

**Protein translocation at the endoplasmic reticulum  
membrane in *Arabidopsis thaliana***

Dissertation der Fakultät für Biologie  
der Ludwig-Maximilians-Universität München

vorgelegt von  
**Melanie Jasmine Mitterreiter**

München, April 2020

Diese Dissertation wurde angefertigt unter der Leitung von PD Dr. Serena Schwenkert an der Fakultät für Biologie der Ludwig-Maximilians-Universität München.

Erstgutachterin: PD Dr. Serena Schwenkert

Zweitgutachter: Prof. Dr. Wolfgang Frank

Tag der Abgabe: 23.04.2020

Tag der mündlichen Prüfung: 30.06.2020

## **Erklärung**

Ich versichere hiermit an Eides statt, dass meine Dissertation selbstständig und ohne unerlaubte Hilfsmittel angefertigt worden ist.

Die vorliegende Dissertation wurde weder ganz, noch teilweise bei einer anderen Prüfungskommission vorgelegt. Ich habe noch zu keinem früheren Zeitpunkt versucht, eine Dissertation einzureichen oder an einer Doktorprüfung teilzunehmen.

München, 23.04.2020

---

Melanie Mitterreiter

## Table of contents

List of figures .....	VII
List of tables .....	IX
Publications .....	X
Abbreviations.....	XI
Summary .....	1
Zusammenfassung .....	2
<b>1. Introduction .....</b>	<b>3</b>
1.1. Protein translocation at the endoplasmic reticulum membrane.....	3
1.2. Endoplasmic reticulum translocation and insertion pathways .....	3
1.3. Co- and post-translational translocation <i>via</i> the Sec translocon.....	6
1.4. The <i>Arabidopsis</i> Sec translocon .....	9
1.4.1. Preprotein guidance by AtTPR7 .....	11
1.4.2. AtSec62 and its homologues in yeast and mammals .....	12
1.5. Aims of this study.....	13
<b>2. Material and Methods.....</b>	<b>14</b>
2.1. Material .....	14
2.1.1. Chemicals, beads and membranes .....	14
2.1.2. Enzymes and Kits.....	14
2.1.3. Molecular weight size marker and DNA standard.....	15
2.1.4. Plant material.....	15
2.1.5. Bacterial strains .....	15
2.1.6. Yeast strains.....	15
2.1.7. Accession numbers .....	16
2.1.8. Vectors and clones .....	17
2.1.9. Oligonucleotides .....	21
2.1.10. Antisera and antibodies .....	25
2.1.11. Statistical analysis .....	25
2.1.12. Computational analysis and software .....	25
2.2. Methods.....	26
2.2.1. Growth conditions.....	26
2.2.1.1. Growth conditions for <i>Escherichia coli</i> and <i>Agrobacterium tumefaciens</i> .....	26

---

2.2.1.2. Growth conditions for <i>Saccharomyces cerevisiae</i> .....	27
2.2.1.3. Growth conditions for <i>Arabidopsis thaliana</i> and <i>Nicotiana benthamiana</i> .....	27
2.2.2. Pollen staining and germination assay .....	28
2.2.3. Microsomal membrane preparation from <i>Arabidopsis thaliana</i> leaves	28
2.2.4. Isolation of soluble and membrane proteins from leaves.....	29
2.2.5. Determination of protein concentration by Bradford .....	29
2.2.6. SDS-Polyacrylamide gel electrophoresis and immunoblotting.....	29
2.2.6.1. SDS-Polyacrylamide gel electrophoresis .....	29
2.2.6.2. Coomassie staining.....	30
2.2.6.3. Semi-dry electro blot .....	30
2.2.6.4. Immunodetection.....	30
2.2.7. Amplification of DNA fragments by Polymerase chain reaction .....	31
2.2.8. Isolation of genomic DNA from <i>Saccharomyces cerevisiae</i> .....	31
2.2.9. Isolation of genomic DNA from <i>Arabidopsis thaliana</i> leaves .....	31
2.2.10. Genotyping using <i>Arabidopsis thaliana</i> genomic DNA .....	32
2.2.11. RNA extraction from <i>Arabidopsis thaliana</i> leaves.....	32
2.2.12. RNA extraction from <i>Saccharomyces cerevisiae</i> .....	32
2.2.13. cDNA synthesis and RT-PCR analysis.....	32
2.2.14. Cloning strategies.....	32
2.2.14.1. Traditional cloning by restriction enzyme digest and ligation .....	33
2.2.14.2. Zero Blunt® Cloning.....	33
2.2.14.3. Gateway® Technology based cloning.....	33
2.2.14.4. Site-directed mutagenesis.....	33
2.2.15. Transformation of <i>Escherichia coli</i> .....	33
2.2.16. Purification of plasmid DNA from <i>Escherichia coli</i> .....	34
2.2.17. Sequencing.....	34
2.2.18. Overexpression of recombinant proteins in <i>Escherichia coli</i> .....	34
2.2.19. Purification of His-/ Strep-tagged proteins .....	35
2.2.20. <i>In vitro</i> transcription and translation using <sup>35</sup> S-methionine.....	35
2.2.21. <i>In vitro</i> pull-down assay .....	36
2.2.22. Detection of radiolabelled proteins .....	36
2.2.23. Transformation and complementation analysis in <i>Saccharomyces cerevisiae</i> .....	36

---

2.2.24. Transformation of <i>Agrobacterium tumefaciens</i> .....	37
2.2.25. <i>Agrobacterium</i> -mediated transient expression of fluorescent proteins in <i>Nicotiana benthamiana</i> .....	37
2.2.26. <i>Agrobacterium</i> -mediated stable transfection of <i>Arabidopsis thaliana</i> ..	38
2.2.27. Immunoprecipitation of GFP-fused proteins using GFP-Trap® Magnetic Agarose beads .....	38
2.2.28. Mass spectrometry .....	39
2.2.29. Transient transformation of isolated <i>Arabidopsis thaliana</i> protoplasts.	39
2.2.30. Confocal microscopy .....	40
<b>3. Results .....</b>	<b>41</b>
3.1. Identification of <i>atsec62</i> and <i>attpr7</i> T-DNA insertion lines.....	41
3.2. Generative defects in <i>atsec62</i> .....	44
3.3. High-temperature and ER stress sensitivity of <i>atsec62</i> .....	46
3.4. AtSec62 localisation and topology analysis .....	47
3.5. Yeast complementation analysis using AtSec62.....	52
3.6. Importance of the AtSec62 C-terminus for its function in plants.....	52
3.7. Identification of potential AtSec62 and AtTPR7 interaction partners by mass spectrometry .....	53
3.8. Verification of AtSec62 associating or interacting proteins.....	57
3.9. Confirmation of potential preproteins for post-translational translocation.....	62
<b>4. Discussion .....</b>	<b>65</b>
4.1. <i>atsec62</i> but not <i>attpr7</i> displays vegetative and generative growth defects similar to other secretory pathway mutants.....	65
4.2. <i>atsec62</i> is sensitive towards high-temperature and ER stress.....	67
4.3. AtSec62 localises to the ER membrane and has three transmembrane domains with its C-terminus being crucial for its function in plants .....	68
4.4. Putative interaction partners of the <i>Arabidopsis</i> Sec translocon .....	70
4.5. Conclusion and future perspectives .....	72
<b>5. References .....</b>	<b>74</b>
Appendix.....	91
<i>Curriculum vitae</i> .....	98
Acknowledgements .....	100

## List of figures

<b>Figure 1:</b> Translocation and insertion pathways at the ER membrane in yeast .....	4
<b>Figure 2:</b> Co- and post-translational protein translocation <i>via</i> the yeast Sec translocon. .....	8
<b>Figure 3:</b> Working model of the <i>Arabidopsis</i> Sec post-translocon .....	10
<b>Figure 4:</b> Confirmation of an <i>attp7</i> T-DNA insertion line .....	41
<b>Figure 5:</b> Isolation of an <i>atsec62</i> T-DNA insertion line and respective complementation lines .....	42
<b>Figure 6:</b> Root morphology of two-week-old <i>atsec62</i> seedlings in comparison to Col-0 .....	43
<b>Figure 7:</b> Reduced seed yield and altered pollen development in <i>atsec62</i> .....	45
<b>Figure 8:</b> ER stress sensitivity of Col-0 and <i>atsec62</i> seedlings. ....	47
<b>Figure 9:</b> Predicted transmembrane domains for Sec62 homologues and AtSec62 constructs used in this study.....	48
<b>Figure 10:</b> Localisation of AtSec62 GFP-fusion proteins in transiently transformed tobacco leaves.....	50
<b>Figure 11:</b> AtSec62 topology analysis in transiently transformed tobacco leaves....	51
<b>Figure 12:</b> Complementation analysis in <i>sec62-ts</i> .....	52
<b>Figure 13:</b> Complementation analysis in <i>atsec62</i> using AtSEC62- $\Delta$ TMD3/C .....	53
<b>Figure 14:</b> GFP-trap <sup>®</sup> pull-down using stable AtSec62 GFP-fusion lines .....	55
<b>Figure 15:</b> rBiFC analysis of AtSec62 and other components of the Sec translocon. .....	58
<b>Figure 16:</b> rBiFC analysis of AtSec62 and potentially interacting or associating proteins .....	59
<b>Figure 17:</b> rBiFC analysis of AtSec62 and components of the GET pathway or tail- anchored proteins.....	60
<b>Figure 18:</b> Recruitment assay for AtGET3a and AtSec62 .....	61
<b>Figure 19:</b> Candidate preproteins for post-translational translocation .....	63
<b>Figure 20:</b> Topology model and amino acid motifs of Sec62 homologues .....	68
<b>Figure 21:</b> Analysis of potential AtSec62 and AtTPR7 interacting/ associating proteins. .....	71

Appendix:

<b>Figure A1:</b> Protein purification for subsequent antibody generation or <i>in vitro</i> pull-down analysis .....	95
<b>Figure A2:</b> Phylogenetic analysis of Sec62 homologues .....	96
<b>Figure A3:</b> Untransformed leaf sample for rBiFC analysis .....	97
<b>Figure A4:</b> AtCA1 $\beta$ -GFP localisation .....	97

---

**List of tables**

<b>Table 1:</b> Accession numbers of proteins used in this study .....	16
<b>Table 2:</b> Constructs used in this study .....	18
<b>Table 3:</b> Oligonucleotides used in this study .....	21
<b>Table 4:</b> Antibiotic agents used for bacterial work in this study .....	26
<b>Table 5:</b> Segregation analysis for progeny plants derived from heterozygous <i>atsec62</i> (+/-) plants .....	44
<b>Table 6:</b> Segregation analysis on sulfadiazine .....	44
<b>Table 7:</b> Pollen tube germination, seed germination and survival of Col-0 and <i>atsec62</i> plants upon high-temperature stress .....	46
<b>Table 8:</b> Candidate preproteins for post-translational translocation <i>via</i> AtTPR7 .....	54
<b>Table 9:</b> Potential AtSec62 interacting/ associating proteins selected for further interaction analysis .....	56

Appendix:

<b>Table A1:</b> Complete list of potential AtSec62 interacting/ associating proteins.....	91
--	----

## Publications

Parts of this study have been published in the following research article:

**Mitterreiter, M.J., Bosch, F.A., Brylok, T., Schwenkert, S.** (2020). The ER luminal C-terminus of AtSec62 is critical for male fertility and plant growth in *Arabidopsis thaliana*. *The Plant Journal* **101** (1), 5-17. <https://doi.org/10.1111/tpj.14483>. Epub 2019 Sep 3.

© 2019 The Authors

*The Plant Journal* published by Society for Experimental Biology and John Wiley & Sons Ltd

The article is licensed under the Creative Commons Attribution 4.0 International license (<https://creativecommons.org/licenses/by/4.0/>). Figures and tables therein have been reused for this thesis (Figure 1, 5, 6, Supplementary Figure S1) or were partially modified or rearranged (Figure 2, 3, 4, Supplementary Figure S2, S3, S4, S5, Table 1, 2).

M.J.M. performed most of the experiments, analysed data, participated in designing experiments, generated all figures and wrote the manuscript, including all text sections that were incorporated into this thesis in exact or almost exact wording. This is hereby confirmed on behalf of all co-authors.

München, 23.04.2020

---

Serena Schwenkert

Parts of the segregation analysis and preliminary work for complementation analysis in *atsec62* originated from the author's master thesis 'The role of Sec62 in protein translocation into the endoplasmic reticulum of *Arabidopsis thaliana*', supervised by PD Dr. Serena Schwenkert and submitted to the Faculty of Biology of the Ludwig-Maximilians-University Munich in September 2017.

München, 23.04.2020

---

Serena Schwenkert

**Abbreviations**

ADP/ ATP	Adenosine-5'-diphosphate/ triphosphate
AIM	Atg8-family interacting motif
amiRNAi	Artificial microRNAi
APS	Ammonium persulfate
BASTA®	Trade name of glufosinolate
BiFC	Bimolecular fluorescence complementation
bp	Base pairs
BSA	Bovine serum albumin ('fraction V')
CBB	Coomassie-Brilliant-Blue
cDNA	Complementary DNA
CFP	Cyan fluorescent protein
Col-0	<i>Arabidopsis thaliana</i> ecotype Columbia
C-terminus	Carboxy-terminus
ddH <sub>2</sub> O	Double-distilled water
DMSO	Dimethyl sulfoxide
DNA	Deoxyribonucleic acid
DTT	1,4-dithiothreitol
ECL	Enhanced chemiluminescence
EDTA	Ethylenediaminetetraacetic acid
EGTA	Ethylene-glycol-bis(β-aminoethyl ether)-N,N,N',N'-tetraacetic acid
ER	Endoplasmic reticulum
ERAD	ER-associated degradation
gDNA	Genomic DNA
GDP/ GTP	Guanosine-5'-diphosphate/ triphosphate
GET	Guided entry of tail-anchored proteins
GFP	Green fluorescent protein
HEPES	4-(2-hydroxyethyl)-1-piperazineethanesulfonic acid
His-tag	Polyhistidine-tag
HSP/ Hsp	Heat shock protein
IPTG	Isopropyl β-D-1-thiogalactopyranoside
LB	Lysogeny broth
LIR	LC3 interacting region

---

MES	2-(N-morpholino)-ethanesulfonic acid
mRNA	Messenger RNA
MS	Murashige-Skoog
NTA	Nitrilotriacetic acid
N-terminus	Amino-terminus
OD	Optical density
PAGE	Polyacrylamide gel electrophoresis
PBS	Phosphate-buffered saline
PCR	Polymerase chain reaction
PEG	Polyethylene glycol
PVDF	Polyvinylidene difluoride
PVP-40	Polyvinylpyrrolidone, average molecular weight: 40000
rBiFC	Ratiometric BiFC
RFP	Red fluorescent protein
RNA	Ribonucleic acid
RNAi	RNA interference
RT-PCR	Polymerase chain reaction based on reverse transcription
SCD	Synthetic complete medium containing 'dropout' mix
SD	Standard deviation
SDS	Sodium dodecyl sulphate
Sec	Sec (secretion) translocation system
SRP	Signal recognition particle
TA	Tail-anchored
TAE	Tris-acetate-EDTA buffer
TBS	Tris-buffered saline
T-DNA	Transferred DNA
TEMED	Tetramethylethylenediamine
TMD	Transmembrane domain
TPR	Tetratricopeptide repeat
Tris	Tris(hydroxymethyl)aminomethane
Tween 20	Polysorbate 20
UPR	Unfolded protein response
UTR	Untranslated region
v/v	Volume per volume

w/v	Weight per volume
WT	Wild-type
YFP	Yellow fluorescent protein
YPD	Yeast extract-peptone-dextrose medium
X-Gal	5-Brom-4-chlor-3-indoxyl- $\beta$ -D-galactopyranoside

## Summary

Protein translocation into or across the endoplasmic reticulum (ER) membrane *via* the Sec translocon occurs either co-translationally or in a post-translational manner. Despite involved components being well investigated in yeast and humans, there is only scarce knowledge regarding the *Arabidopsis* Sec translocon. It is composed of the central Sec61 complex, the J-domain containing AtERdj2A/B and the luminal AtBiP. It additionally involves the recently described chaperone docking protein AtTPR7, the yet uncharacterised AtSec62 as well as cytosolic chaperones for post-translational translocation.

In this study, an *atsec62* T-DNA insertion line was characterised revealing the importance of AtSec62 for vegetative and generative growth resulting in an altered root morphology, impaired growth and reduced male fertility in *atsec62* probably due to the involvement of AtSec62 in protein translocation and subsequent secretion. *atsec62* displayed an increased susceptibility towards high-temperature and ER stress, indicating that it might be involved in ER stress recovery similar to human Sec62. In contrast to its yeast and human homologues, AtSec62 was shown to have an additional third transmembrane domain with its luminal exposed C-terminus being crucial for proper AtSec62 function in *Arabidopsis*.

Potential AtSec62 interacting or associating proteins were identified, including other Sec translocon components like AtTPR7 and subunits of the Sec61 complex, the GET-pathway proteins AtGET1 and AtGET3a and other proteins like AtATG8e, AtCNX1 and the tail-anchored protein AtSYP123. Moreover, the interaction of AtTPR7 with putative candidates for post-translational translocation like AtPYK10 and AtGLL23 was confirmed by *in vitro* pull-down assays.

The investigation of AtSec62 topology as well as AtSec62 and AtTPR7 interacting proteins provides further insight into the composition of the *Arabidopsis* Sec post-translocon and reveals potential translocation substrates. However, the exact function of respective components and the general mechanism of translocation still remain unknown and should be addressed in future studies.

## Zusammenfassung

Der Proteintransport in das endoplasmatische Retikulum (ER) erfolgt entweder co- oder post-translational mithilfe des Sec-Translocons. Obwohl die beteiligten Proteine in Hefe und im Menschen bereits charakterisiert wurden und entsprechend homologe Proteine auch in Pflanzen existieren, sind die Zusammensetzung des Translocons und der genaue Translokationsmechanismus dort noch weitgehend unerforscht. In *Arabidopsis* besteht das Sec-Translocon aus dem zentralen Sec61-Komplex, den Membranproteinen AtERdj2A/B sowie dem luminalen AtBiP. Darüber hinaus beinhaltet es das Rezeptorprotein AtTPR7, welches mit zytosolischen Chaperonen interagiert, und das noch unerforschte AtSec62.

In dieser Arbeit wurde eine *atsec62* T-DNA Insertionslinie charakterisiert, die eine veränderte Wurzelmorphologie, beeinträchtigt Wachstum sowie eine reduzierte männliche Fertilität aufweist, was die Bedeutung von AtSec62 für den Proteintransport und die nachfolgende Proteinsekretion verdeutlicht. Eine erhöhte Empfindlichkeit der *atsec62*-Pflanzen gegenüber Hitze und ER-Stress weist zudem daraufhin, dass AtSec62 wie sein humaner Gegenspieler an der *ER stress recovery* beteiligt sein könnte. AtSec62 besitzt drei Transmembrandomänen und infolgedessen einen luminal-exponierten C-terminus, der für die Proteinfunktion in *Arabidopsis* essentiell ist.

Darüber hinaus wurden potentielle AtSec62 Interaktionspartner oder AtSec62 assoziierte Proteine identifiziert. Dazu zählen beispielsweise andere Proteine des Sec-Translocons wie AtTPR7 und Untereinheiten des Sec61-Komplexes, AtGET1 und AtGET3a sowie AtATG8e, AtCNX1 und das *tail-anchored* AtSYP123. Zudem wurde die Interaktion zwischen AtTPR7 und Kandidaten für den post-translationalen Proteintransport wie AtPYK10 und AtGLL23 bestätigt.

Die Topologie von AtSec62 und die Identifikation möglicher AtSec62 und AtTPR7 Interaktionspartner gewähren nicht nur tiefere Einblicke in die Zusammensetzung des Sec-Translocons in *Arabidopsis*, sondern zeigen auch mögliche Substrate für den Proteintransport auf. Dennoch sind sowohl die genaue Funktion der jeweiligen Proteine als auch der genaue Translokationsmechanismus weiterhin unbekannt und sollten in zukünftigen Experimenten genauer untersucht werden.

## 1. Introduction

### 1.1. Protein translocation at the endoplasmic reticulum membrane

To reach their final destination within the cell, membrane and secretory proteins that are synthesised on cytosolic ribosomes need to be transported into or across the endoplasmic reticulum (ER) membrane for processing and further transport *via* the Golgi apparatus. In contrast to chloroplasts and mitochondria, translocation of preproteins at the ER membrane can occur either co- or post-translationally (reviewed by Rapoport 2007, Cross *et al.* 2009, Hegde and Keenan 2011, Zimmermann *et al.* 2011, Aviram and Schuldiner 2017, Linxweiler *et al.* 2017, Van Puyenbroeck and Vermeire 2018).

Proteins destined for secretion or targeted to the ER lumen usually display an N-terminal, cleavable signal sequence harbouring a section of seven to twelve hydrophobic amino acids, whereas membrane proteins feature at least one transmembrane domain (TMD) of around 20 hydrophobic amino acids (Ng *et al.* 1996, Park and Rapoport 2012, Ast *et al.* 2013, Schibich *et al.* 2016). Both signals can be recognised by the signal recognition particle (SRP) and allow guidance to the ER membrane (Park and Rapoport 2012). In addition, so called tail-anchored (TA) proteins harbour a hydrophobic TMD at their very C-terminus which is only exposed shortly before translation is terminated thereby depending on post-translational translocation (Borgese and Gaetani 1983, Aviram and Schuldiner 2017).

Depending on their signal sequence, preproteins use different translocation and insertion pathways at the ER membrane. However, all following pathways include cytosolic factors for substrate recognition – during or after protein translation – and interaction with receptors located at the ER membrane as well as subsequent translocation and insertion (compare to Aviram and Schuldiner 2017).

### 1.2. Endoplasmic reticulum translocation and insertion pathways

Protein translocation across or into the ER membrane in yeast occurs *via* the SRP-dependent, the SRP-independent or *via* the Guided Entry of Tail-anchored proteins (GET)-pathway (reviewed by Aviram and Schuldiner 2017) (Figure 1).

Co-translational protein transport *via* the SRP-dependent pathway involves the SRP binding to the ribosome-nascent polypeptide chain complex and recruiting it to the ER membrane *via* the SRP receptor, which is composed of two subunits named SRP101p/SR $\alpha$  and SRP102p/SR $\beta$  (Gilmore *et al.* 1982a, Gilmore *et al.* 1982b, Meyer

*et al.* 1982, Young *et al.* 1995). The ribosome-nascent chain complex is then transferred to the heterotrimeric Sec61 complex, which is composed of Sec61p, Sbh1p and Sss1p and forms the translocation channel (Panzner *et al.* 1995, Harada *et al.* 2011). The J-domain containing protein Sec63p and the heat shock protein (Hsp) 70-like, luminal Kar2p (named BiP in mammalian cells) are additionally involved in co-translational translocation to facilitate unidirectional translocation (Linxweiler *et al.* 2017).

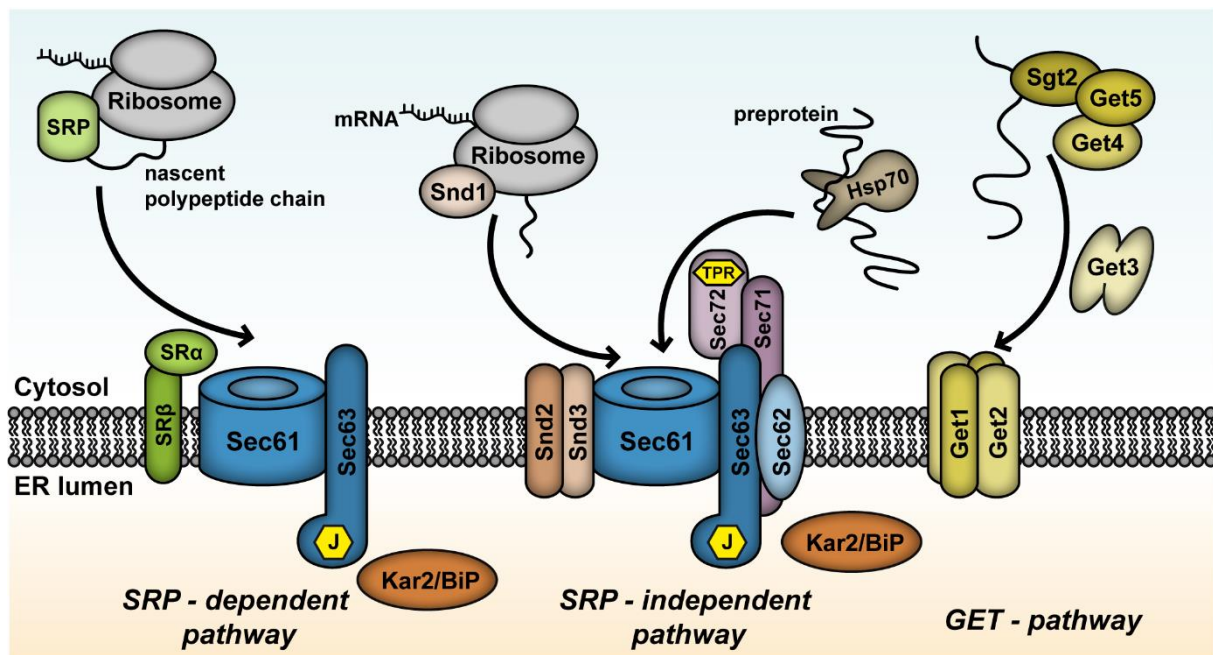


**Figure 1: Translocation and insertion pathways at the ER membrane in yeast.** Co-translational translocation *via* the SRP-dependent pathway features the signal recognition particle (SRP) pausing translation of the emerging polypeptide chain at the ribosome, the SRP receptor, composed of SRP101p/SRα and SRP102p/SRβ, and the Sec61 translocation pore. Alternatively, co-translational translocation *via* the SRP-independent pathway involves the recently identified ribosome-interacting Snd1p and the membrane proteins Snd2p and Snd3p. SRP-independent and post-translational translocation is achieved by preprotein interacting, cytosolic Hsp70-like chaperones, the signal peptide receptor, which is composed of Sec62p, the J-domain containing Sec63p, Sec71p and the TPR protein Sec72p, the Sec61 translocation pore and the luminal Hsp70-like chaperone Kar2p/BiP. Tail-anchored proteins are inserted into the ER membrane by the Guided Entry of Tail-anchored proteins (GET)-pathway featuring the pre-targeting complex (Sgt2p, Get4p and Get5p), the Get3p dimer and the Get1p-Get2p insertase. For simplicity, the suffix 'p' has been omitted in protein names in the actual figure. Reviewed by Saraogi and Shan 2011, Hegde and Keenan 2011, Aviram and Schuldiner 2017, Van Puyenbroeck and Vermeire 2018.

Alternatively, co-translational translocation can occur in an SRP-independent manner with the recently identified ribosome-interacting Snd1p and the membrane proteins

Snd2p and Snd3p, officially named ENV10 and PHO88 (Aviram *et al.* 2016). Snd2p and Snd3p are interacting with the Sec61 complex, indicating that both proteins might be involved in substrate targeting to the ER membrane (Aviram *et al.* 2016). Moreover, it was suggested that the SND-pathway, which also seems to be conserved in mammalian cells (Haßdenteufel *et al.* 2017), deals with a broad substrate range focussing on substrates featuring central TMDs and compensates defects in the SRP-dependent and the GET-pathway (Aviram *et al.* 2016). However, the exact mode of substrate recognition for the SND-pathway still remains unclear (Aviram and Schuldiner 2017).

Small pre-secretory proteins are generally imported post-translationally as their signal sequence is only transcribed shortly before translation is entirely completed (Lakkaraju *et al.* 2012, Ast and Schuldiner 2013). Fully translated preproteins are bound by Hsp70-like chaperones like Ssa1p (Chirico *et al.* 1988, Deshaies *et al.* 1988, Tripathi *et al.* 2017) and targeted to the ER membrane *via* a tetrameric complex, composed of Sec63p, Sec62p and the yeast specific Sec71p and Sec72p, which enables binding to cytosolic chaperones *via* its tetratricopeptide repeat (TPR) domain (Deshaies *et al.* 1991, Fang and Green 1994, Feldheim and Schekman 1994, Panzner *et al.* 1995, Lyman and Schekman 1997, Plath *et al.* 1998, Schlegel *et al.* 2007, Harada *et al.* 2011). As for co-translational translocation, the luminal Hsp70-like chaperone Kar2p facilitates protein translocation *via* the Sec61 protein-conducting channel by binding the translocating preprotein upon interaction with the Sec63p J-domain and thereby preventing the polypeptide from sliding back into the cytosol (Brodsky and Schekman 1993, Brodsky *et al.* 1995, Panzner *et al.* 1995, Osborne *et al.* 2005, Rapoport 2007). Despite small differences regarding the overall composition of the Sec translocon, homologous proteins for the post-translational translocation pathway are present in mammals and plants (summarised by Zimmermann *et al.* 2011, Schweiger and Schwenkert 2013).

Post-translational translocation and subsequent insertion of TA proteins into the ER membrane occurs *via* the GET-pathway. Preproteins are bound by the ribosome-associated chaperone Sgt2p, which is part of the pre-targeting complex together with the cytosolic Get4p and Get5p (Wang *et al.* 2010a, Denic *et al.* 2013). The TA protein is then passed on to the homodimeric ATPase Get3p (Rome *et al.* 2013, Mateja *et al.* 2015), which targets the pre-preprotein to the heterodimeric Get1p-Get2p insertase in the ER membrane (Schuldiner *et al.* 2008). The homologous pathway in mammalian

cells features the chaperone SGTA, GET4/TRC35, the Get5p homologue Ubl4a, the Get3p homologous TRC40 (Stefanovic and Hegde 2007) and the Get1p and Get2p homologues CAML and WRP but also involves additional proteins like Bat3 and Bag6 (Mariappan *et al.* 2010, Yamamoto and Sakisaka 2012, Shao *et al.* 2017). However, the GET-pathway in yeast not only targets TA proteins to the ER membrane but also glycosylphosphatidylinositol-anchored proteins (Ast *et al.* 2013), while mammalian TRC40 was suggested to additionally guide small secretory proteins to the Sec61 complex (Johnson *et al.* 2012). Moreover, homologues of yeast Get1p, Get3p and Get4p have been identified in *Arabidopsis* with AtGET3a guiding TA proteins to the ER membrane localised AtGET1 (Srivastava *et al.* 2017, Xing *et al.* 2017). Even though respective proteins are not essential for plant growth, loss-of-function mutants display defective root hair growth (Xing *et al.* 2017) and an increased susceptibility towards ER stress (Srivastava *et al.* 2017).

### 1.3. Co- and post-translational translocation *via* the Sec translocon

Co- and post-translational protein translocation *via* the Sec translocon including underlying mechanisms (compare to Figure 2) have already been extensively studied in yeast and humans in contrast to the GET-pathway (Schuldiner *et al.* 2008) and the recently discovered SND-pathway (Aviram *et al.* 2016).

For co-translational translocation in yeast and mammals, the large ribonucleoprotein complex SRP binds to the ribosome and the signal peptide of the emerging nascent polypeptide chain at the ribosome *via* a methionine-rich domain of its Srp54p/SRP54 component, thereby arresting protein translation (Krieg *et al.* 1986, Kurzchalia *et al.* 1986, Römisch *et al.* 1990, Zopf *et al.* 1990, Lütcke *et al.* 1992, Saraogi and Shan 2011).

The SRP and the associated ribosome-nascent chain complex are targeted to the ER membrane by the ER localised SRP receptor, which is composed of the soluble SRP101p/SR $\alpha$  and the membrane anchored SRP102p/SR $\beta$  (Gilmore *et al.* 1982a, Gilmore *et al.* 1982b, Meyer *et al.* 1982, Tajima *et al.* 1986, Young *et al.* 1995, Schwartz and Blobel 2003). For stable interaction, the GTPases SRP54 as well as SR $\alpha$  need to be GTP-bound, while GTP-binding of SR $\beta$  is additionally required for its interaction with SR $\alpha$  (Zopf *et al.* 1993, Schwartz and Blobel 2003).

Binding of the SRP to its GTP-bound receptor enables the transfer of the ribosome-nascent chain complex from the SRP to the Sec61 translocon, which interacts with the ribosome mainly *via* the loop region L6 and L8 of Ssh1p, while it is interacting with the

nascent polypeptide chain *via* loop L6 (Becker *et al.* 2009, Saraogi and Shan 2011, Aviram and Schuldiner 2017).

The Sec61 complex is built up by the pore-forming Sec61p and the accessory Sbh1p and Sss1p (Panzner *et al.* 1995, Harada *et al.* 2011) (corresponding to Sec61 $\alpha$ , Sec61 $\beta$  and Sec61 $\gamma$  in mammalian cells, Görlich and Rapoport 1993). The  $\alpha$ -subunit can be divided into the transmembrane segments 1-5 and 6-10 with the loop region serving as a hinge during lateral gate opening (Rapoport 2007). The  $\gamma$ -subunit links those two halves of the  $\alpha$ -subunit, while the  $\beta$ -subunit is non-essential (Rapoport 2007). The Sec61 channel is primed by binding of the ribosome and activated by insertion of the signal peptide into the lateral wall leading to the preprotein being inserted as a loop (Osborne *et al.* 2005, Rapoport 2007).

The SRP-SR $\alpha$ -SR $\beta$  complex dissociates upon GTP hydrolysis, which is coupled to the transfer of the ribosome-nascent chain complex to the Sec61 translocon (Connolly *et al.* 1991, Song *et al.* 2000, Fulga *et al.* 2001, Zhang *et al.* 2009). After dissociation from the SRP, translation continues, while the emerging polypeptide is simultaneously translocated through the Sec61 complex (Saraogi and Shan 2011).

Successful translocation additionally involves the J-domain containing Sec63p and the ER luminal Hsp70-like chaperone Kar2p/BiP, which are essential for co- and post-translational protein translocation (Brodsky *et al.* 1995, Zimmermann *et al.* 2011). Upon interaction of Kar2p/BiP with the J-domain of Sec63p, its ATPase domain is activated and its peptide binding pocket is closed, thereby preventing the still translocating preprotein from sliding back into the cytosol (Brodsky and Schekman 1993, Brodsky *et al.* 1995, Panzner *et al.* 1995, Matlack *et al.* 1999, Osborne *et al.* 2005, Rapoport 2007). Peptide-bound Kar2p/BiP is released by ADP-ATP exchange upon terminated translocation (Osborne *et al.* 2005, Rapoport 2007).

In contrast to the co-translational pathway, post-translational protein translocation at the ER membrane involves cytosolic Hsp70-like chaperones, which bind the translated preprotein in an ATP-dependent manner, preventing molecular crowding and premature folding and which guide preproteins to the Sec translocon (Chirico *et al.* 1988, Deshaies *et al.* 1988, Zimmermann *et al.* 1988, Deshaies *et al.* 1991, Ng *et al.* 1996, Ngosuwana *et al.* 2003, Tripathi *et al.* 2017).

Besides the trimeric Sec61 complex, post-translational translocation in yeast additionally features a tetrameric complex composed of Sec63p, Sec62p, Sec71p and Sec72p (Deshaies *et al.* 1991, Panzner *et al.* 1995, Harada *et al.* 2011).

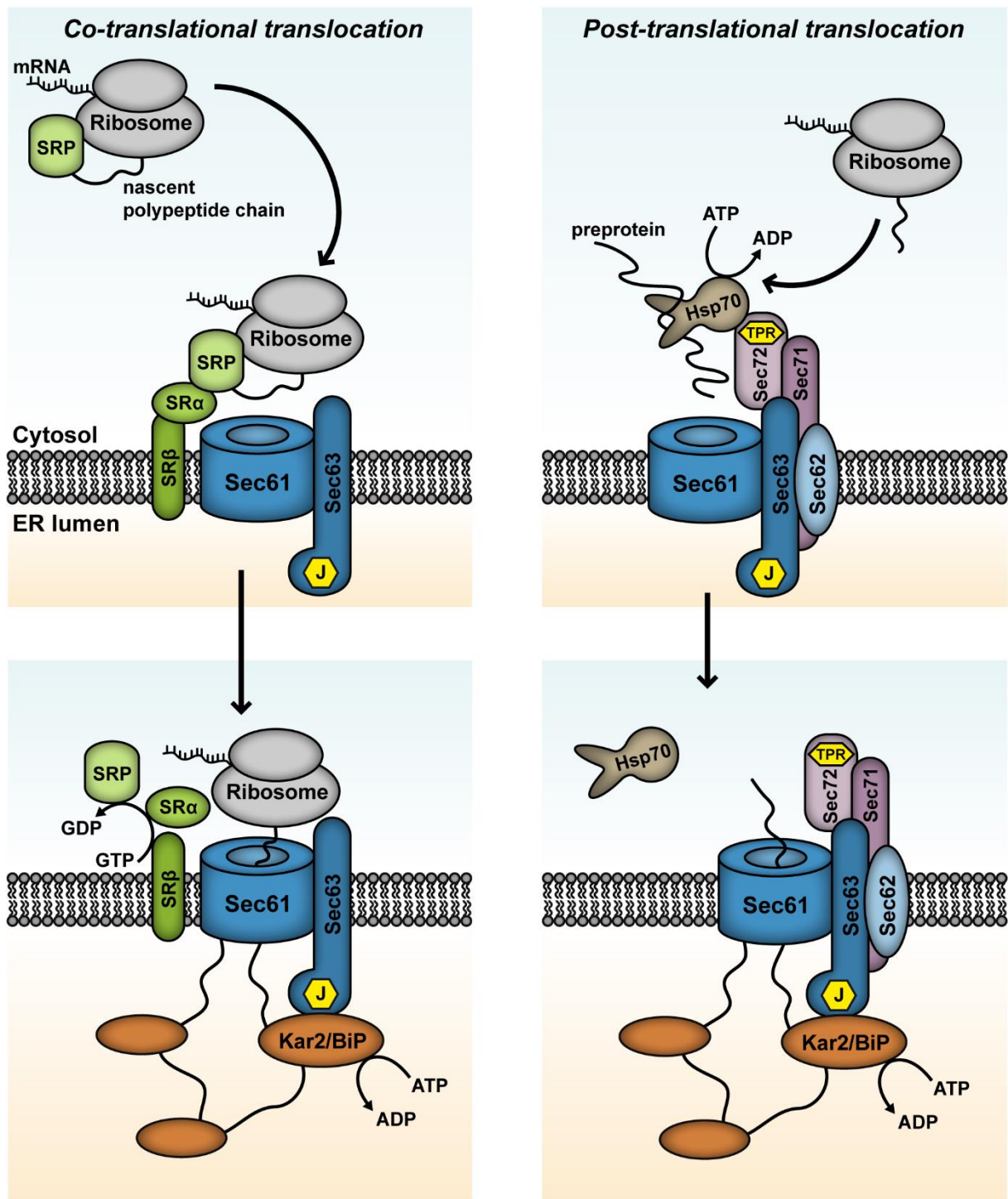


**Figure 2: Co- and post-translational protein translocation via the yeast Sec translocon.**

For co-translational translocation, the signal recognition particle (SRP) pauses translation of the emerging polypeptide chain at the ribosome and its binding to the SRP receptor (SR $\alpha$  and SR $\beta$ ) enables guidance to the Sec61 translocation pore. Upon GTP hydrolysis, the SRP and SR $\alpha$  as well as SR $\beta$  are dissociating. For post-translational translocation, the preprotein is bound by cytosolic Hsp70-like chaperones, which are bound by the TPR protein Sec72p, being part of the signal peptide receptor complex together with Sec71p, Sec62p and Sec63p. Co- and post-translational translocation feature the Sec61 translocation pore and the luminal Hsp70-like chaperone Kar2p/BiP, which is binding the polypeptide upon ATP hydrolysis, thereby preventing the polypeptide from sliding back into the cytosol. Reviewed by Rapoport 2007, Saraogi and Shan 2011, Park and Rapoport 2012, Aviram and Schuldiner 2017.

While Sec61 and Sec63p are involved in co- and post-translational translocation, Sec62p, Sec71p and Sec72p are specifically associated with post-translational translocation and probably act as signal peptide receptor (Deshaies *et al.* 1991, Brodsky and Schekman 1993, Fang and Green 1994, Panzner *et al.* 1995, Lyman and Schekman 1997, Plath *et al.* 1998, Dünwald *et al.* 1999). Sec72p is thereby enabling interaction with cytosolic chaperones *via* its cytosol exposed TPR domain (Feldheim and Schekman 1994, Schlegel *et al.* 2007). Depending on signal sequence characteristics, Sec63p, Sec62p, Sec71p and Sec72p might associate in different combinations for optimal binding to preproteins (Yim *et al.* 2018). The Sec62p-Sec63p complex has additionally been shown to interact with Sec61 *via* Sec63p leading to lateral channel opening and activating Sec61 for subsequent protein translocation (Harada *et al.* 2011, Itskanov and Park 2019, Wu *et al.* 2019).

Post-translational translocation in mammalian cells features auxiliary components like the translocating chain-associating membrane protein TRAM (Hegde *et al.* 1998, Tamborero *et al.* 2011), the translocon-associated protein complex TRAP (Sommer *et al.* 2013, Pfeffer *et al.* 2017) and other additional proteins (summarised by Zimmermann *et al.* 2011).

Protein transport in yeast and mammals further involves modifying enzymes like the signal peptidase complex required for processing/ cleaving the signal peptide, the oligosaccharyltransferase complex for N-linked glycosylation of translocated preproteins (Chen *et al.* 2001, Wild *et al.* 2018) and the glycosylphosphatidylinositol transamidase (Fraering *et al.* 2001, Zhu *et al.* 2005, Zimmermann *et al.* 2011).

#### **1.4. The *Arabidopsis* Sec translocon**

In contrast to yeast and mammals, there is only scarce knowledge concerning the ER Sec translocation complex in plants. The *Arabidopsis* genome encodes three isoforms of the channel-forming Sec61p/Sec61 $\alpha$  homologue, which share 89% sequence identity with each other as well as 52% and 67% identity with their yeast and mammalian counterparts (Schweiger and Schwenkert 2013). Moreover, two homologous isoforms for yeast Sec63p are present in *Arabidopsis*, named AtERdj2A and AtERdj2B, showing 74% sequence identity to each other and 22% and 19% sequence identity to Sec63p and human Sec63 (ERdj2) (Yamamoto *et al.* 2008, Schweiger and Schwenkert 2013). Neither AtERdj2A nor AtERdj2B was able to rescue the thermosensitive growth phenotype of the respective yeast mutant, probably due to their inability to form proper complexes with other components of the yeast Sec

translocon (Yamamoto *et al.* 2008). Whereas AtERdj2B seems to have auxiliary functions only, AtERdj2A is important for proper translocation and subsequent secretion, thereby being indispensable for male fertility in *Arabidopsis*, reflected by lethality of the respective T-DNA insertion line and drastically affected tube germination of *aterdj2a* pollen (Yamamoto *et al.* 2008). Together with the yet uncharacterised AtSec62 and the recently described chaperone docking protein AtTPR7, AtERdj2A/B and the Sec61 complex probably build up the *Arabidopsis* Sec post-translocon (Schweiger *et al.* 2012, Schweiger and Schwenkert 2013) (Figure 3).

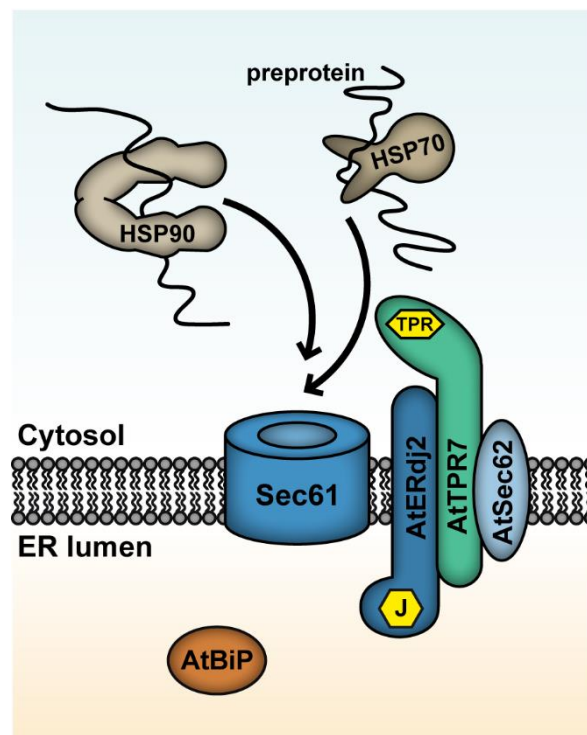


**Figure 3: Working model of the *Arabidopsis* Sec post-translocon.** Post-translational translocation involves the cytosolic HSP70 and HSP90 chaperones, the TPR protein AtTPR7, the Sec61 translocation channel, the J-domain containing AtERdj2A/B, the putative Sec translocon component AtSec62 and the ER luminal AtBiP (Yamamoto *et al.* 2008, Schweiger *et al.* 2012, Schweiger and Schwenkert 2013). Scheme based on Schweiger *et al.* (2012).

For successful translocation, additional chaperone activity is required involving cytosolic HSP70 and HSP90 chaperones (Schweiger *et al.* 2012, Schweiger *et al.* 2013) and ER luminal AtBiP, which is present as three isoforms in *Arabidopsis*, AtBiP1, AtBiP2 and AtBiP3, and probably interacting with the J-domain of AtERdj2A/B (Yamamoto *et al.* 2008, Maruyama *et al.* 2010, Maruyama *et al.* 2014). *AtBIP1/2* are ubiquitously expressed, whereas *AtBIP3* is expressed in pollen, pollen tubes and under ER stress conditions (Maruyama *et al.* 2014). Due to its generally low expression

levels, AtBiP3 can only partially suppress defects in *bip1 bip2* pollen, while *bip1 bip2 bip3* pollen are not even viable probably due to blocked protein secretion, which is especially required during pollen tube germination and growth (Maruyama *et al.* 2014).

#### 1.4.1. Preprotein guidance by AtTPR7

The tail-anchored AtTPR7 was identified by Prasad *et al.* (2010) and has been recently described as part of the *Arabidopsis* Sec post-translocon (Schweiger *et al.* 2012, Schweiger and Schwenkert 2013, Schweiger *et al.* 2013), while it was originally described as the chloroplast outer envelope protein AtOEP61 (von Loeffelholz *et al.* 2011). It was proposed to function as alternative chaperone docking protein at the chloroplast membrane next to AtToc64 (compare to Schwenkert *et al.* 2018), therefore guiding AtHSP70-bound preproteins to the chloroplast (von Loeffelholz *et al.* 2011).

In general, TPR motifs were identified in a wide range of proteins in all eukaryotic organisms and TPR proteins are not only involved in guiding chaperone-bound preproteins to membranes of various cell compartments, thereby being important for proper protein import, but also fulfill other functions in gene expression or protein homeostasis (Schlegel *et al.* 2007, Kriechbaumer *et al.* 2012, Bohne *et al.* 2016, Graham *et al.* 2019). Clamp-type TPR domains consist of three TPR motifs with a 34 amino acid repeat displaying seven conserved positions, which are important for proper TPR domain structure as well as substrate specificity (Sikorski *et al.* 1990, Kriechbaumer *et al.* 2012). They form a peptide binding groove composed of seven  $\alpha$ -helices including a C-terminal stabilisation/ solvation helix and binding to the C-terminus of Hsp70 and Hsp90 (Scheufler *et al.* 2000, Brinker *et al.* 2002, D'Andrea and Regan 2003, Kriechbaumer *et al.* 2012, Schweiger *et al.* 2012).

AtTPR7 possesses such an N-terminal clamp-type TPR domain, which is composed of three TPR repeats, and a C-terminal transmembrane domain (von Loeffelholz *et al.* 2011, Schweiger *et al.* 2012). It is interacting with cytosolic chaperones especially with AtHSP70-1 and the constitutively expressed AtHSP90.2, AtHSP90.3 and AtHSP90.4, while there is only weak interaction with the heat shock-induced AtHSP90.1 (Krishna and Gloor 2001, Schweiger *et al.* 2012, Schweiger *et al.* 2013). Its TPR domain is essential for chaperone interaction and AtTPR7 was suggested to functionally replace the yeast TPR protein Sec72p as well as Sec71p, which anchors Sec72p to the ER membrane (Schweiger *et al.* 2012). However, AtTPR7 is not essential for ER protein translocation and can probably be bypassed as the respective *attp7* T-DNA insertion shows no obvious growth phenotype (Schweiger *et al.* 2012).

AtTPR7 has further been shown to interact with AtERdj2A/B and AtSec62, thereby providing further insights into the *Arabidopsis* Sec post-translocon (Schweiger *et al.* 2012, Schweiger and Schwenkert 2013).

#### 1.4.2. AtSec62 and its homologues in yeast and mammals

In contrast to the Sec61p/Sec61 $\alpha$  and Sec63p/Sec63 homologues in *Arabidopsis*, there is only one homologous isoform for Sec62p/Sec62 encoded, displaying only 12% and 15% sequence identity to its yeast and mammalian counterparts (Schweiger and Schwenkert 2013).

While Sec62p and human Sec62 possess two transmembrane domains, resulting in the N- and the C-terminus being exposed to the cytosol, a third transmembrane domain is only predicted for plant Sec62 homologues (Schweiger and Schwenkert 2013). However, the actual AtSec62 topology and its exact function still remain unknown, whereas the involvement of its yeast and mammalian homologues in ER protein translocation is largely investigated.

Sec62p is part of a tetrameric complex together with Sec63p, Sec71p and Sec72p and is associated with post-translational translocation only (Deshaies *et al.* 1991, Panzner *et al.* 1995, Harada *et al.* 2011). Its positively charged N-terminus is important for its interaction with Sec63p (Wittke *et al.* 2000, Willer *et al.* 2003, Müller *et al.* 2010, Jung *et al.* 2014) and its C-terminus probably has an essential function during signal peptide recognition (Deshaies and Schekman 1990, Dünwald *et al.* 1999, Wittke *et al.* 2000). According to recent studies, the Sec62p-Sec63p complex might even be involved in membrane protein insertion and topogenesis of signal anchor proteins (Reithinger *et al.* 2013, Jung *et al.* 2014, Jung *et al.* 2019).

Mammalian Sec62 and Sec63 are not only associated with the Sec61 complex (Meyer *et al.* 2000, Tyedmers *et al.* 2000) but are also involved in recruiting BiP and translocation substrates to the translocon with Sec62 ensuring efficient post-translational translocation of proteins shorter than around 160 amino acids and being crucial for proteins up to a length of 100 amino acids (Müller *et al.* 2010, Lakkaraju *et al.* 2012). Sec62 has a C-terminal EF-hand motif and is generally important for Ca<sup>2+</sup> homeostasis due to its Ca<sup>2+</sup>-sensitive interaction with Sec61 channel (Linxweiler *et al.* 2013). Furthermore, a C-terminal region of human Sec62 has been shown to be required for delivering proteins to the autolysosomal system, indicating an additional role of Sec62 in ER stress recovery (Fumagalli *et al.* 2016) and correlating its

overexpression to various tumors and pathologies (Zimmermann *et al.* 2006, Greiner *et al.* 2011a, Greiner *et al.* 2011b, Linxweiler *et al.* 2013, Bergmann *et al.* 2017).

Two oligopeptide motifs exclusively found in mammalian Sec62 enable an interaction with the ribosomal tunnel exit, suggesting that Sec62 additionally functions in co-translational protein translocation, which is the favoured pathway in mammalian cells (Müller *et al.* 2010). However, ribosome binding by Sec62 might only be relevant in coordinating protein translocation across the ER membrane as *SEC62* silencing only impairs post-translational import of small, presecretory proteins, whereas post-translational membrane insertion of TA proteins and co-translational translocation remain unaffected (Lang *et al.* 2012).

### **1.5. Aims of this study**

While protein translocation into or across the ER membrane is well studied in yeast and mammals, the actual components involved in translocation as well as potential candidates for co- and post-translational translocation still remain hardly investigated in plants.

For this reason, the putative *Arabidopsis* Sec translocon component AtSec62 should be characterised in this study, especially regarding its presumably altered topology (Schweiger and Schwenkert 2013) and importance in ER protein translocation also being reflected by its impact on plant development and growth.

General growth, root morphology and gametophytic defects in an *atsec62* T-DNA insertion line should be investigated, besides examination of *atsec62* susceptibility towards high-temperature and ER stress. The expected ER localisation of AtSec62 should be confirmed by GFP-fusion, whereas topology analysis should be conducted using Split-GFP. The importance of the *Arabidopsis* AtSec62 C-terminal region should additionally be studied by performing complementation analyses.

To further elucidate ER protein-translocation and the post-translational pathway in particular, potential AtSec62 and AtTPR7 associating or interacting proteins should be identified by mass spectrometric analyses and should be subsequently confirmed by rBiFC and pull-down experiments.

## 2. Material and Methods

### 2.1. Material

#### 2.1.1. Chemicals, beads and membranes

Chemicals used in the following experiments were purchased from bts Biotech Trade & Service (Kraichtal, Germany), Duchefa Biochemie (Haarlem, Netherlands), J.T. Baker Chemicals (Deventer, Netherlands), Fluka (Buchs, Schweiz), Merck (Darmstadt, Germany), New England Biolabs (Frankfurt am Main, Germany), Serva (Heidelberg, Germany), Sigma-Aldrich (Taufkirchen, Germany), ThermoFisher Scientific (Braunschweig, Germany) and Roth (Karlsruhe, Germany).  $^{35}\text{S}$ -methionine was received from PerkinElmer (Walluf, Germany). Ni-NTA-Agarose beads were obtained from Macherey-Nagel (Düren, Germany), GFP-Trap<sup>®</sup> Magnetic Agarose (MA) beads from ChromoTek (Planegg-Martinsried, Germany) and Strep-Tactin<sup>®</sup> Sepharose<sup>®</sup> and D-desthiobiotin from IBA (Göttingen, Germany). PVDF transfer membrane was purchased from Millipore (Billerica, MA, USA) and the blotting paper from Macherey-Nagel (Düren, Germany).

#### 2.1.2. Enzymes and Kits

Restriction endonucleases, T4 DNA Ligase, Q5 DNA Polymerase, SP6 RNA Polymerase and Phusion<sup>®</sup> High Fidelity DNA Polymerase were purchased from New England Biolabs (Frankfurt am Main, Germany), DFS-Taq DNA Polymerase from Bioron (Ludwigshafen, Germany) and M-MLV Reverse Transcriptase from Promega (Madison, WI, USA). BP and LR Clonase<sup>®</sup> II mix and Proteinase K for Gateway<sup>®</sup> cloning were purchased from Invitrogen (Karlsruhe, Germany). Cellulase Onozuka R10 and macerozyme R10 were received from Serva (Heidelberg, Germany) and zymolase from Roth (Karlsruhe, Germany). Wheat Germ Extract and rRNasin<sup>®</sup> Ribonuclease Inhibitor were obtained from Promega (Madison, WI, USA) and cComplete<sup>™</sup> Mini EDTA-free Protease Inhibitor Cocktail from Roche (Penzberg, Germany).

T<sub>N</sub>T<sup>®</sup> Coupled Reticulocyte Lysate Systems for *in vitro* transcription/ translation were purchased from Promega (Madison, WI, USA). The NucleoSpin<sup>®</sup> Plasmid EasyPure Kit and the NucleoBond<sup>®</sup> Xtra Midi or NucleoBond<sup>®</sup> PC 100 Kit from Macherey-Nagel (Düren, Germany) were used for plasmid isolation from *Escherichia coli*. Gel extraction or purification of PCR products were performed using the NucleoSpin<sup>®</sup> Gel and PCR Clean-up Kit from Macherey-Nagel (Düren, Germany). Isolation of RNA was done with

the RNeasy<sup>®</sup> (Plant) Mini Kit from Qiagen (Hilden, Germany). Site-directed mutagenesis was performed with the Q5<sup>®</sup> Site-Directed Mutagenesis Kit from New England Biolabs (Frankfurt am Main, Germany) and Zero Blunt<sup>®</sup> Cloning with the Zero Blunt<sup>®</sup> PCR Cloning Kit from Invitrogen (Karlsruhe, Germany).

### 2.1.3. Molecular weight size marker and DNA standard

Protein Marker I (unstained), peqGOLD (VWR, Ismaning, Germany) was used as molecular weight marker, displaying following sizes: 116, 66.2, 45, 35, 25, 18.4 and 14.4 kDa. HindIII and EcoRI digested  $\lambda$ -phage DNA (New England Biolabs, Frankfurt am Main, Germany) was used as DNA standard, resulting in following fragments: 21226, 5148, 4973, 4268, 3530, 2027, 1904, 1584, 1375, 947, 831 and 564 bp.

### 2.1.4. Plant material

*Arabidopsis thaliana* ecotype Columbia (Col-0) was used as wild-type (WT). The *attpr7* T-DNA insertion line (SALK\_057977) was obtained from the SALK collection (<http://signal.salk.edu/>) (compare to Schweiger *et al.* 2012), while the *atsec62* T-DNA insertion line (GK-871A06) was obtained from the European Arabidopsis Stock Centre (<http://arabidopsis.info/>). *Arabidopsis* seeds were stored in the dark at room temperature. *Nicotiana benthamiana* was used for *Agrobacterium*-mediated transient transfection.

### 2.1.5. Bacterial strains

For cloning and general plasmid amplification, chemically competent *Escherichia coli* Top10 cells were used, whereas *ccdB*-resistant DB3.1 cells were used for amplification of empty Gateway<sup>®</sup> cloning vectors. *Escherichia coli* BL21(DE3)pLysS and BL21-CodonPlus(DE3)-RIPL cells were used for heterologous protein overexpression. Stable transfection of *Arabidopsis* plants as well as transient transfection of tobacco leaves (*Nicotiana benthamiana*) was performed using *Agrobacterium tumefaciens* Agl1 (Carbenicillin resistance) or GV3101 (Rifampicin/ Gentamycin resistance). Chemically competent cells used in this study were prepared by Tamara Bergius and Carina Engstler.

### 2.1.6. Yeast strains

The *Saccharomyces cerevisiae* strain W303 was used as wild-type and was provided by Nikola Wagener. The thermosensitive *sec62-ts* yeast mutant (BY4741; MATa; ura3D0; leu2D0; his3D1; met15D0; *sec62-ts:kanMX*) was purchased from EUROSCARF (<http://euroscarf.de/>).

### 2.1.7. Accession numbers

Accession numbers of genes or proteins used in this study are listed in Table 1. Detailed sequence data can be found under respective accession numbers in the NCBI data libraries (<https://www.ncbi.nlm.nih.gov/>).

**Table 1: Accession numbers of proteins used in this study.**

Protein	Accession number	Species
ATG8e	At2g45170	<i>Arabidopsis thaliana</i>
BiP2	At5g42020	<i>Arabidopsis thaliana</i>
CA1 $\beta$	At3g01500	<i>Arabidopsis thaliana</i>
CNX1	At5g61790	<i>Arabidopsis thaliana</i>
CYP83A1	At4g13770	<i>Arabidopsis thaliana</i>
DGL1	At5g66680	<i>Arabidopsis thaliana</i>
ERdj2A	At1g79940	<i>Arabidopsis thaliana</i>
GET1	At4g16444	<i>Arabidopsis thaliana</i>
GET3a	At1g01910	<i>Arabidopsis thaliana</i>
GET4	At5g63220	<i>Arabidopsis thaliana</i>
GLL23	At1g54010	<i>Arabidopsis thaliana</i>
HSP70-1	At5g02500	<i>Arabidopsis thaliana</i>
HSP90.2/ HSP81.2	At5g56030	<i>Arabidopsis thaliana</i>
PHB3	At5g40770	<i>Arabidopsis thaliana</i>
PBP1	At3g16420	<i>Arabidopsis thaliana</i>
pSSU	XP_016440853/ XP_016481946	<i>Nicotiana tabacum</i>
PYK10/ BGLU23	At3g09260	<i>Arabidopsis thaliana</i>
Sec61 $\alpha$ 1	At2g34250	<i>Arabidopsis thaliana</i>
Sec61 $\beta$ 1	At2g45070	<i>Arabidopsis thaliana</i>
Sec61 $\gamma$ 1	At5g50460	<i>Arabidopsis thaliana</i>
Sec62	XP_006838327	<i>Amborella trichopoda</i>
	At3g20920	<i>Arabidopsis thaliana</i>
	XP_003573202	<i>Brachypodium distachyon</i>
	NP_495908	<i>Caenorhabditis elegans</i>
	XP_001701717	<i>Chlamydomonas reinhardtii</i>
	NP_001020701	<i>Danio rerio</i>
	XP_017075746	<i>Drosophila eugracilis</i>
	NP_001012620	<i>Gallus gallus</i>
	XP_003551357	<i>Glycine max</i>
	XP_003532206	<i>Glycine max</i>
	NP_003253	<i>Homo sapiens</i>
	XP_003712053	<i>Magnaporthe oryzae</i>
	MARPO_0080s0045	<i>Marchantia polymorpha</i>
	XP_003600465	<i>Medicago truncatula</i>
NP_081292	<i>Mus musculus</i>	
AFJ68748.1	<i>Nannochloropsis gaditana</i>	

Protein	Accession number	Species
Sec62	XP_016469805	<i>Nicotiana tabacum</i>
	XP_015627309	<i>Oryza sativa</i>
	XP_024398141	<i>Physcomitrella patens</i>
	NP_015231	<i>Saccharomyces cerevisiae</i>
	NP_594256	<i>Schizosaccharomyces pombe</i>
	XP_002969339	<i>Selaginella moellendorffii</i>
	XP_002970672	
	XP_004250935	<i>Solanum lycopersicum</i>
	XP_004228518	
	NP_001121518	<i>Xenopus tropicalis</i>
XP_008681002	<i>Zea mays</i>	
SHD	At4g24190	<i>Arabidopsis thaliana</i>
SYP123	At4g03330	<i>Arabidopsis thaliana</i>
SYP43	At3g05710	<i>Arabidopsis thaliana</i>
TGG1/ BGLU38	At5g26000	<i>Arabidopsis thaliana</i>
TPR7/ OEP61	At5g21990	<i>Arabidopsis thaliana</i>
VHA-A	At1g78900	<i>Arabidopsis thaliana</i>

### 2.1.8. Vectors and clones

Split-GFP vectors for topology analysis (pSP-GFP1-10-HDEL, pGFP1-10, pGFP11-GW and pGW-GFP11) were provided by Hans Thordal-Christensen (compare to Cabantous *et al.* 2005, Xie *et al.* 2017). The modified Gateway® vectors facilitate N- and C-terminal fusion of the eleventh  $\beta$ -sheet to the protein of interest, while control plasmids encode the GFP  $\beta$ -sheets 1-10, being expressed either in the cytosol (GFP1-10) or in the ER lumen by an integrated ER retention signal (GFP1-10-HDEL) (Xie *et al.* 2017). The ER marker used for localisation studies consists of a fluorophore with an N-terminal ER targeting signal and a C-terminal ER retention signal (compare to Nelson *et al.* 2007, Schweiger *et al.* 2012). pDONR221-P1P4 and pDONR221-P3P2 as well as pBiFCt-2in1-NN, pBiFCt-2in1-NC, pBiFCt-2in1-CN and pBiFCt-2in1-CC were provided by Christopher Grefen (compare to Grefen and Blatt 2012). Gateway® vectors pBGW, pB7CWG2, pB7FWG2, pB7YWG2, pK7FWG2, pK7WGF2 and pAG425GPD-ccdB have been described recently (Karimi *et al.* 2002, Alberti *et al.* 2007, Karimi *et al.* 2007). The helper plasmid p19 was additionally added if necessary, to enhance protein expression in transiently transfected tobacco plants.

Constructs used for this study are listed in Table 2, also indicating restriction sites used for cloning and the purpose of generated constructs. As indicated, constructs were partially generated under the control of the endogenous promoter of *AtSEC62* (base

pairs 800-1899) and encode the full length genomic *AtSEC62* (amino acids 1-365), the *AtSec62* N-terminus (*AtSec62-N*, amino acids 1-160) or a truncated *AtSec62* version lacking the C-terminal region and the putative third transmembrane domain (amino acids 1-247), named *AtSec62-ΔTMD3/C*.

**Table 2: Constructs used in this study.** Genes and vectors, detailed sequence description, restriction sites for cloning and purpose of use are indicated.

No.	Gene	Vector	Description <sup>2</sup>	Restriction site	Purpose <sup>3</sup>
1	<i>AtATG8e</i>	pDONR221-P1P4	-	Gateway <sup>®</sup>	rBiFC
2	<i>AtBIP2</i>	pDONR221-P1P4	no stop	Gateway <sup>®</sup>	rBiFC
3	<i>AtCA1β</i>	pDONR207	no stop	Gateway <sup>®</sup>	L
4	<i>AtCA1β</i>	pDONR221-P1P4	no stop	Gateway <sup>®</sup>	rBiFC
5	<i>AtCA1β</i>	pK7FWG2	no stop	Gateway <sup>®</sup>	L
6	<i>AtCNX1</i>	pDONR221-P1P4	no stop	Gateway <sup>®</sup>	rBiFC
7	<i>AtCYP83A1</i>	pDONR221-P1P4	no stop	Gateway <sup>®</sup>	rBiFC
8	<i>AtERDJ2A</i>	pDONR221-P1P4	no stop	Gateway <sup>®</sup>	rBiFC
9	<i>AtDGL1</i>	pDONR221-P1P4	no stop	Gateway <sup>®</sup>	rBiFC
10	<i>AtGET1</i>	pDONR221-P1P4	no stop	Gateway <sup>®</sup>	rBiFC
11	<i>AtGET3A</i>	pB7CWG2	no stop	Gateway <sup>®</sup>	R
12	<i>AtGET3A</i>	pDONR207	no stop	Gateway <sup>®</sup>	R
13	<i>AtGET3A</i>	pDONR221-P1P4	no stop	Gateway <sup>®</sup>	rBiFC
14	<i>AtGET4</i>	pDONR221-P1P4	no stop	Gateway <sup>®</sup>	rBiFC
15	<i>AtGLL23</i>	pCR Blunt	-	EcoRI/ Sall	Cloning
16	<i>AtGLL23</i>	pSP65	-	EcoRI/ Sall	T
17 <sup>1</sup>	<i>AtHSP70-1</i>	pET51b	-	BamHI/ HindIII	O
18 <sup>1</sup>	<i>AtHSP90.2</i>	pET51b	-	KpnI/ NotI	O
19	<i>AtPBP1</i>	pCR Blunt	-	SacI/ Sall	Cloning
20	<i>AtPBP1</i>	pSP65	-	SacI/ Sall	T
21	<i>AtPHB3</i>	pCR Blunt	-	EcoRI/ Sall	Cloning
22	<i>AtPHB3</i>	pSP65	-	EcoRI/ Sall	T
23	<i>AtPYK10</i>	pCR Blunt	-	EcoRI/ Sall	Cloning
24	<i>AtPYK10</i>	pSP65	-	EcoRI/ Sall	T
25	<i>AtSEC61α1</i>	pDONR221-P1P4	-	Gateway <sup>®</sup>	rBiFC
26	<i>AtSEC61β1</i>	pDONR221-P1P4	-	Gateway <sup>®</sup>	rBiFC
27	<i>AtSEC61γ1</i>	pDONR221-P1P4	-	Gateway <sup>®</sup>	rBiFC
28	<i>AtSEC62</i>	pAG425GPD-ccdB	-	Gateway <sup>®</sup>	C (yeast)
29	<i>AtSEC62</i>	pAG425GPD-ccdB	ΔTMD3/C, stop	Gateway <sup>®</sup>	C (yeast)
30	<i>AtSEC62</i>	pB7FWG2	no stop	Gateway <sup>®</sup>	L
31	<i>AtSEC62</i>	pB7YWG2	amino acids 1-160	Gateway <sup>®</sup>	R
32	<i>AtSEC62</i>	pB7YWG2	no stop	Gateway <sup>®</sup>	R
33	<i>AtSEC62</i>	pBGW	endogenous promoter, full length (genomic)	Gateway <sup>®</sup>	C (plant)

No.	Gene	Vector	Description <sup>2</sup>	Restriction site	Purpose <sup>3</sup>
34	<i>AtSEC62</i>	pBGW	endogenous promoter, $\Delta$ TMD3/C (genomic)	Gateway <sup>®</sup>	C (plant)
35	<i>AtSEC62</i> <i>AtATG8e</i>	pBiFCt-2in1-NN	Sec62-P3P2, ATG8e-P1P4	Gateway <sup>®</sup>	rBiFC
36	<i>AtSEC62</i> <i>AtBIP2</i>	pBiFCt-2in1-CC	Sec62-P3P2, BiP2-P1P4	Gateway <sup>®</sup>	rBiFC
37	<i>AtSEC62</i> <i>AtCA1<math>\beta</math></i>	pBiFCt-2in1-NC	Sec62-P3P2, CA1 $\beta$ -P1P4	Gateway <sup>®</sup>	rBiFC
38	<i>AtSEC62</i> <i>AtCNX1</i>	pBiFCt-2in1-NC	Sec62-P3P2, CNX1-P1P4	Gateway <sup>®</sup>	rBiFC
39	<i>AtSEC62</i> <i>AtCYP83A1</i>	pBiFCt-2in1-NC	Sec62-P3P2, CYP83A1-P1P4	Gateway <sup>®</sup>	rBiFC
40	<i>AtSEC62</i> <i>AtDGL1</i>	pBiFCt-2in1-NC	Sec62-P3P2, DGL1-P1P4	Gateway <sup>®</sup>	rBiFC
41	<i>AtSEC62</i> <i>AtERDJ2A</i>	pBiFCt-2in1-NC	Sec62-P3P2, ERdj2A-P1P4	Gateway <sup>®</sup>	rBiFC
42	<i>AtSEC62</i> <i>AtGET1</i>	pBiFCt-2in1-NC	Sec62-P3P2, GET1-P1P4	Gateway <sup>®</sup>	rBiFC
43	<i>AtSEC62</i> <i>AtGET3A</i>	pBiFCt-2in1-NC	Sec62-P3P2, GET3a-P1P4	Gateway <sup>®</sup>	rBiFC
43	<i>AtSEC62</i> <i>AtGET4</i>	pBiFCt-2in1-NC	Sec62-P3P2, GET4-P1P4	Gateway <sup>®</sup>	rBiFC
44	<i>AtSEC62</i> <i>AtSEC61<math>\alpha</math>1</i>	pBiFCt-2in1-NN	Sec62-P3P2, Sec61 $\alpha$ 1-P1P4	Gateway <sup>®</sup>	rBiFC
45	<i>AtSEC62</i> <i>AtSEC61<math>\beta</math>1</i>	pBiFCt-2in1-NN	Sec62-P3P2, Sec61 $\beta$ 1-P1P4	Gateway <sup>®</sup>	rBiFC
46	<i>AtSEC62</i> <i>AtSEC61<math>\gamma</math>1</i>	pBiFCt-2in1-NN	Sec62-P3P2, Sec61 $\gamma$ 1-P1P4	Gateway <sup>®</sup>	rBiFC
47	<i>AtSEC62</i> <i>AtSHD</i>	pBiFCt-2in1-CC	Sec62-P3P2, SHD-P1P4	Gateway <sup>®</sup>	rBiFC
48	<i>AtSEC62</i> <i>AtSYP123</i>	pBiFCt-2in1-NN	Sec62-P3P2, SYP123-P1P4	Gateway <sup>®</sup>	rBiFC
49	<i>AtSEC62</i> <i>AtSYP43</i>	pBiFCt-2in1-NN	Sec62-P3P2, SYP43-P1P4	Gateway <sup>®</sup>	rBiFC
50	<i>AtSEC62</i> <i>AtTGG1</i>	pBiFCt-2in1-CC	Sec62-P3P2, TGG1-P1P4	Gateway <sup>®</sup>	rBiFC
51	<i>AtSEC62</i> <i>AtTPR7</i>	pBiFCt-2in1-NN	Sec62-P3P2, TPR7-P1P4	Gateway <sup>®</sup>	rBiFC
52	<i>AtSEC62</i> <i>AtVHA-A</i>	pBiFCt-2in1-NN	Sec62-P3P2, VHA-A-P1P4	Gateway <sup>®</sup>	rBiFC
53 <sup>1</sup>	<i>AtSEC62</i>	pDONR207	-	Gateway <sup>®</sup>	Cloning
54	<i>AtSEC62</i>	pDONR207	amino acids 1-160	Gateway <sup>®</sup>	R
55	<i>AtSEC62</i>	pDONR207	$\Delta$ TMD3/C, stop	Gateway <sup>®</sup>	C (yeast)

No.	Gene	Vector	Description <sup>2</sup>	Restriction site	Purpose <sup>3</sup>
56	<i>AtSEC62</i>	pDONR207	ΔTMD3/C, no ATG, stop	Gateway <sup>®</sup>	Split-GFP
57	<i>AtSEC62</i>	pDONR207	ΔTMD3/C, no stop, C-terminal His-tag	Gateway <sup>®</sup>	Split-GFP
58	<i>AtSEC62</i>	pDONR207	endogenous promoter, full length (genomic)	Gateway <sup>®</sup>	C (plant)
59	<i>AtSEC62</i>	pDONR207	endogenous promoter, ΔTMD3/C (genomic)	Gateway <sup>®</sup>	C (plant)
60 <sup>1</sup>	<i>AtSEC62</i>	pDONR207	no ATG	Gateway <sup>®</sup>	Cloning
61	<i>AtSEC62</i>	pDONR207	no stop	Gateway <sup>®</sup>	Cloning
62	<i>AtSEC62</i>	pDONR221-P3P2	-	Gateway <sup>®</sup>	rBiFC
63	<i>AtSEC62</i>	pDONR221-P3P2	no stop	Gateway <sup>®</sup>	rBiFC
64 <sup>1</sup>	<i>AtSEC62</i>	pET21a	amino acids 1-160	NotI/ NdeI	O
65	<i>AtSEC62</i>	pGFP11-GW	ΔTMD3/C, no ATG, stop	Gateway <sup>®</sup>	Split-GFP
66	<i>AtSEC62</i>	pGFP11-GW	no ATG	Gateway <sup>®</sup>	Split-GFP
67	<i>AtSEC62</i>	pGW-GFP11	ΔTMD3/C, no stop, C-terminal His-tag	Gateway <sup>®</sup>	Split-GFP
68	<i>AtSEC62</i>	pGW-GFP11	no stop	Gateway <sup>®</sup>	Split-GFP
69	<i>AtSEC62</i>	pK7WGF2	no ATG	Gateway <sup>®</sup>	L
70	<i>AtSHD</i>	pDONR221-P1P4	no stop	Gateway <sup>®</sup>	rBiFC
71	<i>AtSYP123</i>	pDONR221-P1P4	-	Gateway <sup>®</sup>	rBiFC
72	<i>AtSYP43</i>	pDONR221-P1P4	-	Gateway <sup>®</sup>	rBiFC
73	<i>AtTGG1</i>	pDONR221-P1P4	no stop	Gateway <sup>®</sup>	rBiFC
74	<i>AtTPR7</i>	pDONR221-P1P4	-	Gateway <sup>®</sup>	rBiFC
75 <sup>1</sup>	<i>AtTPR7</i>	pET21a	ΔTMD	NdeI/ XhoI	O
76 <sup>1</sup>	<i>AtTPR7</i>	pET21a	ΔTPR, ΔTMD	-	O
77	<i>AtVHA-A</i>	pDONR221-P1P4	-	Gateway <sup>®</sup>	rBiFC
78 <sup>1</sup>	pSSU (tobacco)	pSP65	-	-	T
79	<i>ScSEC62</i>	pAG425GPD-ccdB	-	Gateway <sup>®</sup>	C (yeast)
80	<i>ScSEC62</i>	pDONR207	-	Gateway <sup>®</sup>	C (yeast)

<sup>1</sup> Constructs were generated in the laboratories of Jürgen Soll and Serena Schwenkert for previous studies and have been reused for this thesis.

<sup>2</sup> If not stated otherwise, the full-length coding sequence was used for construct generation. ΔTMD3/C: *AtSec62* amino acids 1-247, ΔTMD: *AtTPR7* amino acids 1-500 (compare to Schweiger *et al.* 2012), ΔTPR: *AtTPR7* Δbp 309-636 (compare to Schweiger *et al.* 2012), P1P4/ P3P2: derived from pDONR221-P1P4/ -P3P2.

<sup>3</sup> C: complementation analysis, L: localisation analysis, O: overexpression, R: recruitment assay, rBiFC: interaction analysis (Grefen and Blatt 2012), Split-GFP: topology analysis (Xie *et al.* 2017), T: *in vitro* transcription and translation.

### 2.1.9. Oligonucleotides

Used oligonucleotides are listed in Table 3 and were ordered in standard desalted quality from metabion (Planegg, Germany). Oligonucleotides for Gateway® Cloning were either designed according to the manufacturer's Gateway® Technology manual (<https://tools.thermofisher.com/content/sfs/manuals/gatewayman.pdf>) or based on instructions for 2in1 Gateway® primer design (Grefen laboratory, [https://www.ruhr-uni-bochum.de/botanik/Resources/pdf/Entry\\_clone\\_preparation\\_for\\_2in1\\_cloning.pdf](https://www.ruhr-uni-bochum.de/botanik/Resources/pdf/Entry_clone_preparation_for_2in1_cloning.pdf)).

**Table 3: Oligonucleotides used in this study.** Their 5'- 3' sequence and purpose of use are indicated.

No.	Oligonucleotide	5'- 3' sequence	Purpose
1	35S-Prom-for	G TTCATTTTCATTTGGAGAGGACTC	Sequencing
2	35S-Term-rev	GACTGGTGATTTTTGCGGAC	Sequencing
3	<i>AtSEC62</i> -5'UTR-f	CTTGAAATGTGAGAAAAATGAAATAC	Genotyping
4	<i>AtSEC62</i> -Exon1-f	ATGAAGAAGCCGGTCCGAGCCGAG	RT-PCR
5	<i>AtSEC62</i> -Exon2-r	ATCGTCTGTGTCAAGGTCTTTATC	Genotyping
6	<i>AtSEC62</i> -Exon5-r	TTATGTTTTAAGATCAGAGTCAGTCC	RT-PCR
7	<i>AtSEC62-ΔTMD3/C</i> -r	GGGGACCACTTTGTACAAGAAAGCTGG GTCTTAGTCTTTCTTTGGCCAGAAAC	RT-PCR/ Split-GFP/ pBGW/ pAG425GPD -ccdB
8	<i>AtSEC62</i> -3'UTR-rev	GAATACTTCAGATGTTGCCAC	Genotyping
9	<i>AtTPR7</i> -Exon1-attB-f	GGGGACAAGTTTGTACAAAAAAGCAGG CTTCATGTTTAACGGGTTAATGG	RT-PCR
10	<i>AtTPR7</i> -Exon9-f	GTTTCGAACCAAGCATCCCTTC	Genotyping
11	<i>AtTPR7</i> -Exon11-attB-r	GGGGACCACTTTGTACAAGAAAGCTGG GTCGTTTCCAATATAGCCGAGAC	RT-PCR
12	<i>AtTPR7</i> -Exon11-r	CCAATATAGCCGAGACGGTGAAG	Genotyping
13	BGLU23-EcoR1-for	GAATTCATGGTTTTGCAAAGCTTCC	pSP65
14	BGLU23-Sal1-rev	GTCGACTTAAAGCTCATCCTTCTTGAG	pSP65
15	BiP2-Apal-ATG-for	GTACGGGCCCATGGCTCGCTCGTTTGG AG	RT-PCR
16	BiP2-NotI-nostop-rev	GTACGCGGCCGCAGAGCTCATCGTGAG ACTCATC	RT-PCR
17	CA1β-GFP-for	GGGGACAAGTTTGTACAAAAAAGCAGG CTTCATGGGAACCGAAGCATAAC	pK7FWG2
18	CA1β-GFP-nostop-rev	GGGGACCACTTTGTACAAGAAAGCTGG GTCCAGCTTCCAATGTAGTATGG	pK7FWG2
19	CYC1-Term-rev	GCGTGAATGTAAGCGTGAC	Sequencing
20	Gabi-LB8409	ATATTGACCATCATACTCATTGC	Genotyping
21	GET3a-attB-f	GGGGACAAGTTTGTACAAAAAAGCAGG C TTCATGGCGGCGGATTTG	pB7CWG2

No.	Oligonucleotide	5'- 3' sequence	Purpose
22	GET3a-nostop-attB-r	GGGGACCACTTTGTACAAGAAAGCTGG GTCGCCACTCTTGACCCGTTT	pB7CWG2
23	GFP-for	TG ACTTCAAGATCCGCCACAACA	Sequencing
24	GFP-rev	CTCGCCGGACACGCTGAACTTG	Sequencing
25	GLL23-EcoRI-for	GAATTCATGATGGCAAAAACTGTAATT TAG	pSP65
26	GLL23-Sall-rev	GTCGACTCAGTAATACTCGTAACCGC	pSP65
27	GPD-Prom-for	CGGTAGGTATTGATTGTAATTCTG	Sequencing
28	LBa1	TGGTTCACGTAGTGGGCCATCG	Genotyping
29	M13-for	GTA AACGACGGCCAGT	Sequencing
30	M13-rev	GGAAACAGCTATGACCATG	Sequencing
31	NosT-BiFC-rev	CATCTCATAAATAACGTCATGCATTAC	Sequencing
32	P1P4-ATG8e-for	GGGGACAAGTTTGTACAAAAAAGCAGG CTTAATGAATAAAGGAAGCATC	rBiFC
33	P1P4-ATG8e-stop-rev	GGGGACAAC TTTGTATAGAAAAGTTG GGTTTAGATTGAAGAAGCACC	rBiFC
34	P1P4-BiP2-for	GGGGACAAGTTTGTACAAAAAAGCAGG CTTAATGGCTCGCTCGTTTG	rBiFC
35	P1P4-BiP2-nostop-rev	GGGGACAAC TTTGTATAGAAAAGTTGG GTGGAGCTCATCGTGAGACTC	rBiFC
36	P1P4-CA1 $\beta$ -for	GGGGACAAGTTTGTACAAAAAAGCAGG CTTAATGGGAACCGAAGCATA C	rBiFC
37	P1P4-CA1 $\beta$ -nostop-rev	GGGGACAAC TTTGTATAGAAAAGTTGG GTGCAGCTTCCAATGTAGTATGG	rBiFC
38	P1P4-CNX1-for	GGGGACAAGTTTGTACAAAAAAGCAGG CTTAATGAGACAACGGCAAC	rBiFC
39	P1P4-CNX1-nostop-rev	GGGGACAAC TTTGTATAGAAAAGTTGG GTGATTATCACGTCTCGGTTG	rBiFC
40	P1P4-CYP83A1-for	GGGGACAAGTTTGTACAAAAAAGCAGG CTTAATGGAAGATATCATCATCGG	rBiFC
41	P1P4-CYP83A1-nostop-rev	GGGGACAAC TTTGTATAGAAAAGTTGG GTGATACTTGTTCACTTTCTCTG	rBiFC
42	P1P4-ERdj2A-for	GGGGACAAGTTTGTACAAAAAAGCAGG CTTAATGGCGGCGTCAGAAGAG	rBiFC
43	P1P4-ERdj2A-nostop-rev	GGGGACAAC TTTGTATAGAAAAGTTGG GTGCTCTTCTCCGATCCCGACTC	rBiFC
44	P1P4-DGL1-for	GGGGACAAGTTTGTACAAAAAAGCAGG CTTAATG GTGAACCTCTCGAG	rBiFC
45	P1P4-DGL1-nostop-rev	GGGGACAAC TTTGTATAGAAAAGTTGG GTGCTTATGGTAGAGGTAGACG	rBiFC
46	P1P4-GET1-for	GGGGACAAGTTTGTACAAAAAAGCAGG CTTAATGGAAGGAGAGAAGCTTATAG	rBiFC
47	P1P4-GET1-nostop-rev	GGGGACAAC TTTGTATAGAAAAGTTGG GTGGAAC TCCACGAACCTACACAC	rBiFC

No.	Oligonucleotide	5'- 3' sequence	Purpose
48	P1P4-GET3a-for	GGGGACAAGTTTGTACAAAAAAGCAGG CTTAATGGCGGCGGATTTG	rBiFC
49	P1P4-GET3a-nostop-rev	GGGGACAAC TTTGTATAGAAAAGTTGG GTGGCCACTCTTGACCCGTTT	rBiFC
50	P1P4-GET4-for	GGGGACAAGTTTGTACAAAAAAGCAGG CTTAATGTTCGAGAGAGAGGATC	rBiFC
51	P1P4-GET4-nostop-rev	GGGGACAAC TTTGTATAGAAAAGTTGG GTGGCCCATCATCTTGAAGATGTC	rBiFC
52	P1P4-Sec61 $\alpha$ 1-for	GGGGACAAGTTTGTACAAAAAAGCAGG CTTAATGGGAGGAGGATTTAGAG	rBiFC
53	P1P4-Sec61 $\alpha$ 1-stop-rev	GGGGACAAC TTTGTATAGAAAAGTTGG GT TTAGAACCCGAAGAAGCCG	rBiFC
54	P1P4-Sec61 $\beta$ 1-for	GGGGACAAGTTTGTACAAAAAAGCAGG C TTAATGGTGGGAAGTGGAG	rBiFC
55	P1P4-Sec61 $\beta$ 1-stop-rev	GGGGACAAC TTTGTATAGAAAAGTTGG GT TCATTTGACAAAGTAGAGCTTG	rBiFC
56	P1P4-Sec61 $\gamma$ 1-for	GGGGACAAGTTTGTACAAAAAAGCAGG C TTAATGGACGCCATTGATTCCGTC	rBiFC
57	P1P4-Sec61 $\gamma$ 1-stop-rev	GGGGACAAC TTTGTATAGAAAAGTTGG GT CTAAGTGGCACCGACGATGATG	rBiFC
58	P1P4-SHD-for	GGGGACAAGTTTGTACAAAAAAGCAGG CTTAATGAGGAAGAGGACGCTC	rBiFC
59	P1P4-SHD-nostop-rev	GGGGACAAC TTTGTATAGAAAAGTTGG GTGCAGTTCGTCCTTGGTGTTT	rBiFC
60	P1P4-SYP123-for	GGGGACAAGTTTGTACAAAAAAGCAGG C TTAATGAACGATCTTATCTCAAG	rBiFC
61	P1P4-SYP123-stop-rev	GGGGACAAC TTTGTATAAAAAGTTGGGT TCAAGTTCGAAGTAGAGTG	rBiFC
62	P1P4-SYP43-for	GGGGACAAGTTTGTACAAAAAAGCA GGC TTAATGGCGACTAGGAATCGTAC	rBiFC
63	P1P4-SYP43-stop-rev	GGGGACAAC TTTGTATAGAAAAGTTGG GT TCACAACAGAATCTCCTTG	rBiFC
64	P1P4-TGG1-for	GGGGACAAGTTTGTACAAAAAAGCAGG C TTAATGAAGCTTCTTATGCTCGC	rBiFC
65	P1P4-TGG1-nostop-rev	GGGGACAAC TTTGTATAGAAAAGTTGG GTGTGCATCTGCAAGACTCTTCC	rBiFC
66	P1P4-TPR7-for	GGGGACAAGTTTGTACAAAAAAGCAGG CTTAATGTTTAACGGGTTAATGGATC	rBiFC
67	P1P4-TPR7-stop-rev	GGGGACAAC TTTGTATAGAAAAGTTGG GT CTAGTTTCCAATATAGCCGAG	rBiFC
68	P1P4-VHA-A-for	GGGGACAAGTTTGTACAAAAAAGCAGG CTTAATGCCGGCGTTTTACGG	rBiFC
69	P1P4-VHA-A-stop-rev	GGGACAAC TTTGTATAGAAAAGTTGGGT TTACCGAGTTTCATCTTCCAAG	rBiFC
70	P35S-BiFC-for	GACGCACAATCCCACTATCC	Sequencing

No.	Oligonucleotide	5'- 3' sequence	Purpose
71	P3P2-Sec62-for	GGGGACAACCTTTGTATAATAAAGTTGGA ATGAAGAAGCCGGTCG	rBiFC
72	P3P2-Sec62-nostop-rev	GGGGACCACTTTGTACAAGAAAGCTGG GTGTGTTTTAAGATCAGAGTCAG	rBiFC
73	P3P2-Sec62-stop-rev	GGGGACCACTTTGTACAAGAAAGCTGG GTTTATGTTTTAAGATCAGAGTCAG	rBiFC
74	PBP1-Sac1-for	GAGCTCATGGCCAAAAGGTGGAAGC	pSP65
75	PBP1-Sal1-rev	GTCGACTCAGTTGGATAAAGGACGAAC	pSP65
76	pDONR207-for	TCGCGTTAACGCTAGCATGGATCT	Sequencing
77	pDONR207-rev	GTAACATCAGAGATTTTGAGACAC	Sequencing
78	pDONR221-for	CTTAAGCTCGGGCCCCAAATAATG	Sequencing
79	pDONR221-rev	CCTGCAGCTGGATGGCAAATAATG	Sequencing
80	PHB3-EcoRI-for	GAATTCATGGGAAGCCAACAAGCGGC	pSP65
81	PHB3-Sall-rev	GTCGACTCAACGGTTCAGGGCAAAGAG	pSP65
82	pSP65-for	CACATACGATTTAGGTGACAC	Sequencing
83	pSP65-rev	CAGCTATGACCATGATTACGC	Sequencing
84	ScSec62-attB-ATG-for	GGGGACAAGTTTGTACAAAAAAGCAGG CTATGTCAGCCGTAGGTCCAGG	pAG425GPD -ccdB
85	ScSec62 attB-stop-rev	GGGGACCACTTTGTACAAGAAGCTGGG TCTCAGTTTTGTTCCGGCTTTTTTC	pAG425GPD -ccdB
86	Sec62-ATG-attB-for	GGGGACAAGTTTGTACAAAAAAGCAGG CTTCATGAAG	pAG425GPD -ccdB
87	Sec62-attB-for	ACAAGTTTGTACAAAAAAGCAGGCTTAA GAGCTTCCATGGCAACT	pBGW
88	Sec62-attB-rev	ACCACTTTGTACAAGAAAGCTGGGTTTA TGTTTTAAGATCAGAGT	pBGW
89	Sec62-stop-attB-rev	GGGGACCACTTTGTACAAGAAAGCTGG GTCTTATGTT	RT-PCR/ pAG425GPD -ccdB
90	Sec62-muta-for	GACCCAGCTTTCTTGTAC	Mutagenesis
91	Sec62-muta-rev	TGTTTTAAGATCAGAGTCAG	Mutagenesis
92	Sec62N-attB-for	GGGGACAAGTTTGTACAAAAAAGCAGG CTTCATGAAGAAGCCGGTCGGAGC	pK7FWG2/ pB7YWG2
93	Sec62N-nostop-attB-rev	GGGGACCACTTTGTACAAGAAAGCTGG GTCTAGCGGATGCCGTTTTTTCGA	pK7FWG2/ pB7YWG2
94	Sec62-ΔTMD3/C-attB-for	GGGGACAAGTTTGTACAAAAAAGCAGG CTTCATGAAGAAGCCGGTCGG	Split-GFP
95	Sec62-ΔTMD3/C-His-attB-rev	GGGGACCACTTTGTACAAGAAAGCTGG GTCGTGGTGGTGGTGGTGGTGGTCTTT C TTTGGCCAGAAAC	Split-GFP
96	Sec62-ΔTMD3/C-nostop-rev	CGATCTCGAGGTCTTTCTTTGGCCAGAA AC	RT-PCR
97	T7-Prom-for	TAATACGACTCACTATAGG	Sequencing
98	T7-Term-rev	GCTAGTTATTGCTCAGCGG	Sequencing

### 2.1.10. Antisera and antibodies

Primary  $\alpha$ AtSec62 antiserum (1:500 dilution used in 5% (w/v) milk, 40 mM Tris/HCl (pH 7.5), 270 mM NaCl, 0.05% (v/v) Tween 20) was generated in rabbits by BioGenes (Berlin, Germany). It was raised against the recombinant AtSec62 N-terminus (amino acids 1-160) fused to a C-terminal His-tag, overexpressed and purified by Thomas Brylok (compare to Figure A1a). Primary anti-GFP antibody (1:1,000 dilution) was purchased from Roche (Penzberg, Germany), while secondary anti-rabbit (1:20,000 dilution) as well as anti-mouse (1:6,000 dilution) antibodies coupled to horseradish peroxidase were purchased from Sigma-Aldrich (Taufkirchen, Germany).

### 2.1.11. Statistical analysis

Statistical analysis was accomplished using Statistic R (R Core Team (2019), R version 3.6.1, <http://www.R-project.org/>, including the 'multcompview' package) or Microsoft Excel 2013.

To assess deviations of the observed segregation pattern from the expected Mendelian ratios, chi-squared analysis was performed, while root and seed yield analyses were done using Student's *t*-test (two-sided, equal variance). Pull-down experiments were evaluated by performing one-way ANOVA with subsequent Tukey's post hoc comparison. The significance threshold was set at  $p \leq 0.05$ .

### 2.1.12. Computational analysis and software

Boxplots were generated by using the BoxPlotR software (Spitzer *et al.* 2014, <http://shiny.chemgrid.org/boxplotr/>). Phylogenetic trees were generated with MEGA-X (Kumar *et al.* 2018, version 10.0.5), using the Maximum Likelihood method, having 500 bootstrap replications and applying the Jones-Taylor-Thornton substitution model (Jones *et al.* 1992) and Nearest-Neighbour-Interchange.

NCBI Conserved Domain Search was used to identify the conserved Sec62 domain (compare to <https://www.ncbi.nlm.nih.gov/Structure/cdd/wrpsb.cgi>). Transmembrane domains of Sec62 homologues were defined based on predictions by TMHMM2.0 (<http://www.cbs.dtu.dk/services/TMHMM/>), Phobius (<http://phobius.sbc.su.se/>), DAS-TMfilter (<http://www.enzim.hu/DAS/DAS.html>) and TMpred ([https://embnet.vital-it.ch/software/TMPRED\\_form.html](https://embnet.vital-it.ch/software/TMPRED_form.html)).

Amino acid sequence alignments were generated using CLC Main Workbench (version 7.7) and modified using GeneDoc (version 2.7). General sequence analyses were done using BioEdit (version 7.2.6.1) and UGENE (version 1.29.0). Promoter regions

were narrowed down using PlantPAN2.0 (<http://plantpan2.itps.ncku.edu.tw/>). NEB tools (<https://international.neb.com/tools-and-resources/interactive-tools>) were used for classical cloning, designing site-directed mutagenesis oligonucleotides and for calculating annealing temperatures. Potential restriction sites within coding regions were identified using RestrictionMapper (<http://www.restrictionmapper.org/>).

Microscope images were taken and analysed using Leica Application Suite (version 4.1.0), Leica Application Suite X (version 3.3.0) or Leica Application Suite Advanced Fluorescence (version 2.6.3.8173) for fluorescent images. ImageQuant LAS 4000 (version 3.1) was used to detect chemiluminescent signals. Analysis of fluorescent images for line histograms and general image analyses were done using ImageJ (version 1.51j8)/Fiji (1.52i). Final figures were generated using Adobe Illustrator® CS3 (version 13.0.0) and GIMP (version 2.10.10).

## 2.2. Methods

### 2.2.1. Growth conditions

#### 2.2.1.1. Growth conditions for *Escherichia coli* and *Agrobacterium tumefaciens*

Bacterial strains were grown in LB medium (1% (w/v) peptone ex casein (tryptic digest), 0.5% (w/v) yeast extract, 1% (w/v) NaCl) and 160 rpm (Multitron and Minitron, INFORS HT). Solid media were supplemented with 1.5% (w/v) agar-agar. If not stated otherwise, *Escherichia coli* were grown at 37°C overnight, while *Agrobacterium tumefaciens* cells were grown at 28°C for two to three days. Final concentrations of required antibiotics are listed in Table 4.

**Table 4: Antibiotic agents used for bacterial work in this study.**

Antibiotic agent	Solvent	Stock concentration [mg ml <sup>-1</sup> ]	Final concentration [µg ml <sup>-1</sup> ]
Ampicillin	ddH <sub>2</sub> O	100	100
Carbenicillin	ddH <sub>2</sub> O	100	100
Chloramphenicol	100% EtOH	12.5	25
Gentamycin	ddH <sub>2</sub> O	10	20
Kanamycin	ddH <sub>2</sub> O	50	50
Rifampicin	DMSO	25	100
Spectinomycin	ddH <sub>2</sub> O	100	100

Bacterial glycerol stocks were prepared with 25% (v/v) glycerol and subsequent freezing of the sample in liquid nitrogen, prior to long term storage at -80°C. For short-

term storage, LB medium plates with respective bacterial strains were sealed with Parafilm® “M” Laboratory Film (Bemis) and stored at 4°C.

#### **2.2.1.2. Growth conditions for *Saccharomyces cerevisiae***

Yeast strains were either grown in YPD medium (1% (w/v) bacto yeast extract, 2% (w/v) bacto peptone, 2% (w/v) glucose) or in SCD medium (0.7% (w/v) yeast nitrogen base without amino acids, 2% (w/v) glucose, 0.2% (w/v) dropout mix without leucine). Solid media were supplemented with 2% (w/v) bacto agar. Yeast cells were grown at 30°C and 140 rpm (Minitron, INFORS HT) for liquid cultures, except for complementation analysis using 28°C as permissive and 37°C as restrictive temperature. Yeast glycerol stocks were prepared with 25% (v/v) glycerol and were directly stored at -80°C without freezing in liquid nitrogen.

#### **2.2.1.3. Growth conditions for *Arabidopsis thaliana* and *Nicotiana benthamiana***

*Arabidopsis thaliana* plants were grown on soil either under greenhouse conditions or in climate chambers (Phytotron, Imtech and Percival (models I-36LLVL, I-36L4VL and LT-36VL), CLF Plant Climatics) under long day conditions (16 h light/ 8 h dark, 22°C/18°C, 100  $\mu\text{mol photons m}^{-2} \text{sec}^{-1}$ ). Plants for high-temperature treatment were grown on half-strength MS medium plates (1% (w/v) sucrose, 0.238% (w/v) MS salts including vitamins, 0.05% (w/v) MES (pH 5.7), 0.6% (w/v) Gelrite®), supplemented with 10  $\mu\text{g ml}^{-1}$  sulfadiazine for segregation analysis. Plants for root length analysis were grown vertically on half-strength MS medium plates (0.238% (w/v) MS salts, 0.05% (w/v) MES (pH 5.7), 1.0% (w/v) Phytoagar). For ER stress treatment, the medium was supplemented with DTT (1.5 mM, 2 mM) or Tunicamycin (0.025  $\mu\text{g ml}^{-1}$ , 0.05  $\mu\text{g ml}^{-1}$ ). Seeds were surface sterilised using 0.05% (v/v) Triton X-100 in 70% (v/v) ethanol for 10 min, prior to three times washing in 100% (v/v) ethanol and subsequent drying on sterile filter paper. Seeds were stratified at 4°C for two to three days in the dark, before being transferred to climate chambers featuring long day conditions. For conducting a high-temperature stress treatment according to Yang *et al.* (2009), seeds on half-strength MS medium plates were germinated at 37°C for 48 h and then transferred to 22°C, whereas control seeds were germinated and grown at 22°C.

Kanamycin selection was performed according to Harrison *et al.* (2006). For this purpose, plants were grown on half-strength MS medium plates (0.238% (w/v) MS salts, 0.05% (w/v) MES (pH 5.7), 1.0% (w/v) Phytoagar), supplemented with 50  $\mu\text{g ml}^{-1}$  Kanamycin. Seeds were stratified for two days at 4°C in the dark, then exposed to light

for four to six hours at 22°C, prior to incubation for two days in the dark. Upon subsequent light exposition, resistant plants with green and expanded cotyledons were transferred to soil. For BASTA® selection, plants were grown either on half-strength MS medium plates containing 50 µg ml<sup>-1</sup> BASTA® or on soil with seedlings being sprayed after two as well as three weeks growth.

*Nicotiana benthamiana* was grown in soil under greenhouse conditions for four to six weeks.

### 2.2.2. Pollen staining and germination assay

Alexander staining solution for differential staining of viable and non-viable pollen was prepared according to Alexander (1969) by adding 10 ml 96% (v/v) ethanol, 1 ml of 1% (w/v) malachite green solution in 96% (v/v) ethanol, 50 ml ddH<sub>2</sub>O, 25 ml glycerol, 5 g phenol, 5 g chloral hydrate, 5 ml of 1% (w/v) acid fuchsin solution in ddH<sub>2</sub>O, 0.5 ml of 1% (w/v) Orange G solution in ddH<sub>2</sub>O and 4 ml glacial acetic acid to a light protected bottle. Anthers of opening buds or open flowers were placed on a microscope slide with 40 µl Alexander staining solution. Samples were covered and sealed airtight, then incubated at room temperature for at least 90 min. For *in vitro* pollen germination assays, pollen grains from eight-week-old plants were spread onto solidified germination medium (1 mM MgCl<sub>2</sub>, 0.16 mM H<sub>3</sub>BO<sub>3</sub>, 1 mM CaCl<sub>2</sub>, 1 mM Ca(NO<sub>3</sub>)<sub>2</sub>, 18% (w/v) sucrose, 0.65% (w/v) Phytoagar). Prepared microscope slides were transferred onto watered filter papers in Petri dishes to provide high humidity and samples were incubated at 25°C and 37°C in the dark for 22 h. Pollen staining and pollen tube germination were documented using a binocular microscope (DM1000 with DFC320 or DFC7000 T digital cameras, Leica).

### 2.2.3. Microsomal membrane preparation from *Arabidopsis thaliana* leaves

Microsomal membrane preparation was carried out at 4°C on ice. Plant material from four-week-old *Arabidopsis* plants was frozen in liquid nitrogen and pestled in isolation medium (50 mM Tris/HCl (pH 7.5), 2 mM MgCl<sub>2</sub>, 100 mM KCl and 0.5 M sucrose). Homogenised samples were filtered through gauze and were centrifuged once at 4,200 **g** for 10 min, at 10,000 **g** for 10 min and at 22,000 **g** for 30 min to remove chloroplasts and mitochondria. The remaining supernatant was centrifuged at 100,000 **g** for 1 h to pellet microsomal membranes. For further purification, the resulting pellet was resuspended in 2 ml wash buffer (50 mM Tris/HCl (pH 7.5), 2 mM MgCl<sub>2</sub>, 100 mM KCl and 12% (w/v) sucrose) and loaded onto a step gradient (5 ml of 50%, 5 ml of 30%

and 3 ml of 20% (w/v) sucrose in wash buffer), prior to centrifugation at 100,000 **g** for 1 h. The fraction between 50% and 30% (w/v) sucrose was washed once at 100,000 **g** for 1 h and the remaining pellet was then resuspended in 25 mM Tris/HCl (pH 7.5), 0.33 M sucrose and 0.5 mM DTT and stored at -80°C.

Microsomal membranes for GFP-Trap<sup>®</sup> pull-down experiments (compare to 2.2.27.) were alternatively isolated from four-week-old plants homogenised in 50 mM Tris/HCl (pH 7.5), 0.5 M sucrose and 1 mM EDTA and filtered through gauze. Samples were centrifuged once at 4,200 **g** for 10 min, at 10,000 **g** for 10 min and 100,000 **g** for 1 h.

#### **2.2.4. Isolation of soluble and membrane proteins from leaves**

*Arabidopsis* leaves were ground in 300 µl homogenisation medium (10 mM EDTA, 2 mM EGTA, 50 mM Tris/HCl (pH 8.0), 10 mM DTT) using an electric micro-pestle, prior to adding additional 300 µl homogenisation medium. Alternatively, several *Arabidopsis* leaves or one tobacco leaf were pestled three times in liquid nitrogen and transferred to 2-5 ml homogenisation medium. Homogenised plant material was incubated on ice for 10 min, filtered through gauze and then centrifuged for 10 min at 9,300 **g** and 4°C. The resulting supernatant contained soluble proteins, while membrane proteins were present in the remaining pellet, which was resuspended in appropriate amounts of homogenisation medium. Samples were stored at -80°C.

#### **2.2.5. Determination of protein concentration by Bradford**

1 µl sample was added to 799 µl ddH<sub>2</sub>O, prior to applying 200 µl Bradford solution (0.1 mM coomassie brilliant blue G-250, 5% (v/v) ethanol, 10% (v/v) H<sub>3</sub>PO<sub>4</sub>) and incubating the mixture for 5 min in the dark. The absorbance at 595 nm was then measured against the reference and the protein concentration was calculated based on a BSA calibration curve.

#### **2.2.6. SDS-Polyacrylamide gel electrophoresis and immunoblotting**

Proteins were separated by SDS-PAGE and either transferred onto PVDF membranes (Millipore) for subsequent immunodetection or stained using coomassie staining solution.

##### **2.2.6.1. SDS-Polyacrylamide gel electrophoresis**

Protein separation by discontinuous SDS-PAGE was conducted based on Laemmli (1970) using a 5% stacking gel (125 mM Tris/HCl (pH 6.8), 0.1% (w/v) SDS, 5% (w/v) acrylamide, 0.1% (w/v) APS, 1% (v/v) TEMED) and a 10 – 15% separating gel

(390 mM Tris/HCL (pH 8.8), 0.1% (w/v) SDS, 10 – 15% (w/v) acrylamide, 0.1% (w/v) APS, 1% (v/v) TEMED). Samples were incubated in SDS loading buffer (62.5 mM Tris/HCl (pH 6.8), 2% (w/v) SDS, 10% (v/v) glycerol, 5% (v/v)  $\beta$ -mercaptoethanol, 0.004% (w/v) bromphenol blue) for 5 min at 95°C, then loaded onto SDS-PAGE gels, which were run in SDS running buffer (25 mM Tris/HCl (pH 8.2 – 8.4), 192 mM glycine, 0.1% (w/v) SDS).

#### **2.2.6.2. Coomassie staining**

SDS-PAGE Gels were stained with coomassie staining solution (45% (v/v) methanol, 9% (v/v) acetic acid, 0.2% (w/v) coomassie brilliant blue R-250), destained (45% (v/v) methanol, 9% (v/v) acetic acid) and dried for storage or further analysis.

#### **2.2.6.3. Semi-dry electro blot**

Proteins were transferred from SDS-PAGE gels onto PVDF membranes by semi-dry electro blotting with components assembled on the anode as follows: one blotting paper soaked in anode buffer I (0.3 M Tris/HCl (pH 10.4), 20% (v/v) methanol), two blotting paper soaked in anode buffer II (25 mM Tris/HCl (pH 10.4), 20% (v/v) methanol), PVDF membrane (activated in 100% (v/v) methanol and washed in anode buffer II), SDS-PAGE gel rinsed in cathode buffer (25 mM Tris/HCl (pH 9.4), 40 mM 6-aminohexanoic acid, 20% (v/v) methanol) and three blotting paper soaked in cathode buffer. Alternatively, blotting papers were soaked and PVDF membrane was washed in Towbin buffer (25 mM Tris/HCl (pH 8.2 – 8.4), 192 mM glycine, 0.1% (w/v) SDS, 20% (v/v) methanol). Transfer was performed for 1 h and  $0.8 \text{ mA cm}^{-2}$ , then proteins on PVDF membrane were visualised with Ponceau staining solution (5% (v/v) acetic acid, 0.3% (w/v) Ponceau S).

#### **2.2.6.4. Immunodetection**

PVDF membranes were blocked in 5% (w/v) milk in TBS-T (20 mM Tris/HCl (pH 7.5), 135 mM NaCl, 0.05% (v/v) Tween 20) for 30 min, then membranes were washed twice in TBS-T for 10 min. Incubation with the primary antibody (compare to 2.1.10.) was conducted for 2 h at room temperature before washing the membrane three times in TBS-T for 10 min and subsequently incubating the membrane with the secondary antibody (compare to 2.1.10.) for 2 h. Alternatively, incubation with the primary or secondary antibody was performed overnight at 4°C. After three times washing in TBS-T for 10 min, equal volumes of ECL (enhanced chemiluminescence) detection solution I (0.1 M Tris/HCl (pH 6.8), 1% (w/v) luminol, 0.44% (w/v) coumaric acid) and II (0.1 M

Tris/HCl (pH 6.8), 0.018% (v/v)  $\text{H}_2\text{O}_2$ ) were applied onto the membrane. The chemiluminescent signal was detected using ImageQuant LAS 500/ 4000 (GE Healthcare).

### **2.2.7. Amplification of DNA fragments by Polymerase chain reaction**

Plasmid DNA, genomic DNA and cDNA were used as templates for DNA amplification. DFS-Taq DNA polymerase was used for general PCR reactions according to manufacturer's instructions, whereas PCR for generation of DNA fragments used for subsequent cloning was performed using Phusion<sup>®</sup> High Fidelity DNA Polymerase based on manufacturer's instructions (New England Biolabs). Annealing temperature and elongation time were adjusted depending on used oligonucleotides and fragment length. Samples were run on 1% (w/v) agarose gels containing ethidium bromide in TAE buffer (40 mM Tris/HCl (pH 8.0 – 8.5), 2.6 mM EDTA, 0.1% (v/v) acetic acid). Respective DNA fragments were excised under UV light and purified using the NucleoSpin<sup>®</sup> Gel and PCR Clean-up Kit (Macherey-Nagel) according to manufacturer's instructions. Purified DNA was either frozen at  $-20^\circ\text{C}$  or directly used for subsequent cloning (compare to 2.2.14.).

### **2.2.8. Isolation of genomic DNA from *Saccharomyces cerevisiae***

Yeast genomic DNA was isolated according to Lööke *et al.* (2011). For this purpose, one yeast colony was suspended in 100  $\mu\text{l}$  extraction buffer (200 mM LiOAc, 1% (w/v) SDS) and incubated for 5 min at  $70^\circ\text{C}$ . 70% (v/v) ethanol was added for DNA precipitation and the samples were centrifuged for 3 min at 15,000 **g** to spin down DNA. The pellet was washed in 500  $\mu\text{l}$  70% (v/v) ethanol and then centrifuged for 1 min at 15,000 **g**. The remaining pellet was dried at room temperature, before being dissolved in 50  $\mu\text{l}$  ddH<sub>2</sub>O. The sample was centrifuged for 15 sec at 15,000 **g** with the resulting supernatant being used for PCR.

### **2.2.9. Isolation of genomic DNA from *Arabidopsis thaliana* leaves**

Single leaves of three- to four-week-old *Arabidopsis* plants were homogenised in 500  $\mu\text{l}$  extraction buffer (1 M Tris/HCl (pH 7.5), 0.05 M NaCl, 0.05 M EDTA (pH 8.0), 1% (w/v) PVP-40) using the TissueLyser (Qiagen). 66  $\mu\text{l}$  of 10% (w/v) SDS solution and 166  $\mu\text{l}$  5 M KOAc solution (3 M potassium acetate, 11.5% (v/v) glacial acetic acid (pH 5.8)) were added and samples were mixed by inverting several times. Samples were then centrifuged for 15 min at 16,100 – 21,000 **g** and the supernatant was transferred to a new tube, prior to the addition of 0.7 volumes of isopropanol,

subsequent mixing by inverting and incubation at -20°C for at least 30 min. Following centrifugation for 15 min at 16,100 – 21,000 **g**, the pellet was washed in 500 µl 70% (v/v) ethanol and centrifuged for 5 min at 16,100 – 21,000 **g**. The remaining pellet was dried for 10 min at 50°C and dissolved in 30 µl ddH<sub>2</sub>O. Isolated genomic DNA (gDNA) was stored at -20°C.

#### **2.2.10. Genotyping using *Arabidopsis thaliana* genomic DNA**

Genotyping was conducted twice for each sample using DFS-Taq DNA polymerase, 2 µl of gDNA template and specific oligonucleotides (compare to Table 3).

#### **2.2.11. RNA extraction from *Arabidopsis thaliana* leaves**

RNA was isolated from leaves of four- to five-week-old *Arabidopsis* plants using the RNeasy® Plant Mini Kit (Qiagen) according to manufacturer's instructions but performing the DNase I digest for 30 min at room temperature and resuspending the final pellet in 30 µl RNase free H<sub>2</sub>O. RNA concentration was measured and RNA quality was investigated by loading samples onto 1% (w/v) agarose gels. RNA was stored at -80°C.

#### **2.2.12. RNA extraction from *Saccharomyces cerevisiae***

RNA from 10 ml overnight cultures was extracted using the RNeasy® Mini Kit (Qiagen) according to manufacturer's instructions, however 2 mg ml<sup>-1</sup> zymolase were used for spheroplast generation. Further steps were performed as described in section 2.2.11.

#### **2.2.13. cDNA synthesis and RT-PCR analysis**

cDNA was synthesised from 0.5 µg RNA using the M-MLV Reverse transcriptase (Promega) according to manufacturer's instructions and was stored at -20°C. Subsequent reverse transcription PCR (RT-PCR) was conducted using respective oligonucleotides (compare to Table 3).

#### **2.2.14. Cloning strategies**

Constructs were generated by traditional cloning, Zero Blunt® Cloning, Gateway® Cloning or by site-directed mutagenesis and transformed into competent *Escherichia coli* Top10 cells (compare to 2.1.5.). To confirm the presence of respective inserts, colony PCR using DFS Taq-DNA polymerase was performed by directly adding individual colonies to the PCR reaction mix. Proper insertion was verified by sequencing (compare to 2.2.17.).

#### **2.2.14.1. Traditional cloning by restriction enzyme digest and ligation**

Double digest of vectors and DNA fragments was performed for 1 h at 37°C using appropriate restriction endonucleases (compare to Table 2) based on manufacturer's instructions (New England Biolabs). Digested samples were loaded onto 1% (w/v) agarose gels and subsequently purified using the NucleoSpin® Gel and PCR Clean-up Kit (Macherey-Nagel) according to manufacturer's instructions. Ligation with T4 DNA Ligase was conducted for 3 h at room temperature based on manufacturer's instructions (New England Biolabs) using 50 ng vector DNA and a vector to insert ratio of at least 1:3.

#### **2.2.14.2. Zero Blunt® Cloning**

Zero Blunt® Cloning was done using the Zero Blunt® PCR Cloning Kit (Invitrogen) according to manufacturer's instructions. Ligation was carried out for 3 h at room temperature using T4 DNA Ligase as described in section 2.2.14.1. but only using 25 ng vector DNA.

#### **2.2.14.3. Gateway® Technology based cloning**

Based on manufacturer's instructions (Invitrogen), DNA fragments possessing respective *attB*-flanking sequences were cloned into the entry vectors pDONR207, pDONR221-P1P4 or pDONR221-P3P2, prior to transfer into binary destination vectors (pGFP11-GW, pGW-GFP11, pBiFCt-2in1-NN, pBiFCt-2in1-NC, pBiFCt-2in1-CN, pBiFCt-2in1-CC, pAG425GPD-*ccdB*, pBGW, pB7CWG2, pB7FWG2, pB7YWG2, pK7FWG2, pK7WGF2).

#### **2.2.14.4. Site-directed mutagenesis**

Site-directed mutagenesis was performed using the Q5® Site-Directed Mutagenesis Kit (New England Biolabs) according to manufacturer's instructions.

#### **2.2.15. Transformation of *Escherichia coli***

Chemically competent *Escherichia coli* cells were prepared based on Hanahan (1983), all centrifugation steps were performed at 4°C. 500 ml LB medium were inoculated with an overnight preculture and grown to an OD<sub>600</sub> of 0.4. Cells were incubated for 15 min in ice water, prior to centrifugation for 5 min at 4,400 **g**. Pelleted cells were resuspended in 250 ml of 100 mM MgCl<sub>2</sub>, then centrifuged for 10 min at 2,800 **g**. *Escherichia coli* cells were solved in 500 ml of 100 mM CaCl<sub>2</sub>, incubated for 10 min on ice and pelleted at 2,800 **g** for 10 min. The pellet was resuspended in 5 ml 85 mM

CaCl<sub>2</sub> and 15% (v/v) glycerol and 50 µl aliquots of chemically competent cells were frozen in liquid nitrogen and stored at -80°C.

For transformation, plasmid DNA was added to competent *Escherichia coli* cells and the suspension was incubated for 30 min on ice. Subsequent heat shock was performed at 42°C for 45 sec, then cells were transferred back to ice before adding 250 µl LB medium. Cells were grown for 1 h at 37°C and 750 rpm (ThermoMixer®, eppendorf). Cells were pelleted at 1,500 g for 4 min, resuspended in 50 µl LB medium and plated on LB medium plates containing appropriate antibiotics.

For blue-white selection, 40 µl of 0.1 M (w/v) IPTG and 40 µl of 40 mg ml<sup>-1</sup> X-Gal (dissolved in DMSO) were spread on selective LB medium plates before plating bacterial suspensions.

#### **2.2.16. Purification of plasmid DNA from *Escherichia coli***

Plasmid DNA was isolated from 3 ml or 50 – 100 ml overnight culture using the NucleoSpin® Plasmid EasyPure Kit or the NucleoBond® Xtra Midi/ PC 100 Kit (Macherey-Nagel) according to manufacturer's instructions. Plasmid concentrations were determined using a Nanophotometer (IMPLEN) and isolated plasmid DNA was stored at -20°C.

#### **2.2.17. Sequencing**

Sequencing of used plasmids and generated constructs was performed by the Sequencing Service of the Genomics Service Unit of the Ludwig-Maximilians-University Munich (<http://www.gi.bio.lmu.de/sequencing/help/index.html>). Required amounts of samples (compare to <http://www.gi.bio.lmu.de/sequencing/help/protocol>, sequencing service: *Cycle, Clean & Run* with *BigDye v3.1* sequencing chemistry) were submitted in 10 mM Tris/HCl (pH 8.5) with appropriate oligonucleotides (compare to Table 3).

#### **2.2.18. Overexpression of recombinant proteins in *Escherichia coli***

Prior to growing large scale cultures, transformed *Escherichia coli* cells were tested according to the manufacturer's BL21-CodonPlus Competent Cells instruction manual (<https://www.agilent.com/cs/library/usermanuals/public/230240.pdf>).

After successful testing, *Escherichia coli* precultures were grown overnight and used for inoculating 1 L selective LB medium. Overexpression was induced at an OD<sub>600</sub> of 0.4 – 0.6 by 1 mM (w/v) IPTG and cultures were grown overnight at 18°C. Cells were

then pelleted for 15 min at 3,300 **g** and 4°C and used for subsequent protein purification.

### **2.2.19. Purification of His-/ Strep-tagged proteins**

For purifying His-tagged proteins, pelleted cells were resuspended in 30 ml lysis buffer (20 mM Tris/HCl (pH 7.5), 200 mM NaCl, 20 mM imidazol) and broken using a microfluidizer (Microfluidics). The suspension was centrifuged for 30 min at 20,000 **g** and 4°C and the supernatant was rotated 2 h at room temperature or overnight at 4°C with 100 µl Ni-NTA-Agarose beads per 10 ml supernatant. The sample was transferred onto an equilibrated column, washed three times with 5 ml His-tag wash buffer (20 mM Tris/HCl (pH 7.5), 200 mM NaCl, 40 mM imidazol) and proteins were eluted four times with 300 µl His-tag elution buffer (20 mM Tris/HCl (pH 7.5), 200 mM NaCl, 200 mM imidazol) after 5 min incubation each. Samples were stored at -80°C.

Strep-tagged proteins were purified exactly as His-tagged proteins, but pelleted cells were resuspended in Strep-tag wash buffer (100 mM Tris/HCl (pH 8.0), 150 mM NaCl), 100 µl Strep-Tactin® Sepharose® per 10 ml supernatant were used for overnight incubation, subsequent washing was performed with 5 ml Strep-tag wash buffer and proteins were eluted five times with 300 µl Strep-tag elution buffer (100 mM Tris/HCl (pH 8.0), 150 mM NaCl, 1 mM EDTA, 2.5 mM desthiobiotin).

### **2.2.20. *In vitro* transcription and translation using <sup>35</sup>S-methionine**

Linearisation of respective plasmids was conducted for 1 h at 37°C using 50 µg plasmid DNA and NheI-HF restriction endonuclease based on manufacturer's instructions (New England Biolabs). DNA was purified using the NucleoSpin® Gel and PCR Clean-up Kit (Macherey-Nagel) according to manufacturer's instructions.

*In vitro* transcription was performed based on manufacturer's instructions (New England Biolabs), using 0.5 µg linearised template and 40 units SP6 RNA Polymerase. Following incubation for 2 h at 40°C, RNA integrity was analysed on 1% (w/v) agarose gels and RNA was stored at -80°C.

*In vitro* translation in Wheat Germ Extract using <sup>35</sup>S-methionine was conducted according to manufacturer's instructions (Promega) with 5 µl RNA template but without potassium acetate. The mixture was incubated at 25°C for 110 min.

Alternatively, *in vitro* transcription and translation were performed simultaneously using the T<sub>N</sub>T® Coupled Reticulocyte Lysate System (Promega) according to manufacturer's

instructions, however Wheat Germ Extract was used instead of Reticulocyte Lysate and magnesium acetate was added in appropriate amounts if necessary.

#### **2.2.21. *In vitro* pull-down assay**

For pull-down experiments, 20 µg of recombinant protein (compare to 2.2.19.) and 15 µl translation product (compare to 2.2.20.) were incubated in 300 µl PBS (140 mM NaCl, 2.7 mM KCl, 10 mM Na<sub>2</sub>HPO<sub>4</sub>, 1.8 mM KH<sub>2</sub>PO<sub>4</sub>, pH 7.3), rolling for 1 h at room temperature. 20 – 30 µl Ni-NTA-Agarose beads or Strep-Tactin<sup>®</sup> Sepharose<sup>®</sup> were added and incubated for 1 h, prior to loading onto an equilibrated column (Micro Bio-Spin<sup>®</sup>, Bio-Rad). Washing was repeated three times using 500 µl PBS, containing 50 mM imidazole for His-tagged proteins, and subsequent centrifugation at 1,000 **g** for 1 min. Elution was conducted after 5 min incubation with 20 µl PBS, containing either 300 mM imidazole or 2.5 mM desthiobiotin, and centrifugation at 15,000 **g** for 1 min. Proteins were directly loaded onto SDS-PAGE gels without incubation at 95°C (compare to 2.2.6.1.).

#### **2.2.22. Detection of radiolabelled proteins**

Radiolabelled proteins were visualised by overnight exposure of dried, Coomassie stained SDS-PAGE gels (compare to 2.2.6.2.) on BAS-MS imaging plates (Fujifilm) and detection by a Typhoon Trio Variable Mode Imager (Amersham Biosciences).

For quantification of pull-down experiments, the signal intensity was measured and adjusted based on the actual amount of His-/ Strep-tagged protein in the respective lane on the Coomassie stained SDS-PAGE gel. The ratio of the elution to the mean signal intensity of the respective translation product was then calculated and plotted.

#### **2.2.23. Transformation and complementation analysis in *Saccharomyces cerevisiae***

Preparation of competent yeast cells as well as subsequent transformation was based on Staudinger *et al.* (1995). 50 ml YPD medium were inoculated with overnight pre-culture and harvested at OD<sub>600</sub> 0.5 – 0.6 by centrifugation for 5 min at 700 **g** and 4°C. Pelleted yeast cells were washed once with 50 ml sterile ddH<sub>2</sub>O and centrifuged for 5 min at 700 **g** and 4°C, followed by washing with 12.5 ml sterile filtered LiSorb (100 mM LiOAc, 10 mM Tris/HCl (pH 8), 1 mM EDTA (pH 8.0), 1 M sorbitol). Cells were resuspended in 300 µl LiSorb before adding 42 µl carrier-DNA (2 mg ml<sup>-1</sup> denatured and syringe sheared herring sperm DNA). Competent yeast cells were either stored at -80°C or directly used for transformation. For this purpose, 5 µl plasmid

DNA and 300  $\mu$ l sterile filtered LiPEG (100 mM LiOAc, 10 mM Tris/HCl (pH 8.0), 1 mM EDTA (pH 8.0), 40% (w/v) PEG 3350) were added to 50  $\mu$ l competent cells. The mixture was incubated for 20 min at room temperature, prior to adding 35  $\mu$ l DMSO and performing 15 min heat shock at 42°C. After pelleting at 700 **g** for 90 sec, yeast cells were resuspended in 100  $\mu$ l 0.9% (w/v) sterile filtered NaCl and spread on several SCD medium plates.

For complementation analysis, transformed yeast cells were grown in SCD medium and OD<sub>600</sub> was adjusted to 1.0, then 7.5  $\mu$ l of serial dilutions ( $10^0$ ,  $10^{-1}$ ,  $10^{-2}$ ,  $10^{-3}$  and  $10^{-4}$  in SCD medium) were spotted onto SCD medium plates and yeast cells were grown at 28°C and 37°C for 48 h.

#### **2.2.24. Transformation of *Agrobacterium tumefaciens***

For preparation of chemically competent cells, 500 ml LB medium were inoculated with an *Agrobacterium tumefaciens* preculture and grown to an OD<sub>600</sub> of 1.0. Cells were pelleted at 3,000 **g** for 15 min, resuspended in 10 ml ice-cold 10 mM CaCl<sub>2</sub> and 100  $\mu$ l aliquots were frozen in liquid nitrogen and stored at -80°C.

Chemically competent *Agrobacterium tumefaciens* cells were thawed on ice before adding 1 – 2  $\mu$ g plasmid DNA. Cells were incubated for 5 min on ice, then 5 min in liquid nitrogen followed by 5 min heat shock at 37°C. 800  $\mu$ l LB medium were added and cells were grown for 4 h at 28°C and 750 rpm (ThermoMixer®, eppendorf). Following centrifugation for 2 min at 1,500 **g**, pelleted cells were resuspended in 100  $\mu$ l LB medium and plated onto LB medium plates containing appropriate antibiotics.

#### **2.2.25. *Agrobacterium*-mediated transient expression of fluorescent proteins in *Nicotiana benthamiana***

Infiltration of four- to six-week-old *Nicotiana benthamiana* leaves and subsequent protoplast isolation were performed as described previously (Koop *et al.* 1996, Schweiger and Schwenkert 2014).

Transformed *Agrobacterium tumefaciens* cells were grown in selective LB medium, pelleted at 3,200 **g** and 4°C for 15 min and resuspended in infiltration medium (10 mM MES (pH 6.0), 100 – 200  $\mu$ M acetosyringone (in 60% (v/v) ethanol), 10 mM MgCl<sub>2</sub>) with an OD<sub>600</sub> of 1.0. Cells were rotated at room temperature for two to four hours in the dark and mixed in a 1:1 ratio in case of co-infiltration, before infiltrating tobacco leaves. Plants were covered overnight and protoplasts were isolated after two to three days growth.

Centrifugation steps for protoplast isolation were performed at room temperature with low acceleration and deceleration, osmolality of buffers was adjusted to 550 mosmol kg<sup>-1</sup> and protoplasts were slowly pipetted with cut tips. One tobacco leaf was cut into approximately 1 cm x 1 cm pieces in 10 ml enzyme solution (1% (w/v) cellulase Onozuka R10, 0.3% (w/v), macerozyme R10, 0.1% (w/v) BSA in F-PIN solution containing 10 mM KNO<sub>3</sub>, 3 mM CaCl<sub>2</sub>, 1.5 mM MgSO<sub>4</sub>, 1.2 mM KH<sub>2</sub>PO<sub>4</sub>, 20 mM NH<sub>4</sub>-succinate (4 M KOH (pH 5.8), 2 M succinic acid, 2 M NH<sub>4</sub>Cl), 2 mM MES (pH 5.8), 4.5 μM KI, 0.1 mM EDTA iron(III) sodium salt, 0.05 mM H<sub>3</sub>BO<sub>3</sub>, 60 μM MnSO<sub>4</sub>, 7 μM ZnSO<sub>4</sub>, 1 μM Na<sub>2</sub>MoO<sub>4</sub>, 0.1 μM CuSO<sub>4</sub>, 0.1 μM CoCl<sub>2</sub>, 120 g L<sup>-1</sup> (approximately 350 mM) sucrose). Following vacuum infiltration for 30 sec, leaf pieces were shaken at 40 rpm for 90 min in the dark on an orbital shaker. Protoplasts were released at 80 rpm for 1 min, filtered through a nylon mesh/gauze and overlaid with 2 ml F-PCN (same as F-PIN solution but 80 g L<sup>-1</sup> (approximately 440 mM) glucose instead of sucrose). Intact protoplasts accumulated at the interface between enzyme solution and F-PCN after 10 min at 70 **g** and were transferred to new tubes, before washing with 10 ml W5 buffer (125 mM CaCl<sub>2</sub>, 5 mM KCl, 2 mM MES (pH 5.7), 7 g L<sup>-1</sup> (approximately 120 mM) NaCl). Protoplasts were then pelleted for 10 min at 50 **g** and gently resuspended in 0.5 ml W5 buffer.

#### **2.2.26. *Agrobacterium*-mediated stable transfection of *Arabidopsis thaliana***

Stable transfection of *Arabidopsis* plants was conducted by floral dip (compare to Clough and Bent 1998). 400 ml selective LB medium were inoculated with transformed *Agrobacterium tumefaciens* preculture and grown for 24 h. Cells were pelleted at 2,800 **g** and 4°C for 20 min and solved in equal volume of sucrose solution (5% (w/v) sucrose, 0.05% (v/v) Silwet L-77). Four- to five-week-old plants were dipped into bacterial suspensions for 10 sec, covered overnight and then grown under greenhouse conditions. Floral dipping was repeated once after five to seven days.

#### **2.2.27. Immunoprecipitation of GFP-fused proteins using GFP-Trap<sup>®</sup> Magnetic Agarose beads**

GFP-Trap<sup>®</sup> pull-down was conducted based on manufacturer's instructions (ChromoTek). Microsomal membranes (compare to 2.2.3.) were resuspended in 200 μl 20 mM HEPES (pH 7.5), 40 mM KCl, 1 mM EDTA, 0.1% (w/v) DTT, 0.1% (w/v) n-dodecyl-β-D-maltosid and 1x protease inhibitor cocktail. 50 μl GFP-Trap<sup>®</sup> MA beads were equilibrated in 500 μl wash buffer (20 mM HEPES (pH 7.5), 40 mM KCl, 1 mM

EDTA, 0.1% (w/v) DTT, 1x protease inhibitor cocktail) for three times, then 150  $\mu$ l of equilibrated beads were added per 2 mg isolated microsomal membranes and tumbled overnight at 4°C. Beads were separated magnetically and samples were washed three times in 500  $\mu$ l wash buffer, before proteins were eluted twice in 50  $\mu$ l SDS loading buffer at 95°C for 10 min. Eluted samples were run on a 5% stacking SDS-PAGE gel, excised and frozen at -20°C, prior to submitting for mass spectrometric analysis (compare to 2.2.28.).

### 2.2.28. Mass spectrometry

Mass spectrometric analysis (proteomics) was done by the MSBioLMU service unit (Mass Spectrometry of Biomolecules at the Ludwig-Maximilians-University Munich, for information concerning sample preparation compare to [http://www.en.biologie.uni-muenchen.de/core\\_facilities/massspectrometry/index.html](http://www.en.biologie.uni-muenchen.de/core_facilities/massspectrometry/index.html)).

For subsequent evaluation, the score obtained from mass spectrometric analysis was aggregated for all protein sequences derived from the same accession number. Stable *Arabidopsis* lines expressing either GFP-AtSec62 or AtSec62-GFP were used for analysis, while non-transformed wild-type plants were used as control. Protein sequences which were present in equal amounts in the control and the actual samples were omitted.

### 2.2.29. Transient transformation of isolated *Arabidopsis thaliana* protoplasts

Centrifugation steps for *Arabidopsis* protoplast isolation were performed at room temperature with low acceleration and deceleration, osmolality of buffers was adjusted to 550 mosmol kg<sup>-1</sup> and protoplasts were slowly pipetted with cut tips. 10 – 20 leaves of four-week-old *Arabidopsis* plants were gently incised in 10 ml enzyme solution (1% (w/v) cellulase Onozuka R10, 0.3% (w/v), macerozyme R10, 0.1% (w/v) BSA, 20 mM MES (pH 5.7), 400 mM mannitol, 20 mM KCl, 10 mM CaCl<sub>2</sub>), vacuum infiltrated for 30 sec and shaken for 90 min at 40 rpm in the dark on an orbital shaker. Protoplasts were released by applying 80 rpm for 1 min, filtered through a nylon mesh/gauze and centrifuged at 100 **g** for 2 min. Pelleted protoplasts were resuspended in 500  $\mu$ l MMg buffer (4 mM MES (pH 5.7), 400 mM mannitol, 15 mM CaCl<sub>2</sub>) and layered onto a gradient consisting of 9 ml MSC buffer (10 mM MES (pH 5.8), 20 mM MgCl<sub>2</sub>, 120 g L<sup>-1</sup> (approximately 350 mM) sucrose) and 2 ml MMg buffer, prior to 10 min centrifugation at 70 **g**. Intact protoplasts at the interface between MMg and MSC buffer were transferred to new tubes with 5 ml W5 buffer (same as in 2.2.25.) and pelleted at 100 **g**

for 2 min. Protoplasts were resuspended in MMg buffer, counted using a haemocytometer (Neubauer improved) and adjusted to approximately  $4 \times 10^{-6}$  protoplasts  $\text{ml}^{-1}$ . 100  $\mu\text{l}$  of isolated protoplasts were mixed with 20  $\mu\text{g}$  plasmid DNA, before adding 110  $\mu\text{l}$  PEG/Ca solution (2 g PEG 4000 with 1.75 ml  $\text{H}_2\text{O}$ , 1 ml of 1 M mannitol solution and 0.5 ml of 1 M  $\text{Ca}(\text{NO}_3)_2$  solution). Samples were incubated in the dark for 10 min, prior to adding 500  $\mu\text{l}$  W5 buffer and 1 min centrifugation at 100 **g**. Pelleted protoplasts were resuspended in 1 ml W5 buffer, sealed with Parafilm® “M” Laboratory Film (Bemis) and incubated at room temperature overnight in the dark.

### **2.2.30. Confocal microscopy**

Fluorescent signals in leaves or protoplasts were detected at room temperature by confocal laser scanning microscopy (Leica TCS SP5, objective: HCX PL APO, magnification: 63x, imaging medium: glycerol) using the Leica Application Suite Advanced Fluorescence for image acquisition (compare to Schweiger and Schwenkert 2014).

Pictures were taken in 512 x 512 or 1024 x 1024 format (width x height) and a scan speed of 100 Hz. The maximum distance between stacks for z-stackings of isolated protoplasts was set at 0.67  $\mu\text{m}$ .

### 3. Results

#### 3.1. Identification of *atsec62* and *attpr7* T-DNA insertion lines

An *attpr7* T-DNA insertion line has been described recently with the insertion being located in exon 9 of *AT5G21990* (*AtTPR7*) (Schweiger *et al.* 2012, Figure 4a). Homozygous *attpr7* plants were confirmed by PCR using the oligonucleotides *AtTPR7*-Exon9-f, *AtTPR7*-Exon11-r and LBa1 (Figure 4b). Even though *AtTPR7* transcript was absent in mutant plants, no obvious phenotype was observable in comparison with Col-0 (compare to Schweiger *et al.* 2012, Figure 4c, d).

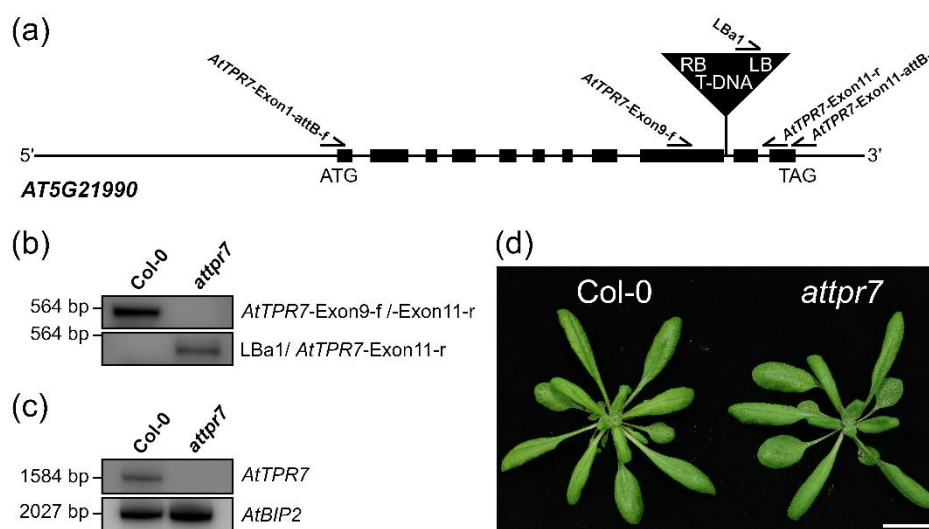


**Figure 4: Confirmation of an *attpr7* T-DNA insertion line.** (a) *AT5G21990* (*AtTPR7*) gene structure and location of the T-DNA insertion (black triangle) in exon 9, also indicating the T-DNA left (LB) and right border (RB). Exons are indicated by black boxes. Based on Schweiger *et al.* (2012). (b) Genotyping PCR for Col-0 and *attpr7* using the oligonucleotides *AtTPR7*-Exon9-f, *AtTPR7*-Exon11-r and LBa1. Oligonucleotide binding sites in *AtTPR7* are indicated in (a). (c) RT-PCR for *AtTPR7* and the control *AtBIP2* using Col-0 and *attpr7*. Oligonucleotide binding sites for *AtTPR7*-Exon1-attB-f and *AtTPR7*-Exon11-attB-r in *AtTPR7* are indicated in (a). (d) Phenotype of four-week-old Col-0 and *attpr7* plants. Scale bar represents 2 cm. Compare to Schweiger *et al.* (2012) for initial characterisation of *attpr7*.

The insertion of the identified *atsec62* T-DNA insertion line is located in Exon 1 of *AT3G20920* (*AtSEC62*) and homozygous mutant plants were selected by PCR using the oligonucleotides *Sec62*-5'UTR-for, *Sec62*-Exon2-rev and Gabi-LB8409 (Figure 5a, b). *atsec62* plants displayed an impaired growth in comparison with wild-type plants after four weeks growth (Figure 5c), although no obvious aerial phenotype was observable during initial growth. Absence of *AtSEC62* transcripts in *atsec62* was verified by RT-PCR using the oligonucleotides *AtSec62*-Exon1-f and *AtSec62*-Exon5-r,

while the absence of AtSec62 protein was confirmed by using a specific  $\alpha$ AtSec62 antibody leading to a detectable signal at the expected molecular weight of 41.9 kDa only in isolated wild-type microsomal membranes (Figure 5d, e).

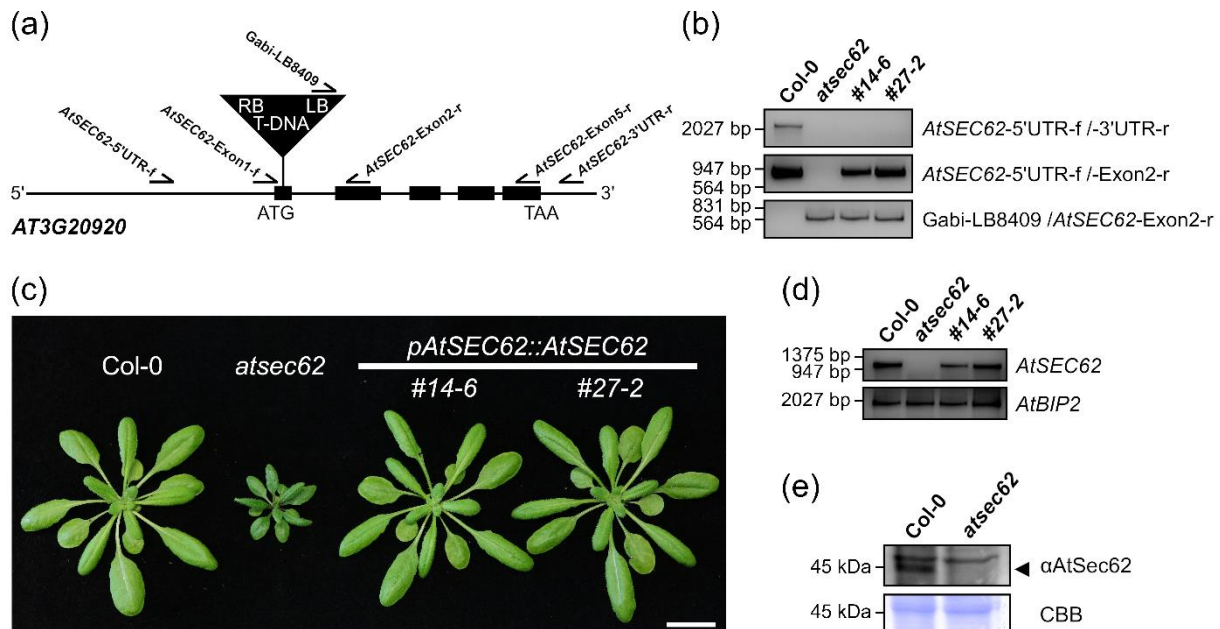


**Figure 5: Isolation of an *atsec62* T-DNA insertion line and respective complementation lines.** (a) *AT3G20920* (*AtSEC62*) gene structure and location of the T-DNA insertion (black triangle) in exon 1, also indicating the T-DNA left (LB) and right border (RB). Exons are indicated by black boxes. (b) Genotyping PCR for *Col-0* and *atsec62* plants as well as complementation lines *pAtSEC62::AtSEC62* #14-6 (#14-6) and *pAtSEC62::AtSEC62* #27-2 (#27-2) using the oligonucleotides *AtSEC62*-5'UTR-f, *AtSEC62*-Exon2-r and *Gabi-LB8409*. Oligonucleotide binding sites in *AtSEC62* are indicated in (a). (c) Phenotype of four-week-old *Col-0* and *atsec62* as well as #14-6 and #27-2 plants. Scale bar represents 2 cm. (d) RT-PCR for *AtSEC62* and the control *AtBIP2* using *Col-0*, *atsec62*, #14-6 and #27-2. Oligonucleotide binding sites for *AtSEC62*-Exon1-f and *AtSEC62*-Exon5-r in *AtSEC62* are indicated in (a). (e) Immunodetection of *Col-0* and *atsec62* microsomal membranes using an  $\alpha$ AtSec62 antiserum (upper panel) and Coomassie stain (lower panel). Putative signal for AtSec62 is indicated by black arrow. Figure taken from Mitterreiter *et al.* (2020).

For complementation analysis, *AtSEC62* encoded under the control of the endogenous promoter was transformed into *atsec62* mutant plants and the presence of respective transcripts was confirmed for two independent lines, named *pAtSEC62::AtSEC62* #14-6 (#14-6) and *pAtSEC62::AtSEC62* #27-2 (#27-2) (Figure 5b, d). The observed growth phenotype of *atsec62* plants was rescued in both lines upon expression of endogenous AtSec62 (Figure 5c).

In contrast to the aerial phenotype, an altered root morphology of *atsec62* was already visible in two-week-old seedling plants, which were grown vertically on half-strength

MS medium (Figure 6a – d). *atsec62* seedlings displayed a primary root length of  $3.67 \pm 1.15$  cm in comparison to wild-type roots with  $5.32 \pm 0.82$  cm length (shown as mean  $\pm$  SD,  $n = 36$  (Col-0),  $n = 37$  (*atsec62*), Figure 6a, b), whereas the number of lateral roots was increased by nearly 50%, with *atsec62* seedlings having  $23.46 \pm 10.73$  lateral roots per plant in comparison to wild-type seedlings only having  $15.69 \pm 4.03$  (shown as mean  $\pm$  SD,  $n = 36$  (Col-0),  $n = 37$  (*atsec62*), Figure 6a, c, d).

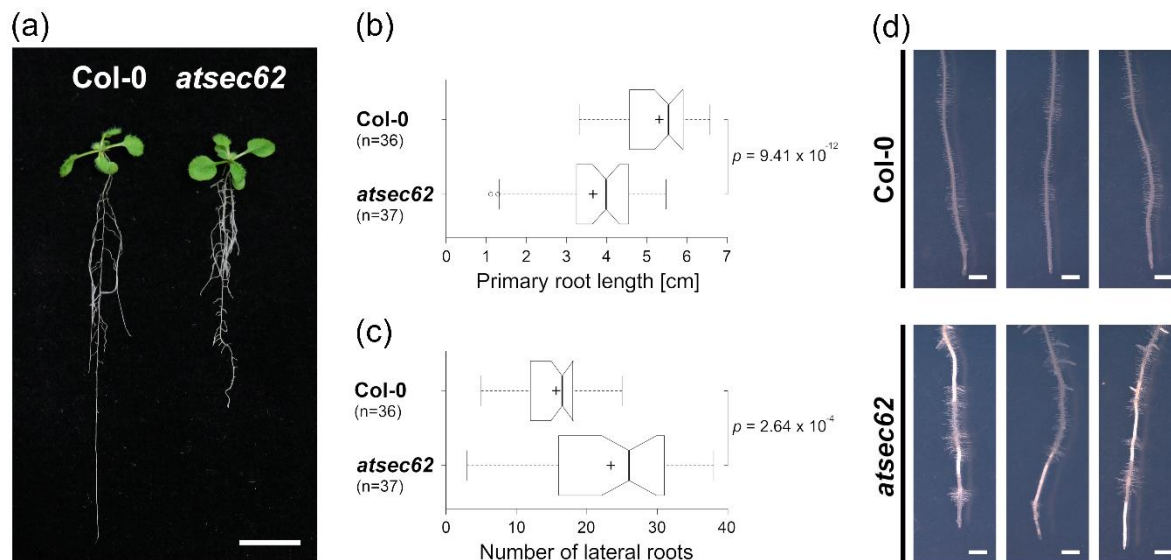


**Figure 6: Root morphology of two-week-old *atsec62* seedlings in comparison to Col-0.** (a) Root phenotype of Col-0 and *atsec62* seedlings. Scale bar represents 1 cm. (b) Boxplot depicting primary root length of Col-0 and *atsec62* seedlings. Centre lines of boxes show the medians with limits at 25<sup>th</sup> and 75<sup>th</sup> percentiles. Tukey – whiskers extend to 1.5 x interquartile range; notches indicate 95% confidence interval; outliers are represented by dots; sample means are indicated by black crosses; sample size  $n = 36$  (Col-0), 37 (*atsec62*). Differences between genotypes were validated by Student's *t*-test. (c) Boxplot as in (b), showing number of lateral roots per seedling for *atsec62* in comparison to Col-0. Sample size  $n = 36$  (Col-0), 37 (*atsec62*). (d) Primary root tips of Col-0 and *atsec62* seedlings. Scale bars represent 1 mm. Figure taken from Mitterreiter *et al.* (2020).

Beside the visible growth phenotype, a very low number of homozygous mutant plants was observable during initial screening. For this reason the segregation pattern of progeny plants derived from heterozygous *atsec62* plants (+/-) was investigated to identify potential defects of *atsec62*. Only 8.83% homozygous progeny plants, but 40.38% wild-type and 50.79% heterozygous progeny plants were identified ( $n = 317$ ), significantly differing from the expected Mendelian ratio that would imply 50% heterozygous progeny, 25% wild-type and 25% homozygous progeny (Table 5).

**Table 5: Segregation analysis for progeny plants derived from heterozygous *atsec62* (+/-) plants.** Progeny genotypes were identified by PCR using *AtSEC62* and T-DNA specific oligonucleotides (compare to Figure 5a, b). Table taken from Mitterreiter *et al.* (2020), modified.

Genotype	wild-type progeny	heterozygous progeny	homozygous progeny	$p_{1:2:1}$
<i>atsec62</i> (+/-)	128	161	28	$1.92 \times 10^{-4}$

Due to their T-DNA insertion, homozygous as well as heterozygous *atsec62* plants should be resistant towards sulfadiazine, whereas wild-type plants remain sensitive, resulting in 75% resistant progeny plants derived from *atsec62* (+/-). Again an altered segregation pattern was observable with only 58.63% resistant plants ( $n = 278$ ), rather resembling a 3:2 ratio than the expected 3:1 ratio, but also significantly differing from a 1:1 ratio, which would be typically expected for male and female gametophyte mutants (Liu and Qu 2008, Drews and Koltunow 2011) (Table 6).

**Table 6: Segregation analysis on sulfadiazine.** Number of sulfadiazine resistant (Sulfa<sup>R</sup>) and sensitive (Sulfa<sup>S</sup>) Col-0, *atsec62* as well as *pAtSEC62::AtSEC62* #14-6 (#14-6) and *pAtSEC62::AtSEC62* #27-2 (#27-2) plants.  $p$ -value for expected segregation, validation by  $\chi^2$  analysis. Table taken from Mitterreiter *et al.* (2020), modified.

Genotype	Sulfa <sup>R</sup>	Sulfa <sup>S</sup>	Sulfa <sup>R</sup> [%]	$p_{3:1}$	$p_{1:1}$	$p_{3:2}$
Col-0	0	100	0	-	-	-
<i>atsec62</i> (+/-)	163	115	58.63	$2.94 \times 10^{-10}$	0.0040	0.6418
#14-6	98	0	100	-	-	-
#27-2	103	0	100	-	-	-

### 3.2. Generative defects in *atsec62*

For further investigation of potential gametophytic defects in *atsec62*, siliques, anthers and pollen of mutant plants were examined. Siliques of six- to seven-week-old *atsec62* plants seemed to be aborted and had a reduced length of only  $0.45 \pm 0.09$  cm in contrast to wild-type plants having siliques of  $1.74 \pm 0.07$  cm length and complementation lines with  $1.70 \pm 0.13$  cm (#14-6) and  $1.77 \pm 0.08$  cm (#27-2) (shown as mean  $\pm$  SD,  $n = 32$ ) (Figure 7a, b). Additionally, most of *atsec62* siliques were empty resulting in a drastically reduced seed yield of  $3.79 \pm 2.42$  mg seeds per plant ( $n = 28$ ), whereas wild-type plants yielded  $440.50 \pm 26.33$  mg seeds per plant ( $n = 7$ ) (shown as mean  $\pm$  SD,  $p = 4.86 \times 10^{-40}$ , compare to Figure 7c).

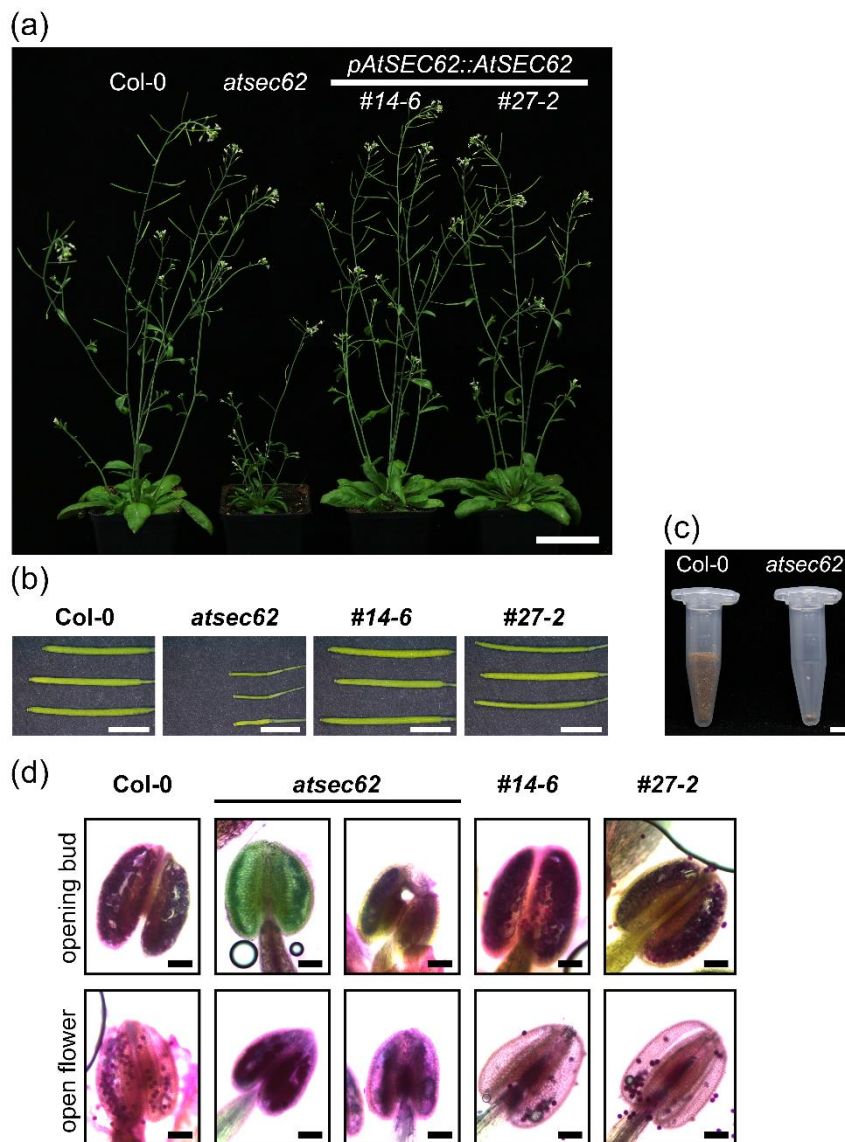


**Figure 7: Reduced seed yield and altered pollen development in *atsec62*.** (a) Phenotype of six-to seven-week-old Col-0 and *atsec62* as well as *pAtSEC62::AtSEC62* #14-6 (#14-6) and *pAtSEC62::AtSEC62* #27-2 (#27-2) plants. Scale bar represents 4 cm. (b) Siliques of six- to seven-week-old Col-0, *atsec62*, #14-6 and #27-2 plants. Scale bars represent 5 mm. (c) Col-0 and *atsec62* seed yield from one single plant. Scale bar represents 5 mm. (d) Alexander staining of anthers from opening buds (upper panels) and open flowers (lower panels) of eight-week-old Col-0, *atsec62*, #14-6 and #27-2 plants. Scale bars represent 100  $\mu$ m. Figure partially taken from Mitterreiter *et al.* (2020), modified.

When investigating siliques of *atsec62* (+/-) neither a reduced seed set nor defective seeds were observable, indicating that the female gametophyte was still functional (Liu and Qu 2008, Drews and Koltunow 2011). Upon investigation of pollen viability by Alexander staining, which allows discrimination between viable (violet staining) and non-functional pollen grains (greenish staining) (Alexander 1969), Col-0 and both complementation lines showed violet and clearly distinguishable pollen grains, which

were already visible in anthers of opening buds, while the majority of *atsec62* anthers appeared greenish with only occasionally faint violet staining and no pollen-like structures observable (Figure 7d). Only upon testing anthers of already open flowers, corresponding to dehiscent wild-type anthers, violet staining of clustered pollen-like structures was observable for *atsec62*. (Figure 7d).

For subsequent *in vitro* pollen germination, *atsec62* pollen were hardly released from the anthers and their germination rate was reduced by 57% in comparison to wild-type pollen when incubated at 25°C (Table 7).

### 3.3. High-temperature and ER stress sensitivity of *atsec62*

To identify other defects in *atsec62* besides general vegetative and generative defects, *in vitro* pollen tube germination was additionally conducted at 37°C, leading to mutant pollen hardly germinating at all (Table 7). High-temperature sensitivity was then further investigated according to Yang *et al.* (2009). Seeds were either germinated at 37°C for 48 h and then transferred to 22°C or directly germinated and grown at 22°C. Seed germination rate was determined after seven days growth, so five days after the actual heat treatment, whereas the survival rate upon high-temperature stress was examined after 14 days growth. *atsec62* seed germination was reduced by 15% even without heat treatment, while there was no further effect caused by high-temperature stress (Table 7). However, the survival rate of germinated *atsec62* plants was decreased with 25.96% of *atsec62* seedlings suffering and dying due to the preceding heat treatment, whereas germinated wild-type plants remained unaffected (Table 7).

**Table 7: Pollen tube germination, seed germination and survival of Col-0 and *atsec62* plants upon high-temperature stress.** Numbers indicate percentage of germinated pollen and seeds or percentage of germinated plants that survived high-temperature stress. Table taken from Mitterreiter *et al.* (2020), modified.

Line	Pollen tube germination [%] <sup>1</sup>		Seed germination [%] <sup>2</sup>		Survival [%] <sup>3</sup>	
	25°C	37°C	22°C	37°C	22°C	37°C
Col-0	24.56	15.78	97.80	96.12	100.00	99.24
<i>atsec62</i>	10.50	0.82	83.46	81.40	96.43	74.04

<sup>1</sup> Col-0 at 25°C (n = 950), Col-0 at 37°C (n = 928), *atsec62* at 25°C (n = 203), *atsec62* at 37°C (n = 164).

<sup>2</sup> Col-0 at 22°C (n = 139), Col-0 at 37°C (n = 129), *atsec62* at 22°C (n = 133), *atsec62* at 37°C (n = 129).

<sup>3</sup> Col-0 at 22°C (n = 133), Col-0 at 37°C (n = 131), *atsec62* at 22°C (n = 112), *atsec62* at 37°C (n = 104).

*atsec62* susceptibility towards ER stress was tested by growing plants on different concentrations of DTT or Tunicamycin. In both cases accumulation of misfolded or

unfolded proteins triggers the unfolded protein response (UPR) with DTT preventing the formation of disulphide bonds and Tunicamycin blocking N-linked glycosylation. While increased concentrations of DTT were affecting *atsec62* seedlings slightly more than the wild-type control, there was no observable effect of Tunicamycin on *atsec62* (Figure 8a, b).

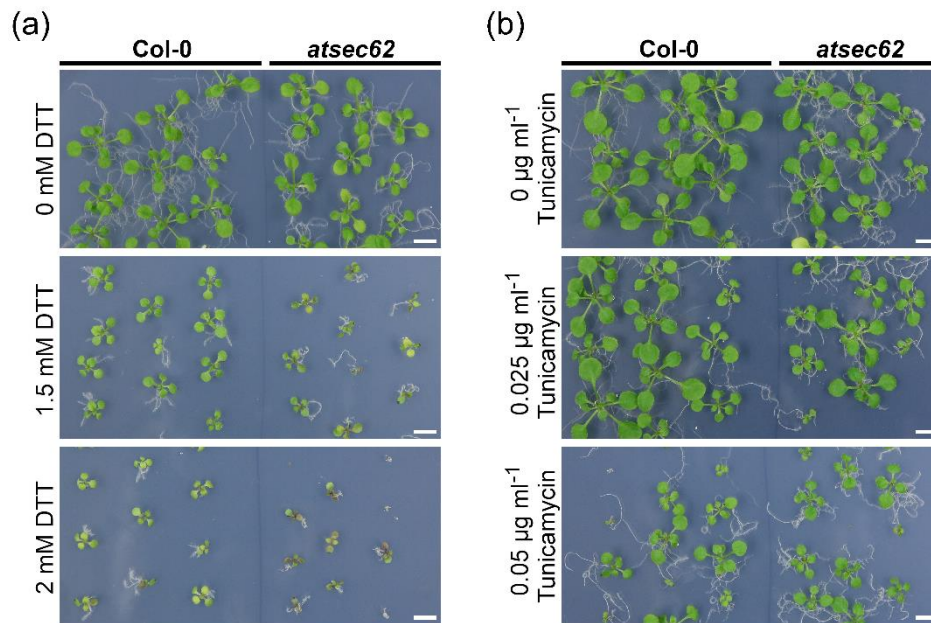
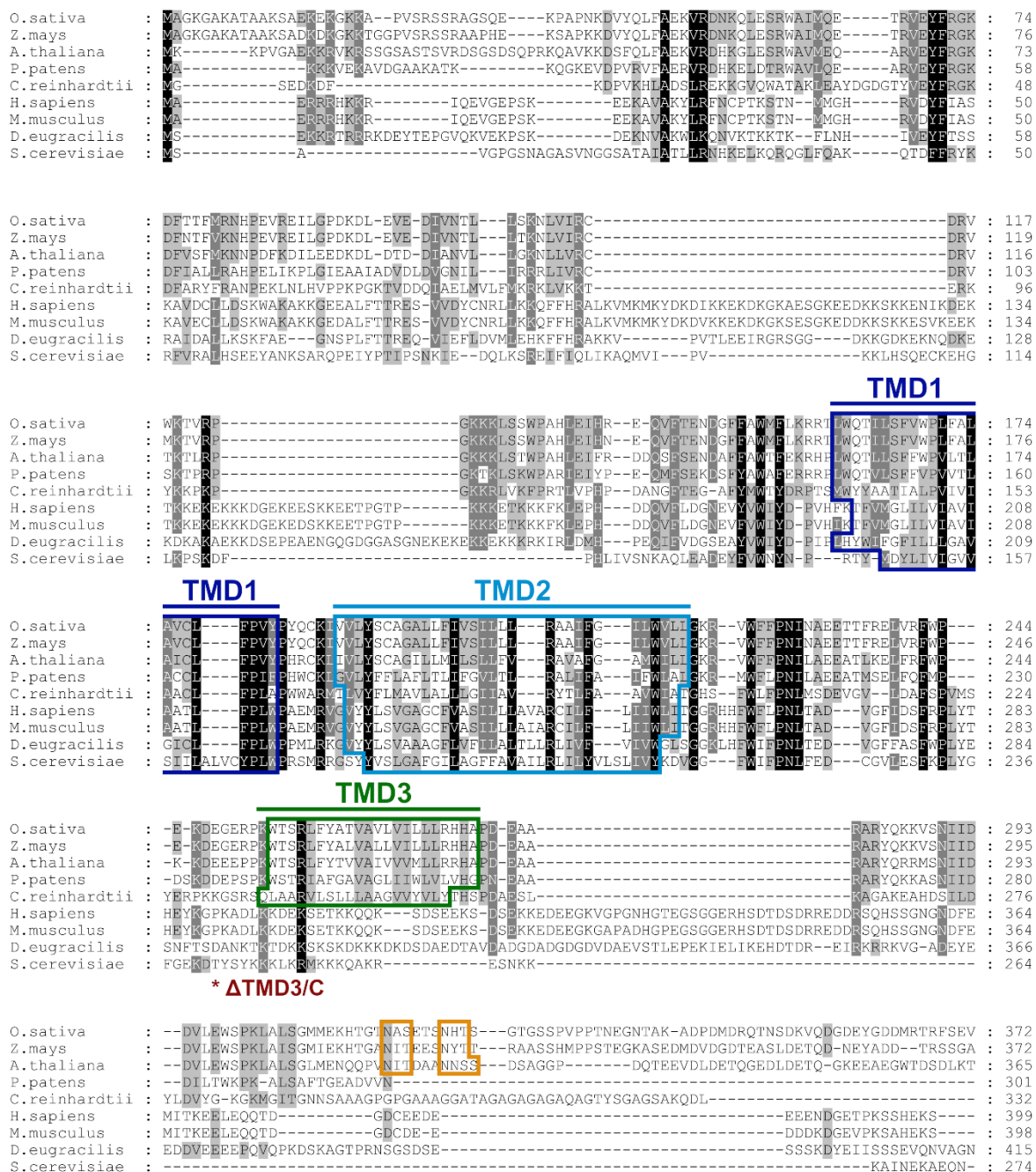


**Figure 8: ER stress sensitivity of Col-0 and *atsec62* seedlings.** Sensitivity of two-week-old plants towards DTT (1.5 mM, 2 mM) (a) and Tunicamycin (0.025 µg ml<sup>-1</sup>, 0.05 µg ml<sup>-1</sup>) (b) induced ER stress. Scale bar represent 5 mm. Figure partially taken from Mitterreiter *et al.* (2020).

### 3.4. AtSec62 localisation and topology analysis

Besides its role in plant growth and development, AtSec62 localisation and topology were investigated, as it has been suggested that AtSec62 possesses a third transmembrane domain (Schweiger and Schwenkert 2013), resulting in an altered topology in contrast to its yeast and mammalian counterparts (Deshaies and Schekman 1989, 1990, Müller *et al.* 2010). Amino acid sequences of various Sec62 homologues were therefore compared regarding their predicted transmembrane domains, including higher plants like *Arabidopsis thaliana*, *Oryza sativa* and *Zea mays*, the moss *Physcomitrella patens*, the unicellular green algae *Chlamydomonas reinhardtii*, mammals like *Homo sapiens* and *Mus musculus*, *Drosophila eugracilis* and the yeast *Saccharomyces cerevisiae* (Figure 9a, for complete phylogenetic tree including additional species see Figure A2).

(a)



(b)

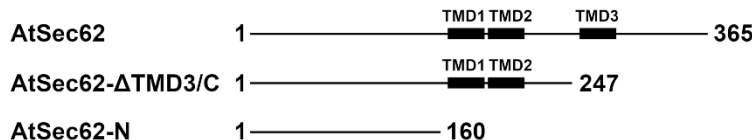


**Figure 9: Predicted transmembrane domains for Sec62 homologues and AtSec62 constructs used in this study.** (a) Amino acid sequence alignment of Sec62 homologues from *Oryza sativa*, *Zea mays*, *Arabidopsis thaliana*, *Physcomitrella patens*, *Chlamydomonas reinhardtii*, *Homo sapiens*, *Mus musculus*, *Drosophila eugracilis* and *Saccharomyces cerevisiae*. Detailed information regarding accession numbers is given in section 2.1.7. Conserved amino acids are shaded in black/ grey. (continued on next page)

---

Predicted transmembrane domains are indicated in dark blue (TMD1), light blue (TMD2) and green (TMD3), putative N-glycosylation sites are shown in orange. (b) Scheme of AtSec62 constructs used in this study. AtSec62 (amino acids 1-365), AtSec62- $\Delta$ TMD3/C (amino acids 1-247) and AtSec62-N (amino acids 1-160) are shown with potential transmembrane domains (black boxes). The stop codon inserted for generation of the AtSec62- $\Delta$ TMD3/C construct is indicated in red in (a). Figure taken from Mitterreiter *et al.* (2020), modified.

---

While two transmembrane domains were predicted for all analysed Sec62 homologues, a third transmembrane domain harbouring many hydrophobic amino acids was only predicted for plant Sec62 (Figure 9a). Potential N-glycosylation sites with the consensus motif N-X-S/T (with X being any amino acid except proline) (compare to Marshall 1972) were additionally found in higher plants, but were absent in mosses, algae as well as yeast and mammals (Figure 9a).

For localisation and topology analyses, full-length AtSec62 and AtSec62- $\Delta$ TMD3/C were used with AtSec62- $\Delta$ TMD3/C lacking the C-terminal region of AtSec62 including the putative third transmembrane domain (Figure 9b).

To initially confirm the predicted ER localisation of AtSec62 and to test whether GFP-fusion might affect proper AtSec62 targeting, N- and C-terminal GFP-fusion constructs, named *GFP-AtSEC62* and *AtSEC62-GFP*, were transiently expressed in tobacco leaves together with an ER marker (compare to Nelson *et al.* 2007, Schweiger *et al.* 2012). Following co-infiltration of tobacco leaves with *Agrobacteria* carrying respective constructs, fluorescent signals were detected by confocal laser scanning microscopy in intact leaves and isolated protoplasts (Figure 10a, b). For both GFP-fusion proteins the fluorescent signal co-localised with the ER marker confirming the putative ER localisation of AtSec62 (Figure 10c, d). The presence of full-length GFP-AtSec62 and AtSec62-GFP with an expected molecular weight of 68.8 kDa (41.9 kDa for AtSec62 and 26.9 kDa for GFP) was proven by isolating proteins out of infiltrated tobacco leaves (Figure 10e).

Subsequent topology analysis was performed by fusing the eleventh GFP  $\beta$ -sheet to the N- or the C-terminus of AtSec62 or AtSec62- $\Delta$ TMD3/C, thereby generating constructs for expression of GFP11-AtSec62, AtSec62-GFP11, GFP11-AtSec62- $\Delta$ TMD3/C and AtSec62- $\Delta$ TMD3/C-GFP11 constructs (compare to Cabantous *et al.* 2005, Xie *et al.* 2017). The *AtSEC62- $\Delta$ TMD3/C-GFP11* fusion construct contained an additional C-terminal His-tag as linker between the actual *AtSEC62* coding region and the GFP encoding section.

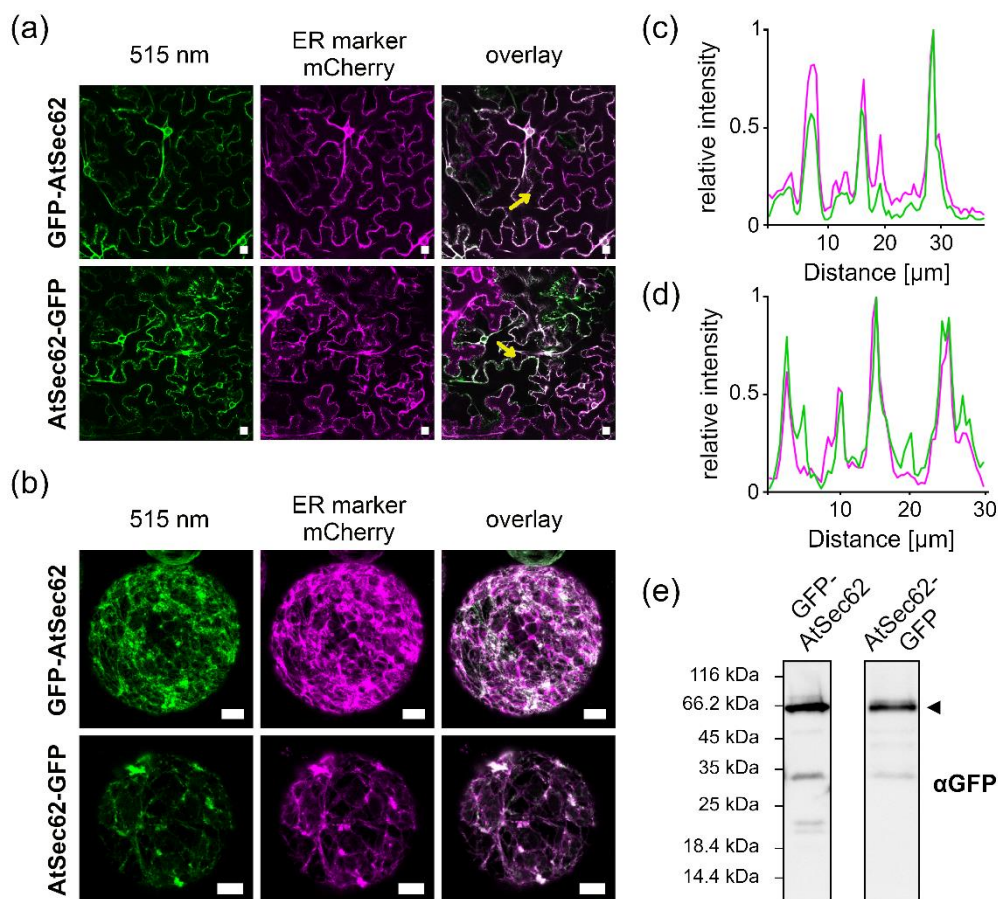


**Figure 10: Localisation of AtSec62 GFP-fusion proteins in transiently transformed tobacco leaves.** Tobacco leaves were co-transformed with *Agrobacteria* carrying constructs for an ER marker (mCherry) and constructs for GFP-AtSec62 or AtSec62-GFP. Fluorescent signals were detected by confocal laser scanning microscopy in intact leaves (a) or isolated protoplasts (b). Scale bars represent 10  $\mu\text{m}$ . Line histograms along the yellow arrow indicated in (a), depict the relative fluorescence intensity of GFP-AtSec62 (c) or AtSec62-GFP (d) (green) and the ER marker (magenta). (e) Membrane proteins were isolated from infiltrated tobacco leaves and GFP-fusion proteins (indicated by black arrow) were detected using an anti-GFP antibody ( $\alpha\text{GFP}$ ). Figure partially taken from Mitterreiter *et al.* (2020), modified.

Respective constructs were co-transformed into tobacco leaves together with plasmids encoding the GFP  $\beta$ -sheets 1-10 (compare to Cabantous *et al.* 2005), which are either localised to the cytosol (GFP1-10) or to the ER lumen by an integrated ER retention signal (GFP1-10-HDEL) (Xie *et al.* 2017). While fluorescent signals for GFP11-AtSec62, GFP11-AtSec62- $\Delta\text{TMD3/C}$  and AtSec62- $\Delta\text{TMD3/C}$ -GFP11 were detectable when co-expressed with cytosolic GFP1-10, signals for AtSec62-GFP11 were only monitored upon co-expression with the ER luminal GFP1-10-HDEL (Figure 11a, b). These results indicate that AtSec62 has indeed an altered topology in comparison to its yeast and mammalian counterparts with its C-terminus facing the ER lumen (Figure 11c).

On top of its possibly altered topology, AtSec62 shares only 12% and 15% overall sequence identity with its yeast and human homologues and even regarding the predicted Sec62 domain (compare to Schweiger and Schwenkert 2013), it shows only 14% sequence identity, while yeast Sec62p and human Sec62 share 19% sequence identity.

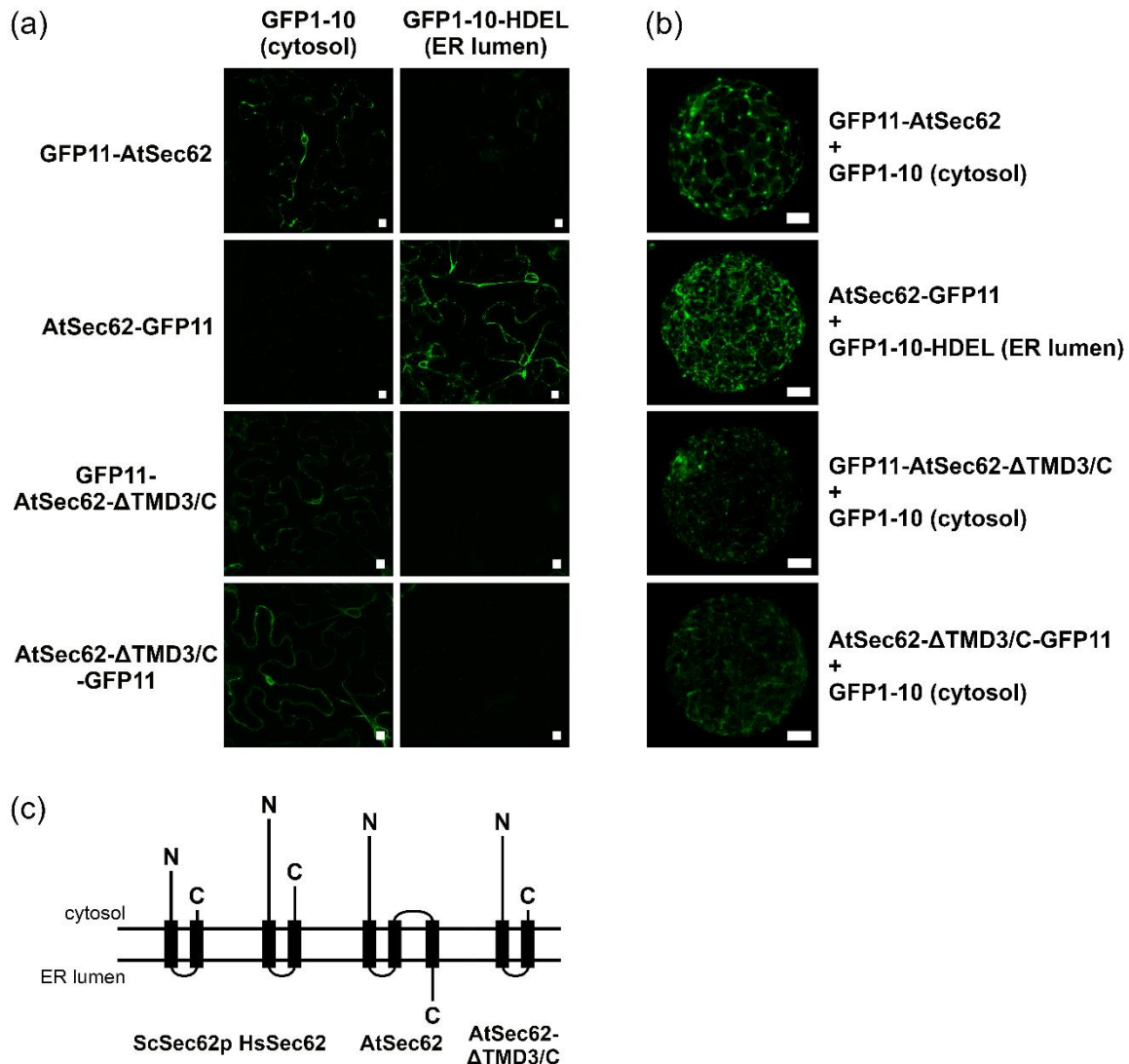


**Figure 11: AtSec62 topology analysis in transiently transformed tobacco leaves.** Tobacco leaves were co-transformed with *Agrobacteria* carrying constructs for either GFP11-AtSec62, AtSec62-GFP11, GFP11-AtSec62-ΔTMD3/C or AtSec62-ΔTMD3/C-GFP11 and cytosolic GFP1-10 or ER luminal GFP1-10-HDEL (compare to Xie *et al.* 2017). Fluorescent signals were detected by confocal laser scanning microscopy in intact leaves (a) or isolated protoplasts (b). Scale bars represent 10  $\mu$ m. (c) Proposed topology model for AtSec62 and AtSec62-ΔTMD3/C in comparison to yeast Sec62p (ScSec62p) and human Sec62 (HsSec62). Figure taken from Mitterreiter *et al.* (2020), modified.

### 3.5. Yeast complementation analysis using AtSec62

To test whether AtSec62 or AtSec62- $\Delta$ TMD3/C can nonetheless rescue the growth phenotype of the *sec-ts* yeast mutant despite its low sequence identity with Sec62p and its possibly altered topology, complementation analysis in yeast was conducted. *sec62-ts* is thermosensitive due to an amino acid substitution (G37D) in Sec62p, enabling normal growth only at permissive temperature (28°) but not at restrictive temperature (37°C). While growth was restored upon expression of the endogenous Sec62p, neither AtSec62 nor AtSec62- $\Delta$ TMD3/C was able to rescue the thermosensitive growth phenotype, even though respective transcripts were present as verified by RT-PCR (Figure 12a, b).

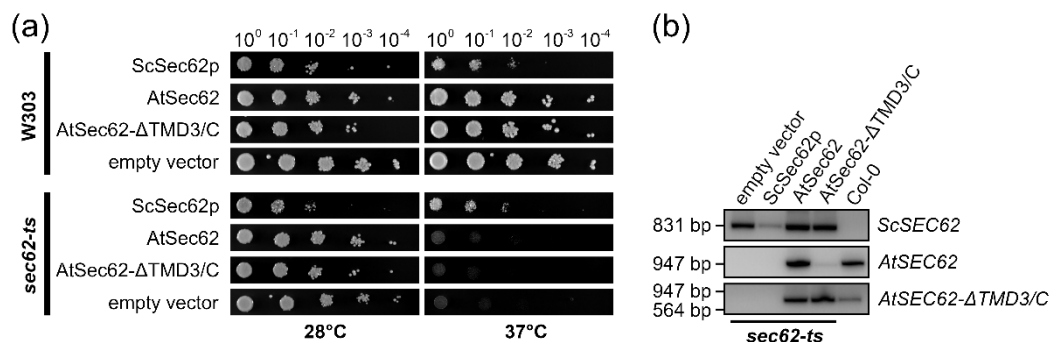


**Figure 12: Complementation analysis in *sec62-ts*.** (a) Wild-type yeast (W303) and thermosensitive *sec62-ts* were transformed with constructs for expression of yeast Sec62p (ScSec62p), AtSec62, AtSec62- $\Delta$ TMD3/C or the empty vector control. Serial dilutions were dropped onto solid SCD medium plates and yeast cells were grown at either permissive (28°C) or restrictive (37°C) temperature for 48h. (b) RT-PCR for *ScSEC62*, *AtSEC62* and *AtSEC62- $\Delta$ TMD3/C* using Col-0 and *sec62-ts* transformed with constructs as described in (a). Figure taken from Mitterreiter *et al.* (2020).

### 3.6. Importance of the AtSec62 C-terminus for its function in plants

For further examination of the AtSec62 C-terminal region, complementation analysis in *atsec62* was conducted by using an *AtSEC62- $\Delta$ TMD3/C* construct under the control of the endogenous promoter (Figure 9b, Figure 13a). Two lines of homozygous *atsec62* plants carrying respective constructs were identified and named *pAtSEC62::AtSEC62- $\Delta$ TMD3/C* #30-23 and *pAtSEC62::AtSEC62- $\Delta$ TMD3/C* #12-22 (Figure 13b). In contrast to complementation with the full-length AtSec62, the truncated AtSec62- $\Delta$ TMD3/C was neither able to rescue the *atsec62* growth phenotype nor the observed silique phenotype, even though respective transcripts were present (Figure 13c – e). Siliques of seven- to eight-week-old #30-23 and #12-22 plants have a length of  $0.55 \pm 0.29$  cm ( $n = 14$ ) and  $0.52 \pm 0.14$  cm ( $n = 18$ ) similar to *atsec62* with

$0.51 \pm 0.15$  cm ( $n = 17$ ), while wild-type siliques have a length of  $1.59 \pm 0.13$  cm ( $n = 16$ ) (shown as mean  $\pm$  SD). These results indicate that the AtSec62 C-terminal region and especially the C-terminus facing the ER lumen, is critical for proper AtSec62 function or stability.

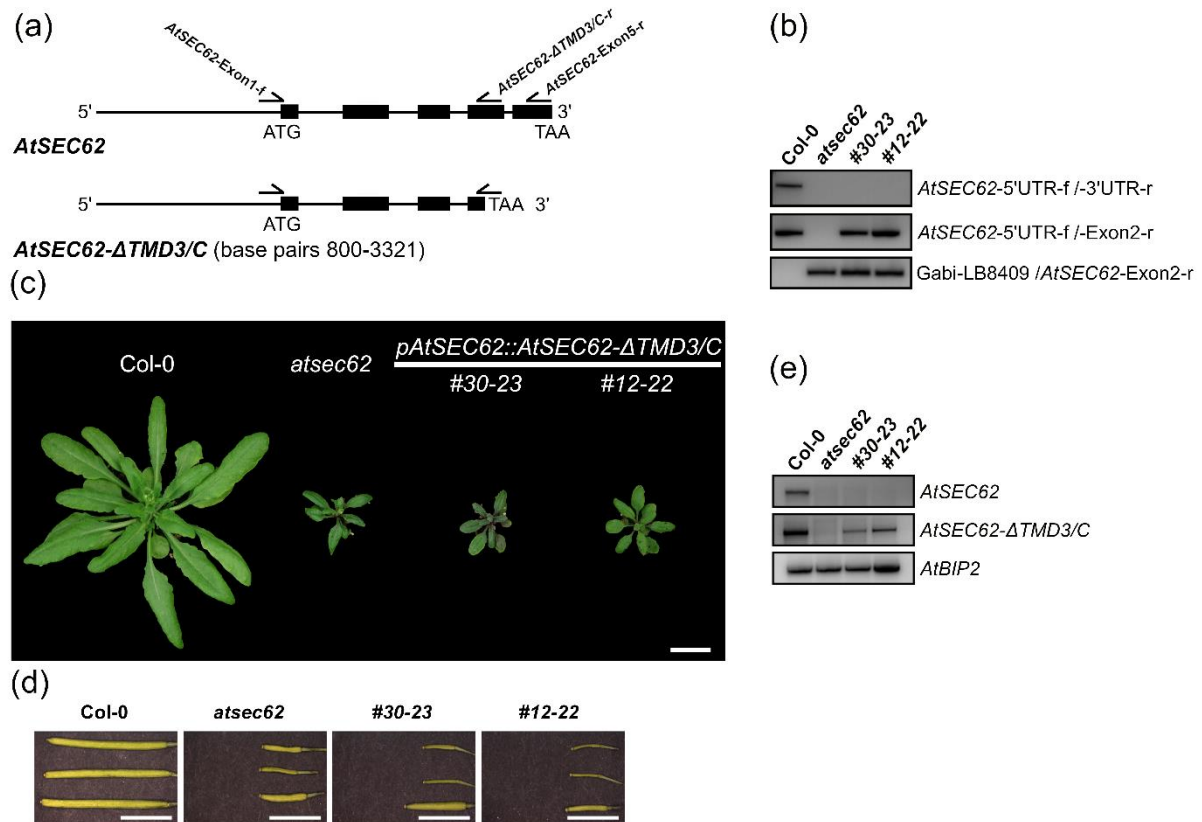


**Figure 13: Complementation analysis in *atsec62* using *AtSEC62-ΔTMD3/C*.** (a) Scheme of full length *AtSEC62* and the truncated *AtSEC62-ΔTMD3/C* construct. (b) Genotyping PCR for Col-0 and *atsec62* plants as well as lines carrying constructs for expression of *AtSEC62-ΔTMD3/C*, *AtSEC62-ΔTMD3/C* #30-23 and #12-22, using the oligonucleotides indicated in Figure 5a. (c) Phenotype of five-week-old Col-0 and *atsec62* as well as #30-23 and #12-22 plants. Scale bar represents 2 cm. (d) Siliques of seven- to eight-week-old Col-0, *atsec62*, #30-23 and #12-22 plants. Scale bars represent 5 mm. (e) RT-PCR for *AtSEC62* or *AtSEC62-ΔTMD3/C* and the control *AtBIP2* using Col-0, *atsec62*, #30-23 and #12-22. Oligonucleotide binding sites for *AtSEC62-Exon1-f*, *AtSEC62-ΔTMD3/C-r* and *AtSEC62-Exon5-r* in *AtSEC62* or *AtSEC62-ΔTMD3/C* are indicated in (a). Figure taken from Mitterreiter *et al.* (2020).

### 3.7. Identification of potential AtSec62 and AtTPR7 interaction partners by mass spectrometry

Since AtSec62 and AtTPR7 are putative components of the *Arabidopsis* Sec post-translocon (Schweiger *et al.* 2012, Schweiger and Schwenkert 2013), potential interaction partners or preproteins destined for translocation should be identified. Respective candidates for AtTPR7 have been identified recently by isolating

microsomal membranes from an inducible *srα* RNAi-line and subsequent mass spectrometric analysis (Dissertation of Brylok 2018). Among identified proteins were the  $\beta$ -glycosyl hydrolase AtPYK10 (Matsushima *et al.* 2003, Nagano *et al.* 2005, Nagano *et al.* 2008), the GDSL-like lipase AtGLL23 (Nagano *et al.* 2008, Jancowski *et al.* 2014) and the AtPYK10 interacting AtPBP1 (Nagano *et al.* 2005, Nagano *et al.* 2008) being involved in glucosinolate biosynthesis as well as the prohibitin AtPHB3 (Christians and Larsen 2007, Van Aken *et al.* 2007, Wang *et al.* 2010b) (summarised in Table 8). Chloroplast localised pSSU from tobacco was additionally used for following analyses as AtTPR7 was initially suggested to be an outer envelope protein associating with pSSU (von Loeffelholz *et al.* 2011).

**Table 8: Candidate preproteins for post-translational translocation via AtTPR7.** Proteins were selected based on mass spectrometric analysis (Dissertation of Brylok 2018) or recent publications (von Loeffelholz *et al.* 2011).

Protein	Localisation <sup>1</sup>	Biological process/ complex/ protein class <sup>1</sup>
AtGLL23	ER (transiently)	GDSL-like lipase
AtPBP1	cytosol	inhibitor-type lectin/ PYK10 interacting
AtPHB3	nucleus/ mitochondria/ plasma membrane	mitochondrial and cell metabolism and biogenesis/ ethylene and NO signalling
pSSU	chloroplast	RuBisCO
AtPYK10	ER bodies	$\beta$ -glucosidase

<sup>1</sup> Localisation and biological process/ complex or protein class of proteins based on aramemnon (<http://aramemnon.uni-koeln.de/>) and UniProt (<https://www.uniprot.org/>) and references therein.

For identifying potential AtSec62 associating or interacting proteins, microsomal membranes were isolated out of wild-type plants either expressing GFP-Atsec62 or AtSec62-GFP (Figure 14a) or untransformed wild-type plants which were used as control.

Mass spectrometric analysis was performed after conducting GFP-trap<sup>®</sup> pull-down experiments to isolate GFP-fusion proteins and associated proteins out of the plant lysate (Figure 14b).

The obtained score was aggregated for all protein sequences of the same accession number and protein sequences which were present in equal amounts in the wild-type control and the actual samples were omitted. Proteins were selected for further analysis based on their overall score, their predicted localisation and their potential involvement in certain cellular pathways or processes.

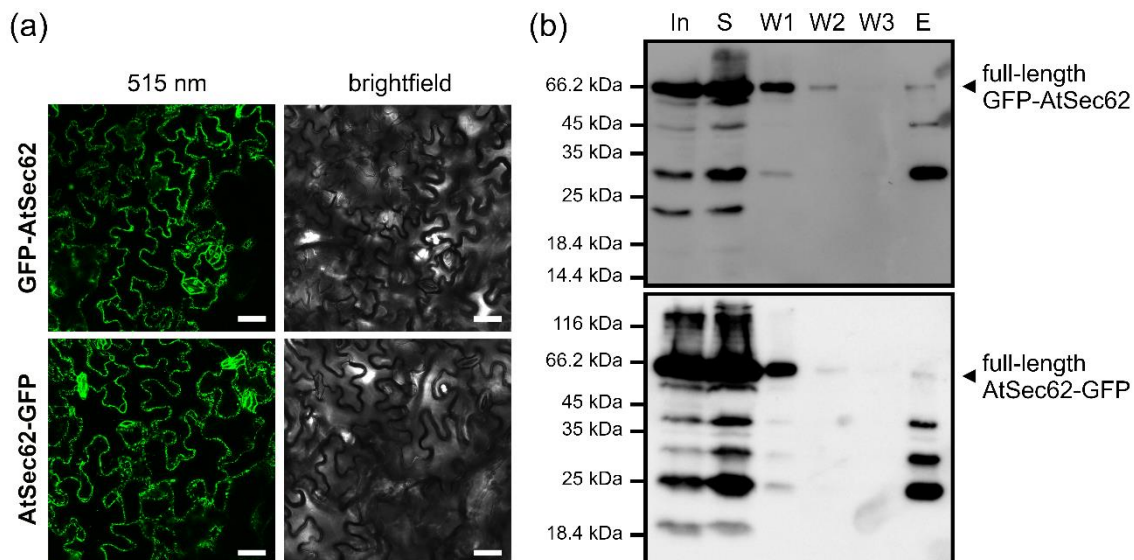


**Figure 14: GFP-trap<sup>®</sup> pull-down using stable AtSec62 GFP-fusion lines.** (a) Col-0 plants expressing GFP-AtSec62 or AtSec62-GFP upon stable transfection by floral dip. Fluorescent signals were detected by confocal laser scanning microscopy in intact leaves. Scale bars represent 50  $\mu\text{m}$ . (b) GFP-trap<sup>®</sup> pull-down using microsomal membranes isolated from plants expressing either GFP-AtSec62 or AtSec62-GFP. 2% of the input (In, corresponding to 25  $\mu\text{g}$  microsomal membranes), 2.5% supernatant (S), 3% of washes (W1 – W3) and 5% elution (E) were loaded onto SDS-PAGE gels. Immunodetection of GFP-fusion proteins was performed using an anti-GFP antibody. Full length proteins are indicated by black arrows.

Hereby identified proteins included the ER luminal HSP70-like chaperone AtBiP1/2 (Maruyama *et al.* 2010, Maruyama *et al.* 2014), the HSP90-type chaperone AtSHD (Krishna and Gloor 2001, Ishiguro *et al.* 2002, Chong *et al.* 2015), the calnexin-type lectin chaperone AtCNX1 (Liu *et al.* 2017, Vu *et al.* 2017), the cytochrome P450 monooxygenase AtCYP83A1 being involved in glucosinolate biosynthesis (Bak and Feyereisen 2001, Hemm *et al.* 2003, Naur *et al.* 2003), AtDGL1 being a putative component of the oligosaccharyltransferase complex (Lerouxel *et al.* 2005), the putative thioglucoside glucohydrolase AtTGG1 (Zhao *et al.* 2008), the vacuolar V-type ATPase component AtVHA-A (Sze *et al.* 2002, Jaquinod *et al.* 2007) and the  $\beta$ -carbonic anhydrase AtCA1 $\beta$  (Fabre *et al.* 2007, Hu *et al.* 2015, Huang *et al.* 2017) (compare to Table 9, protein names and putative functions based on aramemnon (<http://aramemnon.uni-koeln.de/>) and UniProt (<https://www.uniprot.org/>), for full list of identified proteins see Table A1).

**Table 9: Potential AtSec62 interacting/ associating proteins selected for further interaction analysis.** Score is given for proteins identified by GFP-trap® pull-down with AtSec62-GFP or GFP-AtSec62 and subsequent mass spectrometric analysis.

Protein	Localisation <sup>1</sup>	Biological process/ complex/ protein class <sup>1</sup>	Origin <sup>2</sup>	Score <sup>3</sup>	
				AtSec62 -GFP	GFP- AtSec62
AtATG8e	cytosol/ autophagosome	autophagy	P	-	-
AtBiP2	ER	Sec translocation pathway/ chaperone	MS	468.91	n.d.
AtCA1β	chloroplast/ cytosol	β-carbonic anhydrase	MS	861.56	n.d.
AtCNX1	ER	ER stress response	MS	865.66	1250.723
AtCYP83A1	ER	glucosinolate biosynthesis	MS	602.83	674.437
AtDGL1	ER	N-linked glycosylation	MS	n.d.	611.146
AtERdj2A	ER	Sec translocation pathway	IS	-	-
AtGET1	ER	GET pathway	CG	-	-
AtGET3a	cytosol	GET pathway	IS	-	-
AtGET4	cytosol	GET pathway	IS	-	-
AtSec61α1	ER	Sec translocation pathway	IS	-	-
AtSec61β1	ER	Sec translocation pathway	IS	-	-
AtSec61γ1	ER	Sec translocation pathway	IS	-	-
AtSHD	ER	chaperone	MS	348.6	1136.636
AtSYP123	ER/ Golgi	vesicle trafficking	CG	-	-
AtSYP43	ER/ Golgi	vesicle trafficking	CG	-	-
AtTGG1	secretory pathway/ vacuole	glucosinolate biosynthesis	MS	234.623	591.76
AtTPR7	ER	Sec translocation pathway	P	-	-
AtVHA-A	vacuole	V-type ATPase	MS	951.937	739.36

<sup>1</sup> Localisation and biological process/ complex or protein class of proteins based on aramemnon (<http://aramemnon.uni-koeln.de/>) and UniProt (<https://www.uniprot.org/>) and references therein.

<sup>2</sup> CG: Christopher Grefen (personal communication), IS: independent selection, MS: identified by mass spectrometric analysis, P: recent publication (AtATG8e in Hu *et al.* 2020, AtTPR7 in Schweiger and Schwenkert 2013).

<sup>3</sup> n.d.: not detected in mass spectrometric analysis.

Besides proteins identified by mass spectrometry, other interesting candidate proteins were selected (Table 9). These include AtATG8e, which was recently proposed to be interacting with AtSec62 during autophagy (Hu *et al.* 2020), as well as other putative components of the *Arabidopsis* Sec translocon like AtSec61 $\alpha$ 1, AtSec61 $\beta$ 1, AtSec61 $\gamma$ 1, AtERdj2A (Yamamoto *et al.* 2008) and AtTPR7 (Schweiger *et al.* 2012), which has already been shown to be interacting with AtSec62 (Schweiger and Schwenkert 2013).

Additionally, AtGET1, AtGET3a and AtGET4 as components of the *Arabidopsis* GET-pathway were selected (Srivastava *et al.* 2017, Xing *et al.* 2017), as AtGET1 was shown to interact with AtSec62 (Christopher Grefen, personal communication). AtSYP123 (Ichikawa *et al.* 2014) and AtSYP43 (Kim and Bassham 2013) were used as exemplary tail-anchored proteins with AtSYP123 being inserted into the ER membrane *via* the GET-pathway (Xing *et al.* 2017). However, most of the proteins identified by mass spectrometry either contained an N-terminal signal sequence or belonged to the class of signal anchor proteins, rather than being tail-anchored proteins.

### **3.8. Verification of AtSec62 associating or interacting proteins**

To confirm association or interaction of identified proteins with AtSec62, rBiFC experiments were performed. The two halves of the fluorophore, nYFP and cYFP, are fused to potentially interacting proteins while cytosolic RFP is expressed as transformation control (Grefen and Blatt 2012). N- and C-terminal fusions of cYFP to proteins were performed depending on the presence of a signal peptide or tail-anchor and functional protein domains. After infiltrating tobacco leaves, fluorescent signals were detected by confocal laser scanning microscopy in intact leaves after two days incubation.

When focusing on the nuclear region, it is evident that the RFP signal is not detected in the YFP channel (compare to Grefen and Blatt 2012). However, as general signal intensity and respective RFP expression drastically varied between samples and due to YFP background signals (compare to Figure A3), quantification of fluorescent signals was not performed in this study.

Interaction of AtSec62 with other Sec translocon components was initially monitored. While the interaction with the chaperone docking protein AtTPR7 was confirmed (compare to Schweiger and Schwenkert 2013), no distinct fluorescent signal was detectable for AtSec62 and AtBiP2 or AtERdj2A (Figure 15). Intense fluorescent

signals were observable for the putative components of the Sec61 protein-conducting channel, AtSec61 $\beta$ 1 and AtSec61 $\gamma$ 1, whereas only faint signals were detectable for AtSec61 $\alpha$ 1 (Figure 15).

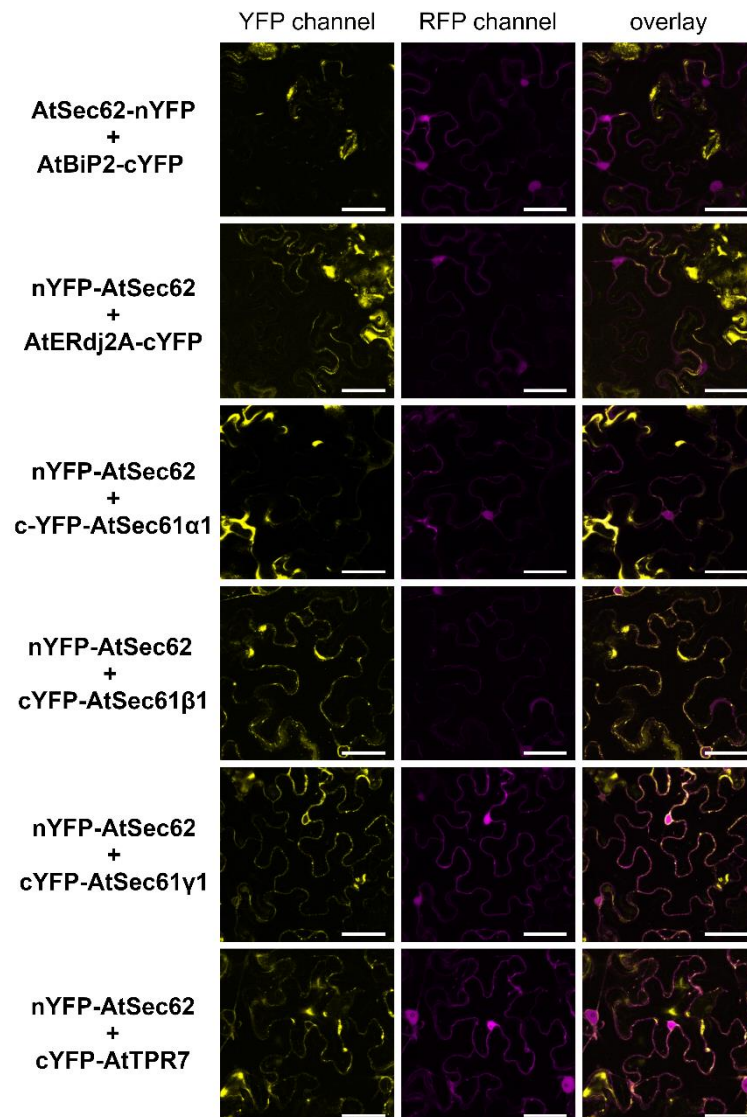


**Figure 15: rBiFC analysis of AtSec62 and other components of the Sec translocon.** Tobacco leaves were transformed with *Agrobacteria* carrying rBiFC constructs for expression of nYFP-AtSec62 or AtSec62-nYFP and AtBiP2-cYFP, AtERdj2A-cYFP, cYFP-AtSec61 $\alpha$ 1, cYFP-AtSec61 $\beta$ 1, cYFP-AtSec61 $\gamma$ 1 or cYFP-AtTPR7 as well as cytosolic RFP. Fluorescent signals were detected by confocal laser scanning microscopy in intact leaves. Scale bars represent 50  $\mu$ m.

Besides observed signals with other Sec translocon components, fluorescent signals were also detectable for AtSec62 and AtATG8e (Figure 16), confirming the proposed interaction of both proteins based on co-localisation upon ER stress (Hu *et al.* 2020). Moreover, fluorescent signals were monitored for proteins identified *via* GFP-trap pull-down experiments, including AtCNX1, AtCYP83A1, AtDGL1 and AtCA1 $\beta$ , which was

localised to the cytosol in this study (Figure A4, compare to Fabre *et al.* 2007, Hu *et al.* 2015, Huang *et al.* 2017), whereas no signal was detectable for AtSHD, AtTGG1 and AtVHA-A (Figure 16).

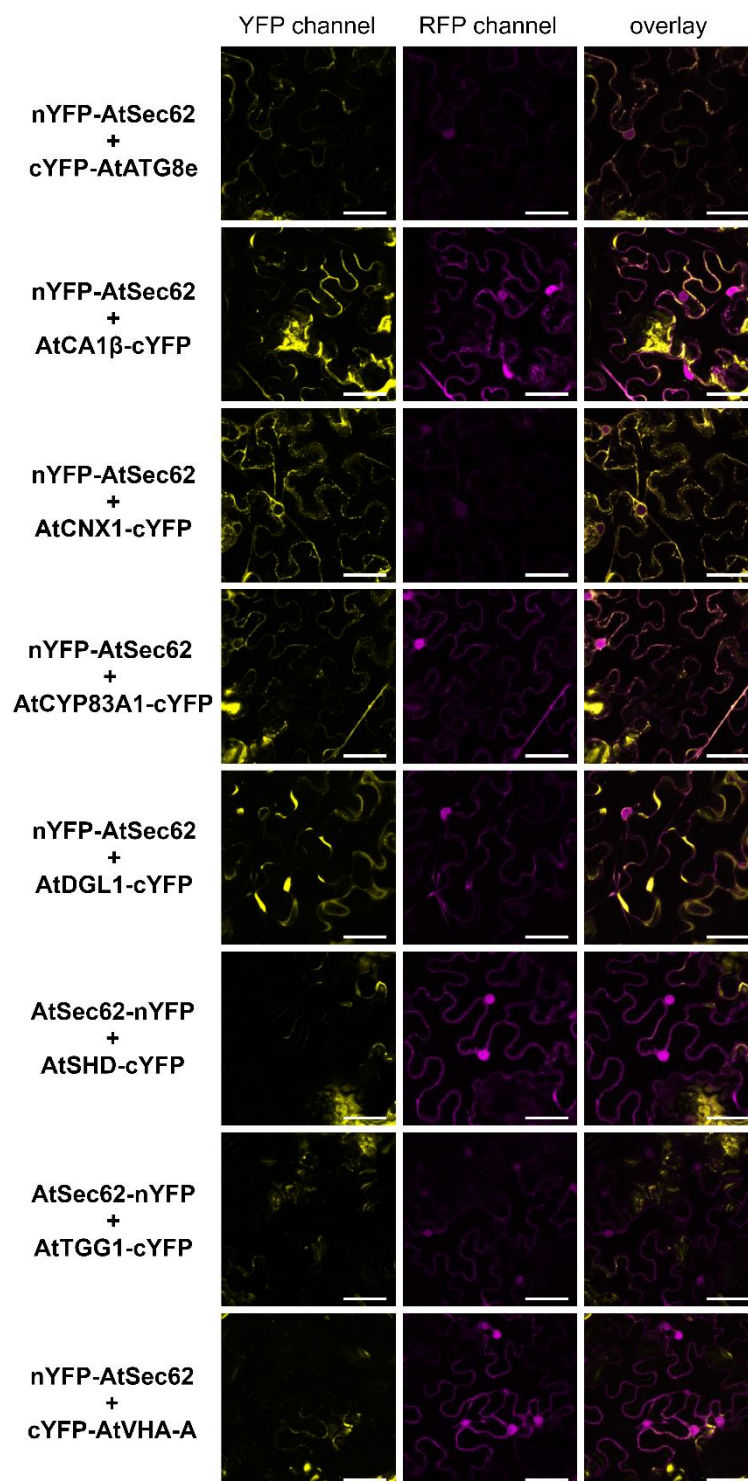


**Figure 16: rBiFC analysis of AtSec62 and potentially interacting or associating proteins.** Tobacco leaves were transformed with *Agrobacteria* carrying rBiFC constructs for expression of nYFP-AtSec62 or AtSec62-nYFP and cYFP-AtATG8e, AtCA1β-cYFP, AtCNX1-cYFP, AtCYP83A1-cYFP, AtDGL1-cYFP, AtSHD-cYFP, AtTGG1-cYFP or cYFP-AtVHA-A as well as cytosolic RFP. Fluorescent signals were detected by confocal laser scanning microscopy in intact leaves. Scale bars represent 50 μm.

When testing for potential interactions with GET-pathway components and exemplary tail-anchored proteins, fluorescent signals were only detectable for AtSec62 and AtGET1, AtGET3a or AtSYP123 but not for AtGET4 or AtSYP43 (Figure 17). These results indicate that AtSec62 might be additionally involved in the GET-pathway.

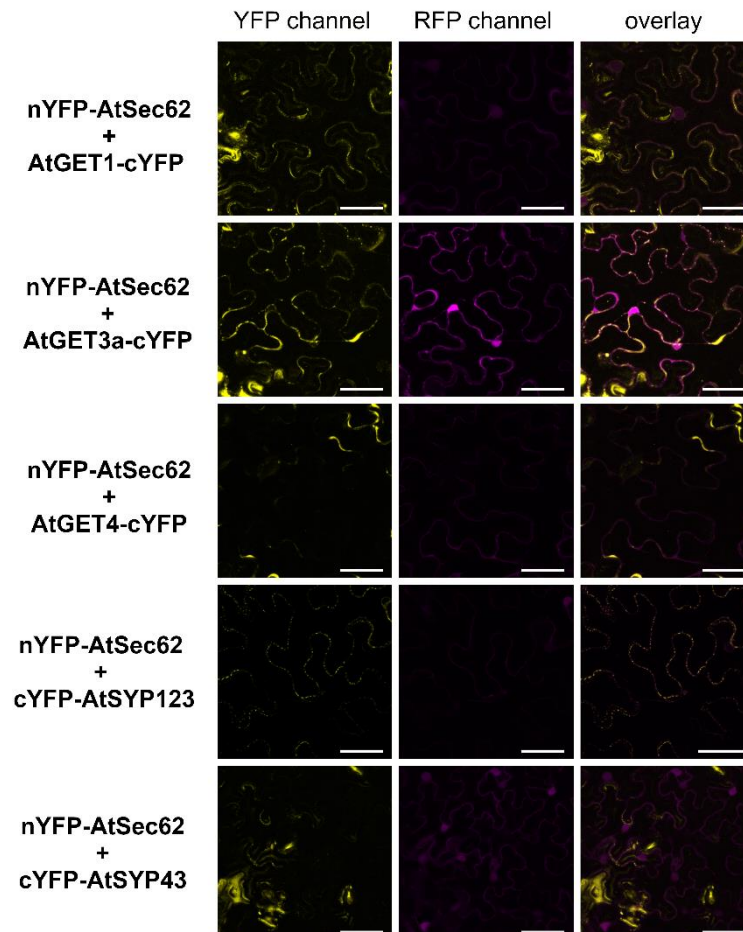


**Figure 17: rBiFC analysis of AtSec62 and components of the GET pathway or tail-anchored proteins.** Tobacco leaves were transformed with *Agrobacteria* carrying rBiFC constructs for expression of nYFP-AtSec62 and AtGET1-cYFP, AtGET3a-cYFP, AtGET4-cYFP, cYFP-AtSYP123 or cYFP-AtSYP43 as well as cytosolic RFP. Fluorescent signals were detected by confocal laser scanning microscopy in intact leaves. Scale bars represent 50  $\mu\text{m}$ .

To further test this hypothesis and to investigate whether AtSec62 recruits AtGET3a to the ER membrane in a similar manner than AtGET1, recruitment assays were performed (Christopher Grefen, personal communication) (Figure 18a).

For this purpose, constructs coding for expression of AtGET3a-CFP, AtSec62-YFP and AtSec62-N-YFP were generated and co-transformed into tobacco leaves together with the helper plasmid p19 to enhance protein expression. Fluorescent signals were then monitored by confocal laser scanning microscopy. Faint signals for AtGET3a-CFP were also detectable in the YFP channel, while intense signals for AtSec62-YFP and

AtSec62-N-YFP were only monitored in the YFP channel, confirming that CFP signals in co-transformed tobacco leaves indeed originated from AtGET3a-CFP (Figure 18b).

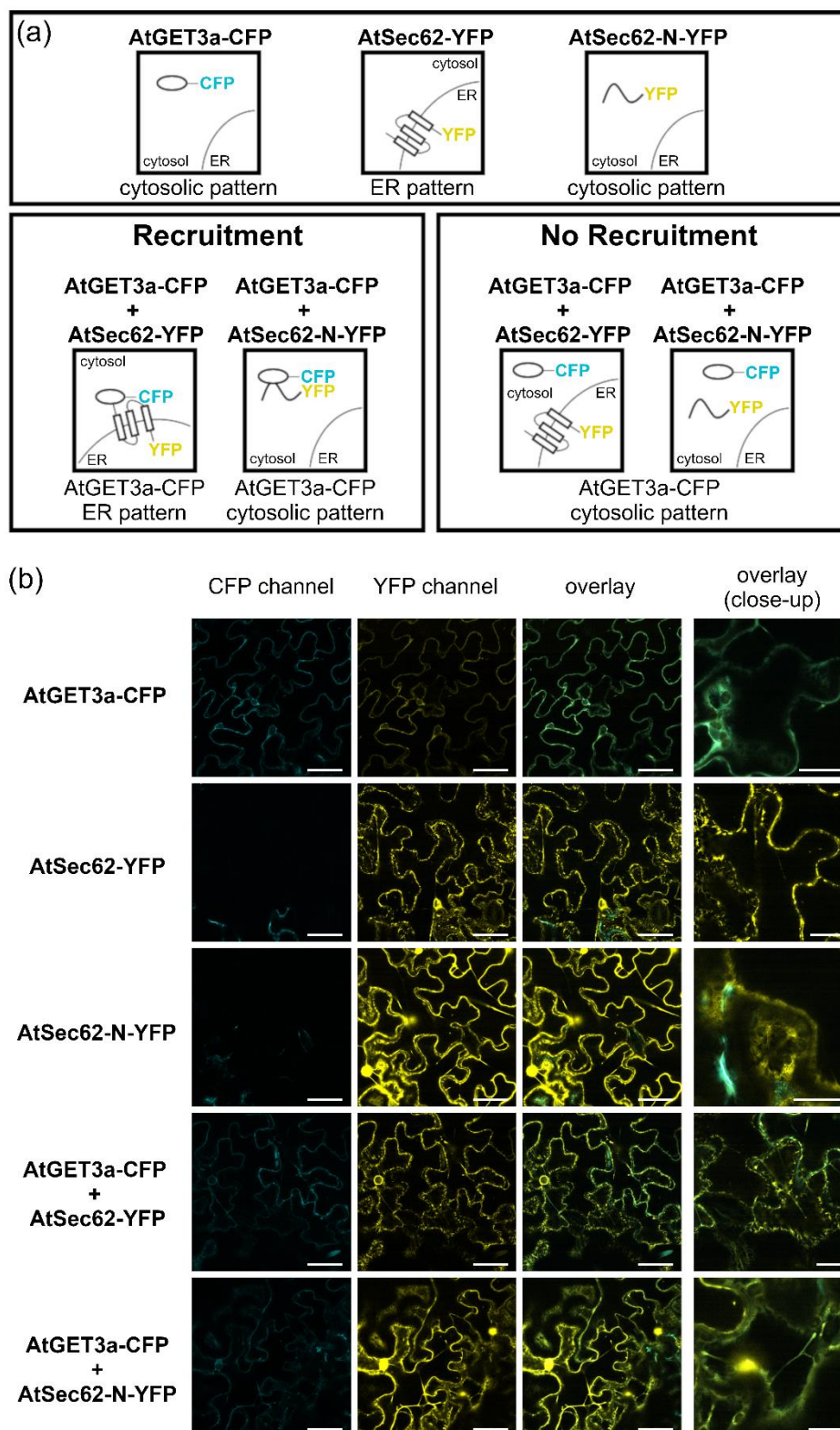


**Figure 18: Recruitment assay for AtGET3a and AtSec62.** (a) Schematic overview of the recruitment assay setup. Upper panel shows single constructs while lower panels show co-transformed constructs in case of recruitment or without recruitment. (*continued on next page*)

(b) Tobacco leaves were co-transformed with *Agrobacteria* carrying the helper plasmid p19 and constructs for AtGET3a-CFP, AtSec62-YFP, AtSec62-N-YFP, AtGET3a-CFP and AtSec62-YFP or AtGET3a-CFP and AtSec62-N-YFP. Fluorescent signals were detected by confocal laser scanning microscopy in intact leaves. An overlay of signals obtained in the CFP and the YFP channel and a close-up are shown. Scale bars represent 50  $\mu\text{m}$  and 20  $\mu\text{m}$  for close-ups.

Similar to previous GFP-localisation experiments, AtSec62-YFP localises to the ER, while AtSec62-N-YFP, lacking all transmembrane domains, localises to the cytosol and also migrates to the nucleus (Figure 18b). Signals for AtGET3a-CFP were detectable in the cytosol when expressed alone or when co-expressed with AtSec62-YFP and AtSec62-N-YFP (Figure 18b), indicating that AtSec62 is not recruiting it to the ER membrane.

### 3.9. Confirmation of potential preproteins for post-translational translocation

To confirm candidate preproteins for post-translation translocation, *in vitro* pull-down experiments were performed. Preproteins were *in vitro* translated and labeled with  $^{35}\text{S}$ -methionine, while Strep-tagged chaperones and His-tagged AtTPR7 constructs were overexpressed in *Escherchia coli* and subsequently purified (Figure A1a, b).

If proteins were destined for post-translational import into the ER *via* AtTPR7, they should be interacting with cytosolic chaperones like AtHSP70-1 and AtHSP90.2. AtPHB3, AtPYK10 and AtGLL23 were bound by AtHSP70-1 as well as AtHSP90.2, whereas an interaction of the cytosolic AtPBP1 with both chaperones was not detectable (Figure 19a). As expected, pSSU was rather bound by AtHSP70-1 than HSP90.2 (May and Soll 2000, Fellerer *et al.* 2011) (compare to Figure 19a).

The interaction of respective candidate preproteins with AtTPR7 should be investigated afterwards. For this purpose, recombinant AtTPR7 $\Delta$ TMD and AtTPR7 $\Delta$ TPR $\Delta$ TMD were used, both lacking the C-terminal transmembrane domain and AtTPR7 $\Delta$ TPR $\Delta$ TMD additionally missing the TPR domain being required for interaction with AtHSP70-1 and AtHSP90.2 (Schweiger *et al.* 2012, Schweiger *et al.* 2013). AtPHB3, AtPYK10 and AtGLL23 were bound by AtTPR7 $\Delta$ TMD, while interaction was slightly reduced for AtTPR7 $\Delta$ TPR $\Delta$ TMD (Figure 19b). No interaction was observable for AtPBP1, whereas a very faint signal was detectable for pSSU corresponding to unspecific binding or low amounts of AtTPR7 being indeed present in chloroplasts (von Loeffelholz *et al.* 2011, Schweiger *et al.* 2012) (Figure 19b).

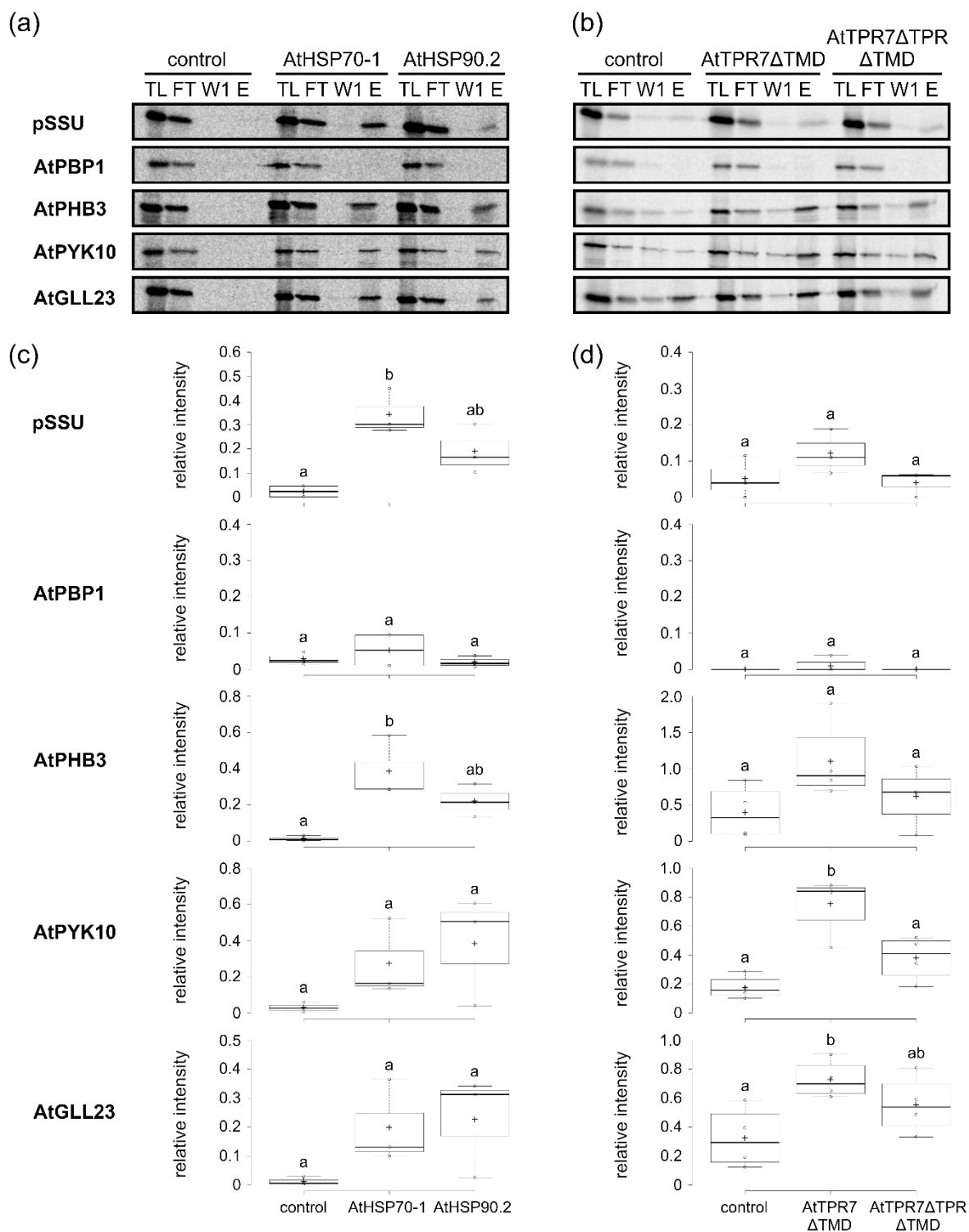


**Figure 19: Candidate preproteins for post-translational translocation.** *In vitro* pull-down assay using  $^{35}\text{S}$ -labelled preproteins (pSSU, AtPBP1, AtPHB3, AtPYK10 and AtGLL23) and purified Strep-tagged AtHSP70-1 and AtHSP90.2 (a) or His-tagged AtTPR7ΔTMD and AtTPR7ΔTPRΔTMD (b). No Strep-/ His-tagged proteins were added for control samples. 5% of the translation product (TL), 2% of the flow-through (FT) and of the first wash (W1) and the complete elution were loaded. (c) Boxplots depicting relative intensity of signals derived from  $^{35}\text{S}$ -labelled preproteins (pSSU, AtPBP1, AtPHB3, AtPYK10 and AtGLL23) that were adjusted to the actual amount of AtHSP70-1 and AtHSP90.2 and ratioed against the mean signal intensity of the translation product. (continued on next page)

---

Centre lines of boxes show the medians with limits at 25<sup>th</sup> and 75<sup>th</sup> percentiles. Tukey – whiskers extend to 1.5 x interquartile range; individual data points are represented by dots; sample means are indicated by black crosses; sample size  $n = 3$  ( $n = 2$  for pSSU/control and AtPBP1/AtHSP70-1). Differences between samples were validated by one-way ANOVA and subsequent Tukey's post hoc comparison. Mean values with unlike letters were significantly differing between samples. (d) Boxplots as in (c), <sup>35</sup>S-derived signals were adjusted to the actual amount of AtTPR7ΔTMD and AtTPR7ΔTPRΔTMD. Sample size  $n = 4$ ,  $n = 3$  (pSSU).

---

When quantifying signals derived from radiolabelled candidate proteins, observed differences were only significant for pSSU and AtPHB3 regarding their interaction with chaperones (Figure 19c) and for AtPYK10 and AtGLL23 regarding their interaction with AtTPR7ΔTMD (Figure 19d). This might be due to large variation between samples and high background signals for the control samples (compare to Figure 19b), even though clear pattern was observable for all candidate preproteins (compare to Figure 19c, d).

## 4. Discussion

In this study, the importance of AtSec62 for plant growth and development was demonstrated especially regarding male fertility. AtSec62 has three transmembrane domains in contrast to its yeast and mammalian homologues and its luminal exposed C-terminus was shown to be crucial for proper AtSec62 function in *Arabidopsis*. In addition, potential AtSec62 and AtTPR7 interacting or associating proteins were identified providing further insight in the composition and translocation substrates of the *Arabidopsis* Sec translocon.

### 4.1. *atsec62* but not *attpr7* displays vegetative and generative growth defects similar to other secretory pathway mutants

An *atsec62* T-DNA insertion line has been isolated and verified on RNA and on protein level and respective complementation lines have proven that lack of AtSec62 is indeed causing the observed generative and vegetative growth defects. Additionally, the absence of respective *AtTPR7* transcript in a recently described *attpr7* mutant line was confirmed and no obvious growth phenotype was detectable in accordance with previous studies (Lister *et al.* 2007, Schweiger *et al.* 2012). These results indicate that AtTPR7 is not essential for ER protein translocation and can probably be bypassed similar to other chaperone docking proteins like chloroplast localised AtToc64 and mitochondrial AtOM64 (Aronsson *et al.* 2007, Lister *et al.* 2007, Schweiger *et al.* 2012), whereas AtSec62 is critical for proper plant growth and development especially regarding male gametophyte development. The observed *atsec62* dwarf-like phenotype and the abnormal pollen morphology have also been shown by another independent study, also confirming the late onset of the aerial phenotype (Hu *et al.* 2020). The altered *atsec62* root morphology with reduced root length but an increased number of lateral roots might be due to disturbed ER protein translocation, also interfering with hormone signalling and root nutrient uptake, for example regarding phosphate (compare to Pérez-Torres *et al.* 2008, Malhotra *et al.* 2018). This would in return also affect growth of aerial plant tissues, thereby contributing to the observed phenotype maybe even in a time-displaced manner.

Besides general vegetative growth defects, *atsec62* displays defects in male gametophyte development. Only clustered pollen-like structures are observable in mutant anthers instead of distinct pollen grains and pollen development appears to be delayed in contrast to wild-type anthers. Due to this delayed pollen development as

well as reduced and probably temperature-dependent pollen tube germination, *atsec62* pollen might not reach the female gametophyte in time for proper pollination leading to drastically reduced seed yield.

Observed generative defects in male transmission in *atsec62* resemble defects in other mutant lines with defective or missing secretory pathway components (Jakobsen *et al.* 2005, Yamamoto *et al.* 2008, Conger *et al.* 2011, Maruyama *et al.* 2014, Vu *et al.* 2017). For example, polar nuclei fusion and pollen tube growth in *bip1 bip2* are affected, whereas *bip1 bip2 bip3* pollen are not even viable (Maruyama *et al.* 2010, Maruyama *et al.* 2014) and *aterdj2a* as well as *atsec24a-1* pollen fail to properly germinate resulting in male sterility (Yamamoto *et al.* 2008, Conger *et al.* 2011). Similar to AtSec62, AtERdj2A is part of the Sec translocon and is indispensable for translocation and subsequent secretion (Yamamoto *et al.* 2008), while AtSEC24A is probably part of the COPII coat, thereby being involved in selective cargo binding in protein ER export (Kuehn *et al.* 1998, Conger *et al.* 2011). Reduced pollen viability and tube growth were also observed for the *cnx1 crt1 crt2 crt3* quadruple mutant, lacking ER resident calnexin and calreticulin, both involved in protein quality control (Vu *et al.* 2017). Moreover, AtMIA is essential for protein secretion due to its involvement in vesicle trafficking and *mia-1* pollen not only fail to germinate *in vitro* but also stick to the anthers probably due to remnants of the pollen mother cell and the callosic wall still attached to the pollen grains (Jakobsen *et al.* 2005). However, protein secretion from tapetal cells is required for degradation of callose and the pollen mother cell wall (Stieglitz 1977, Rhee *et al.* 2003, Lu *et al.* 2014) as well as for pollen exine formation, which among others depends on secreted lipid transfer proteins becoming part of the microspore surface (Huang *et al.* 2013).

Incomplete removal of the callosic wall and the pollen mother cell wall might likewise be the reason for clustered pollen-like structures in *atsec62* next to other effects caused by defective protein translocation and subsequent protein secretion similar to *aterdj2a* (Yamamoto *et al.* 2008).

Defective pollen development and reduced seed germination match the *AtSEC62* expression pattern with high expression levels in mature pollen, seeds and during anther development and only moderate expression in vegetative tissue (*Arabidopsis* eFP browser, <http://bar.utoronto.ca/>, Winter *et al.* 2007). Due to the presence of homozygous *atsec62* plants and to *atsec62* (+/-) progeny plants not segregating in the

expected 1:1 ratio for gametophyte mutants, the absence of AtSec62 can presumably be partially bypassed or compensated by an alternative translocation pathway.

Interestingly, the phenotype of the recently described line with AtGET3a overexpression in an *Atget1-1* background resembles the *atsec62* phenotype, also displaying impaired growth, shorter roots and reduced seed set (Xing *et al.* 2017), while *Atget1-1* alone has no severe phenotype (Srivastava *et al.* 2017, Xing *et al.* 2017). For this reason, Xing *et al.* (2017) suggested that there might be an alternative translocation pathway next to the GET-pathway, which might be disturbed in respective AtGET3a overexpressing lines due to trapping of tail-anchored proteins in the cytosol, thereby causing the observed phenotype. This alternative pathway might be the *Arabidopsis* Sec post-translocon but might involve additional, yet undiscovered components. AtSec62 might otherwise be part of the GET-pathway rather than the actual Sec translocon (Christopher Grefen, personal communication).

#### **4.2. *atsec62* is sensitive towards high-temperature and ER stress**

Besides impaired growth and reduced male fertility of *atsec62* under normal growth conditions, seedling survival after high-temperature treatment is reduced in contrast to wild-type plants and *atsec62* pollen are hardly germinating at all, whereas there is no further effect on seed germination. As storage compounds are already present in seeds, there might only be low ER import rates increasing upon further vegetative growth and therefore causing no effects regarding seed germination.

The increased susceptibility towards high-temperature stress might not only be due to a generally reduced fitness of *atsec62* plants but also to an involvement of AtSec62 in plant thermotolerance.

*atsec62* additionally showed a higher susceptibility towards DTT induced ER stress, while it remained unaffected by Tunicamycin treatment (0.05  $\mu\text{g ml}^{-1}$ ). However, when applying higher concentrations of Tunicamycin (0.1  $\mu\text{g ml}^{-1}$ ), *atsec62* plants turn sensitive with the observed effect being rescued by overexpressing YFP-AtSec62 in an amiRNAi-*atsec62* background (Hu *et al.* 2020). Hu *et al.* (2020) additionally showed an increased sensitivity of *atsec62* and amiRNAi-*atsec62* plants towards NaCl induced salt stress which in return also triggers ER stress in plants. AtSec62 might be involved in the UPR (reviewed by Strasser 2018, Pastor-Cantizano *et al.* 2020, Wang *et al.* 2020) by translocating required components but might also be directly involved in ER stress recovery similar to its mammalian homologues (Linxweiler *et al.* 2013, Fumagalli *et al.* 2016). Hu *et al.* (2020) suggested that AtSec62 acts as an ER-phagy receptor in

plants based on co-localisation of the autophagosome marker AtATG8e as well as on *atsec62*, *atg5* and *atg7* displaying similar survival rates upon Tunicamycin treatment. It was further proposed that AtSec62 has two LC3 interacting region (LIR)/ Atg8-family interacting motifs (AIM) being required for interaction with AtATG8e (Hu *et al.* 2020). Moreover, AtSec62 might also be involved in the salt-induced ER-associated degradation (ERAD) pathway, which was suggested to have an interactive mechanism with the UPR in *Arabidopsis* even though respective mechanisms still remain unknown (Li *et al.* 2017, Hu *et al.* 2020).

#### 4.3. AtSec62 localises to the ER membrane and has three transmembrane domains with its C-terminus being crucial for its function in plants

As expected, due to its interaction with AtTPR7 (Schweiger and Schwenkert 2013) and localisation predictions (<http://aramemnon.uni-koeln.de/>, <https://www.uniprot.org/>), AtSec62 localises to the ER membrane. Hu *et al.* (2020) independently showed that YFP-tagged AtSec62 is an integral membrane protein and co-localises with AtCNX1 and the Sec translocon components AtSec61 $\alpha$ 1 and AtERdj2A.

AtSec62 has a third predicted TMD in contrast to its yeast and mammalian homologues (Deshaies and Schekman 1989, 1990, Müller *et al.* 2010, Schweiger and Schwenkert 2013) and also putative N-glycosylation sites, residing in the C-terminal region, hint towards the AtSec62 C-terminus being exposed to the ER lumen rather than the cytosol (compare to Figure 20). The presence of this putative third transmembrane domain was proven by Split-GFP topology analysis in this study and by protease protection assays of YFP-AtSec62 by Hu *et al.* (2020).

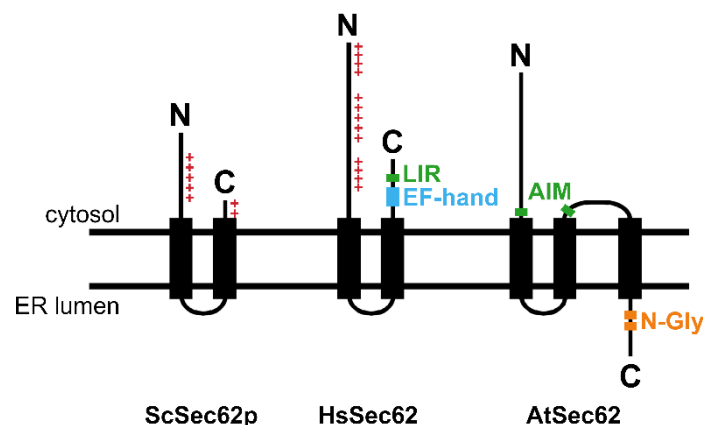


**Figure 20: Topology model and amino acid motifs of Sec62 homologues.** Positively charged regions (red), LIR/ AIM motifs (green), EF-hand motifs (blue) and N-glycosylation sites (N-Gly, orange) in yeast Sec62p (ScSec62p), human Sec62 (HsSec62) and AtSec62 are indicated. Figure taken from Mitterreiter *et al.* 2020, modified. Motifs based on Müller *et al.* 2010, Linxweiler *et al.* 2013, Jung *et al.* 2014, Fumagalli *et al.* 2016 and Hu *et al.* 2020.

To further assess the importance of the prolonged C-terminal region in plants and to test for potential functional conservation, complementation analysis using AtSec62 as well as AtSec62- $\Delta$ TMD3/C was conducted in *atsec62* and *sec62-ts*.

In contrast to full-length AtSec62, AtSec62- $\Delta$ TMD3/C was not able to rescue the observed vegetative and generative growth defects in *atsec62*, indicating that the C-terminal region is essential for proper AtSec62 function in plants. This might also involve membrane insertion of AtSec62 as well as protein stability or folding besides solely functional properties. Its C-terminus might be crucial for interaction with Sec translocon components or translocation substrates. Furthermore, it might be involved in recognising misfolded or unfolded proteins and in promoting further interaction with AtATG8e in course of ER-phagy (Hu *et al.* 2020).

When performing complementation analysis in yeast, neither AtSec62 nor the truncated AtSec62- $\Delta$ TMD3/C was able to restore normal growth of thermosensitive *sec62-ts*, while human Sec62 as well as Sec62 from *Drosophila* and the phytopathogen *Magnaporthe oryzae* were able to rescue the growth phenotype of respective yeast mutants (Noël and Cartwright 1994, Müller *et al.* 2010, Zhou *et al.* 2016). Even though AtSec62- $\Delta$ TMD3/C topology at least resembles Sec62p topology, the inability of plant Sec62 to complement *sec62-ts* might be due to the cytosol exposed C-terminus of Sec62p having an essential function in yeast by contributing to signal peptide recognition (Deshaies and Schekman 1990, Dünwald *et al.* 1999, Wittke *et al.* 2000). Similar to AtERdj2A, AtSec62 might additionally be unable to form proper complexes with yeast Sec translocon components (Yamamoto *et al.* 2008). AtERdj2A as well as AtERdj2B displays only around 20% sequence identity to Sec63p/Sec63, comparable to AtSec62 sharing only 12% and 15% sequence identity with Sec62p and human Sec62 (Yamamoto *et al.* 2008, Schweiger and Schwenkert 2013). Also sequence identity regarding the actual predicted Sec62 domain (compare to Schweiger and Schwenkert 2013) is low with AtSec62 showing only 14% identity to Sec62p/Sec62. Notably, also Sec62p and human Sec62 share only 19% sequence identity regarding the conserved Sec62 domain.

Summarising, AtSec62 and especially its luminal C-terminus is probably not conserved when compared to its yeast and mammalian counterparts and is likely to have acquired a unique function in plants.

#### 4.4. Putative interaction partners of the *Arabidopsis* Sec translocon

To gain further insights into ER protein translocation in *Arabidopsis*, potential interacting/ associating proteins of the Sec translocon components AtSec62 and AtTPR7 were identified also including putative translocation substrates (summarised in Figure 21). An interaction between AtSec62 and AtTPR7 has already been reported (Schweiger and Schwenkert 2013) and was confirmed by rBiFC experiments in this study, while there was no interaction detectable between AtSec62 and AtERdj2A or AtBiP2. This might be due to general low expression of respective constructs and therefore only low signal intensity or it might indicate that AtSec62 is not associating with AtERdj2A in contrast to its yeast and mammalian homologues (Deshaies *et al.* 1991, Panzner *et al.* 1995, Tyedmers *et al.* 2000, Harada *et al.* 2011). Signal peptide recognition in plants might no longer depend on the formation of the Sec62-Sec63 complex but might be conducted by AtSec62 alone and AtERdj2A might only be important for recruiting AtBiP to the translocon (compare to Yamamoto *et al.* 2008). Besides the majority of mammalian Sec62 and Sec63 being not complexed, smaller fractions of Sec62 were associated with Sec61 $\beta$ , while Sec63 was associated with Sec61 $\alpha$  (Meyer *et al.* 2000). Similar results were obtained for the yeast homologues with Sec62p being associated with Sec61 $\beta$ p (Sbh1p) and probably playing a role in TA protein insertion (Tyedmers *et al.* 2000), whereas Sec63p – together with Kar2p – and Sec61 $\alpha$ p (Sec61p) were proposed to be involved in delivering proteins for degradation (Knittler *et al.* 1995, Wiertz *et al.* 1996, Pilon *et al.* 1997, Plemper *et al.* 1997, Tyedmers *et al.* 2000). In line with these observations, fluorescent signals were obtained for AtSec62 together with AtSec61 $\beta$ 1 and additionally with AtSec61 $\gamma$ 1 and faint signals with AtSec61 $\alpha$ 1, indicating that – instead of the respective homologues AtERdj2A/B – AtSec62 might have partially overtaken the function of Sec63p.

A putative interaction or association was observable for AtSec62 and AtGET1, AtGET3a and the TA protein AtSYP123. AtGET3a might not only recruit TA proteins to AtGET1 but also to AtSec62, which might play a comparable role for TA protein insertion as its yeast homologue Sec62p (Tyedmers *et al.* 2000). However, a recruitment of AtGET3a to the ER membrane *via* AtSec62 was not observable in this study. Besides lack of actual recruitment, this might be due to only faint interactions not being detectable due to general low signal intensity of AtGET3a-CFP. As for other potential interacting/ associating proteins, further experiments are required to prove

these interactions and to elucidate the actual function for protein translocation or potential other pathways, thereby also explaining the observed *atsec62* phenotype. Furthermore, an interaction between AtSec62 and AtATG8e was detectable, providing further evidence for the proposed involvement of AtSec62 in ER-phagy (Hu *et al.* 2020). AtSec62 is also interacting with AtCNX1, which is involved in ER quality control (Liu *et al.* 2017, Vu *et al.* 2017), and AtDGL1, which might be part of the oligosaccharyltransferase complex, thereby belonging to the auxiliary Sec translocon machinery (Lerouxel *et al.* 2005). Respective *cnx1 crt1 crt2 crt3* mutant plants – additionally lacking ER resident calreticulin – have a similar phenotype as *atsec62* with drastically affected pollen tube and root growth (Vu *et al.* 2017), indicating that AtSec62 and AtCNX1 might either be involved in the same cellular process or are at least both influencing proper protein translocation and subsequent quality control.

A fluorescent signal was additionally detected for AtSec62 and AtCYP83A1, which is involved in glucosinolate biosynthesis (Bak and Feyereisen 2001, Hemm *et al.* 2003, Naur *et al.* 2003) and might rather be a translocation substrate than a direct AtSec62 interacting protein.

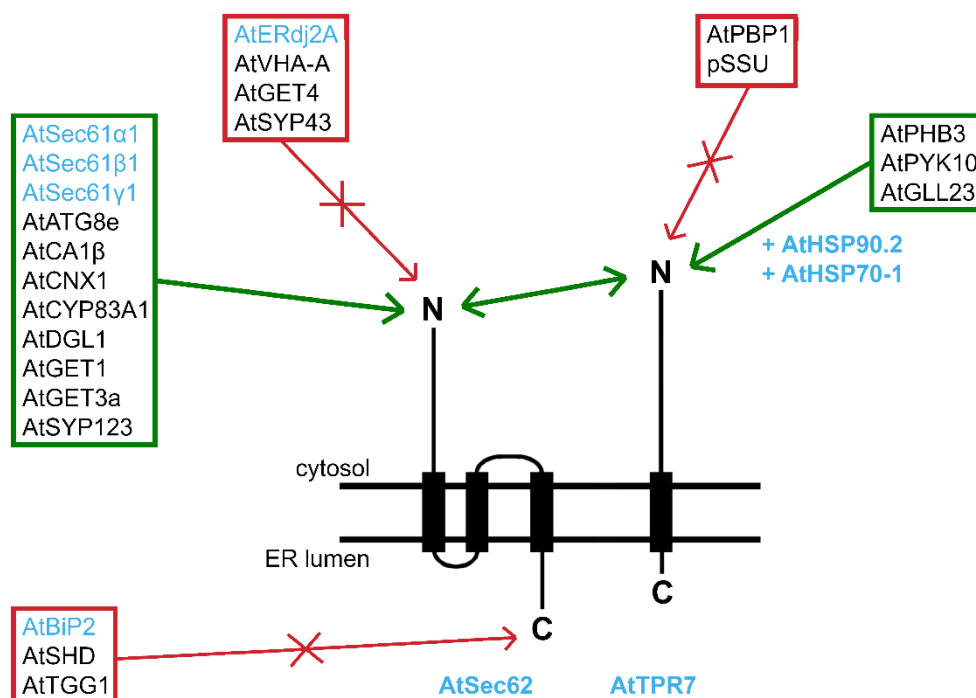


**Figure 21: Analysis of potential AtSec62 and AtTPR7 interacting/ associating proteins.** rBiFC analysis (for AtSec62) and *in vitro* pull-down experiments (for AtTPR7ΔTMD) showed putative interacting/ associating proteins (green boxes and arrows) or non-interacting proteins (red boxes and arrows). Interaction of potential post-translational translocation substrates with AtTPR7 possibly also involves the cytosolic chaperones AtHSP70-1 and/ or AtHSP90.2. Proteins involved in the Sec translocation pathway are highlighted in blue.

Interestingly, an interaction with AtCA1 $\beta$  was observable, which was localised to the cytosol in this study but also shows chloroplast localisation depending on respective splice variants used (Fabre *et al.* 2007, Hu *et al.* 2015). For this reason it might also be considered as translocation substrate similar to other carbonic anhydrases that were reported to enter chloroplasts *via* the ER (Villarejo *et al.* 2005).

As AtTPR7 translocation substrates, proteins were identified that are mainly involved in the glucosinolate pathway, hormone signaling and plant defense (Matsushima *et al.* 2003, Nagano *et al.* 2005, Christians and Larsen 2007, Van Aken *et al.* 2007, Nagano *et al.* 2008, Wang *et al.* 2010b, Jancowski *et al.* 2014). AtPYK10, AtPHB3 and AtGLL23 were shown to interact with cytosolic chaperones as well as with AtTPR7 *via* chaperones as interaction with AtTPR7 lacking the N-terminal TPR domain was reduced (compare to Figure 21). These results provide first insight into potential substrates for post-translational translocation in plants. All three proteins display high overall hydrophobicity scores in contrast to predictions for post-translationally transported yeast proteins (Ng *et al.* 1996, dissertation of Brylok 2018). Substrate recognition by AtTPR7 might occur only for non-essential proteins, thereby explaining the missing *attpr7* phenotype, or AtTPR7 can be bypassed by other proteins – maybe even AtSec62, which might be acting as signal peptide receptor on its own (compare to Schweiger *et al.* 2012).

#### 4.5. Conclusion and future perspectives

In this study, it has been shown that the ER luminal C-terminus of AtSec62 is critical for plant growth and male fertility and that it probably has acquired a unique function in comparison to its yeast and mammalian counterparts.

Potential AtSec62 and AtTPR7 interacting/ associating proteins have been identified but need to be confirmed by additional experiments. For example, ER import experiments should be carried out into plant microsomal membranes to verify potential translocation substrates. Furthermore, additional translocation substrates and potential common features should be identified to predict post-translationally transported proteins in the future.

In summary, this study contributed to understanding ER protein translocation in *Arabidopsis* by providing further insights into the composition of the *Arabidopsis* Sec translocon and by revealing potential translocation substrates.

Nevertheless, the exact function of AtSec62 still remains unknown and will be an interesting issue to address in future studies. These might also reveal whether AtSec62

functions in post-translational translocation only or whether it is also involved in co-translational transport similar to mammalian Sec62 (compare to Panzner *et al.* 1995, Müller *et al.* 2010).

## 5. References

- Alberti, S., Gitler, A. D. and Lindquist, S.** (2007). A suite of Gateway cloning vectors for high-throughput genetic analysis in *Saccharomyces cerevisiae*. *Yeast* **24** (10), 913-919. <https://doi.org/10.1002/yea.1502>.
- Alexander, M. P.** (1969). Differential Staining of Aborted and Nonaborted Pollen. *Stain Technology* **44** (3), 117-122. <https://doi.org/10.3109/10520296909063335>.
- Aronsson, H., Boij, P., Patel, R., Wardle, A., Töpel, M. and Jarvis, P.** (2007). Toc64/OEP64 is not essential for the efficient import of proteins into chloroplasts in *Arabidopsis thaliana*. *The Plant Journal* **52** (1), 53-68. <https://doi.org/10.1111/j.1365-313X.2007.03207.x>.
- Ast, T., Cohen, G. and Schuldiner, M.** (2013). A Network of Cytosolic Factors Targets SRP-Independent Proteins to the Endoplasmic Reticulum. *Cell* **152** (5), 1134-1145. <https://doi.org/10.1016/j.cell.2013.02.003>.
- Ast, T. and Schuldiner, M.** (2013). All roads lead to Rome (but some may be harder to travel): SRP-independent translocation into the endoplasmic reticulum. *Crit Rev Biochem Mol Biol* **48** (3), 273-288. <https://doi.org/10.3109/10409238.2013.782999>.
- Aviram, N., Ast, T., Costa, E. A., Arakel, E. C., Chuartzman, S. G., Jan, C. H., Haßdenteufel, S., Dudek, J., Jung, M., Schorr, S., Zimmermann, R., Schwappach, B., Weissman, J. S. and Schuldiner, M.** (2016). The SND proteins constitute an alternative targeting route to the endoplasmic reticulum. *Nature* **540** (7631), 134-138. <https://doi.org/10.1038/nature20169>.
- Aviram, N. and Schuldiner, M.** (2017). Targeting and translocation of proteins to the endoplasmic reticulum at a glance. *J Cell Sci* **130** (24), 4079-4085. <https://doi.org/10.1242/jcs.204396>.
- Bak, S. and Feyereisen, R.** (2001). The involvement of two p450 enzymes, CYP83B1 and CYP83A1, in auxin homeostasis and glucosinolate biosynthesis. *Plant Physiol* **127** (1), 108-118. <https://doi.org/10.1104/pp.127.1.108>.
- Becker, T., Bhushan, S., Jarasch, A., Armache, J. P., Funes, S., Jossinet, F., Gumbart, J., Mielke, T., Berninghausen, O., Schulten, K., Westhof, E., Gilmore, R., Mandon, E. C. and Beckmann, R.** (2009). Structure of monomeric yeast and mammalian Sec61 complexes interacting with the translating ribosome. *Science* **326** (5958), 1369-1373. <https://doi.org/10.1126/science.1178535>.
- Bergmann, T. J., Fumagalli, F., Loi, M. and Molinari, M.** (2017). Role of SEC62 in ER maintenance: A link with ER stress tolerance in SEC62-overexpressing tumors? *Mol Cell Oncol* **4** (2), e1264351. <https://doi.org/10.1080/23723556.2016.1264351>.
- Bohne, A. V., Schwenkert, S., Grimm, B. and Nickelsen, J.** (2016). Roles of Tetratricopeptide Repeat Proteins in Biogenesis of the Photosynthetic Apparatus. *Int Rev Cell Mol Biol* **324**, 187-227. <https://doi.org/10.1016/bs.ircmb.2016.01.005>.

- Borgese, N. and Gaetani, S.** (1983). In vitro synthesis and post-translational insertion into microsomes of the integral membrane protein, NADH-cytochrome b5 oxidoreductase. *Embo j* **2** (8), 1263-1269.
- Brinker, A., Scheufler, C., von der Mülbe, F., Fleckenstein, B., Herrmann, C., Jung, G., Moarefi, I. and Hartl, F. U.** (2002). Ligand Discrimination by TPR Domains: RELEVANCE AND SELECTIVITY OF EEVD-RECOGNITION IN Hsp70-Hop-Hsp90 COMPLEXES. *Journal of Biological Chemistry* **277** (22), 19265-19275. <https://doi.org/10.1074/jbc.M109002200>.
- Brodsky, J. L., Goeckeler, J. and Schekman, R.** (1995). BiP and Sec63p are required for both co- and posttranslational protein translocation into the yeast endoplasmic reticulum. *Proc Natl Acad Sci U S A* **92** (21), 9643-9646. <https://doi.org/10.1073/pnas.92.21.9643>.
- Brodsky, J. L. and Schekman, R.** (1993). A Sec63p-BiP complex from yeast is required for protein translocation in a reconstituted proteoliposome. *J Cell Biol* **123** (6 Pt 1), 1355-1363. <https://doi.org/10.1083/jcb.123.6.1355>.
- Brylok, T.** (2018). Die SRP-abhängige Proteintranslokation des Chloroplasten und des endoplasmatischen Retikulums. Dissertation, Fakultät für Biologie, Ludwig-Maximilians-Universität München. <https://edoc.ub.uni-muenchen.de/21920/>.
- Cabantous, S., Terwilliger, T. C. and Waldo, G. S.** (2005). Protein tagging and detection with engineered self-assembling fragments of green fluorescent protein. *Nat Biotechnol* **23** (1), 102-107. <https://doi.org/10.1038/nbt1044>.
- Chen, X., VanValkenburgh, C., Liang, H., Fang, H. and Green, N.** (2001). Signal Peptidase and Oligosaccharyltransferase Interact in a Sequential and Dependent Manner within the Endoplasmic Reticulum. *Journal of Biological Chemistry* **276** (4), 2411-2416. <https://doi.org/10.1074/jbc.M007723200>.
- Chirico, W. J., Waters, M. G. and Blobel, G.** (1988). 70K heat shock related proteins stimulate protein translocation into microsomes. *Nature* **332** (6167), 805-810. <https://doi.org/10.1038/332805a0>.
- Chong, L. P., Wang, Y., Gad, N., Anderson, N., Shah, B. and Zhao, R.** (2015). A highly charged region in the middle domain of plant endoplasmic reticulum (ER)-localized heat-shock protein 90 is required for resistance to tunicamycin or high calcium-induced ER stresses. *J Exp Bot* **66** (1), 113-124. <https://doi.org/10.1093/jxb/eru403>.
- Christians, M. J. and Larsen, P. B.** (2007). Mutational loss of the prohibitin AtPHB3 results in an extreme constitutive ethylene response phenotype coupled with partial loss of ethylene-inducible gene expression in Arabidopsis seedlings. *J Exp Bot* **58** (8), 2237-2248. <https://doi.org/10.1093/jxb/erm086>.
- Clough, S. J. and Bent, A. F.** (1998). Floral dip: a simplified method for Agrobacterium-mediated transformation of Arabidopsis thaliana. *Plant J* **16** (6), 735-743. <https://doi.org/10.1046/j.1365-313x.1998.00343.x>.

- Conger, R., Chen, Y., Fornaciari, S., Faso, C., Held, M. A., Renna, L. and Brandizzi, F.** (2011). Evidence for the involvement of the Arabidopsis SEC24A in male transmission. *J Exp Bot* **62** (14), 4917-4926. <https://doi.org/10.1093/jxb/err174>.
- Connolly, T., Rapiejko, P. J. and Gilmore, R.** (1991). Requirement of GTP hydrolysis for dissociation of the signal recognition particle from its receptor. *Science* **252** (5009), 1171-1173. <https://doi.org/10.1126/science.252.5009.1171>.
- Cross, B. C., Sinning, I., Luirink, J. and High, S.** (2009). Delivering proteins for export from the cytosol. *Nat Rev Mol Cell Biol* **10** (4), 255-264. <https://doi.org/10.1038/nrm2657>.
- D'Andrea, L. D. and Regan, L.** (2003). TPR proteins: the versatile helix. *Trends in Biochemical Sciences* **28** (12), 655-662. <https://doi.org/10.1016/j.tibs.2003.10.007>.
- Denic, V., Dötsch, V. and Sinning, I.** (2013). Endoplasmic reticulum targeting and insertion of tail-anchored membrane proteins by the GET pathway. *Cold Spring Harb Perspect Biol* **5** (8), a013334. <https://doi.org/10.1101/cshperspect.a013334>.
- Deshaies, R. J., Koch, B. D., Werner-Washburne, M., Craig, E. A. and Schekman, R.** (1988). A subfamily of stress proteins facilitates translocation of secretory and mitochondrial precursor polypeptides. *Nature* **332** (6167), 800-805. <https://doi.org/10.1038/332800a0>.
- Deshaies, R. J., Sanders, S. L., Feldheim, D. A. and Schekman, R.** (1991). Assembly of yeast Sec proteins involved in translocation into the endoplasmic reticulum into a membrane-bound multisubunit complex. *Nature* **349** (6312), 806-808. <https://doi.org/10.1038/349806a0>.
- Deshaies, R. J. and Schekman, R.** (1989). SEC62 encodes a putative membrane protein required for protein translocation into the yeast endoplasmic reticulum. *J Cell Biol* **109** (6), 2653-2664. <https://doi.org/10.1083/jcb.109.6.2653>.
- Deshaies, R. J. and Schekman, R.** (1990). Structural and functional dissection of Sec62p, a membrane-bound component of the yeast endoplasmic reticulum protein import machinery. *Mol Cell Biol* **10** (11), 6024-6035. <https://doi.org/10.1128/MCB.10.11.6024>.
- Drews, G. N. and Koltunow, A. M.** (2011). The female gametophyte. *Arabidopsis Book* **9**, e0155. <https://doi.org/10.1199/tab.0155>.
- Dünnwald, M., Varshavsky, A. and Johnsson, N.** (1999). Detection of transient in vivo interactions between substrate and transporter during protein translocation into the endoplasmic reticulum. *Mol Biol Cell* **10** (2), 329-344. <https://doi.org/10.1091/mbc.10.2.329>.
- Fabre, N., Reiter, I. M., Becuwe-Linka, N., Genty, B. and Rumeau, D.** (2007). Characterization and expression analysis of genes encoding alpha and beta carbonic anhydrases in Arabidopsis. *Plant Cell Environ* **30** (5), 617-629. <https://doi.org/10.1111/j.1365-3040.2007.01651.x>.
- Fang, H. and Green, N.** (1994). Nonlethal sec71-1 and sec72-1 mutations eliminate proteins associated with the Sec63p-BiP complex from *S. cerevisiae*. *Mol Biol Cell* **5** (9), 933-942. <https://doi.org/10.1091/mbc.5.9.933>.

- Feldheim, D. and Schekman, R.** (1994). Sec72p contributes to the selective recognition of signal peptides by the secretory polypeptide translocation complex. *J Cell Biol* **126** (4), 935-943. <https://doi.org/10.1083/jcb.126.4.935>.
- Fellerer, C., Schweiger, R., Schöngruber, K., Soll, J. and Schwenkert, S.** (2011). Cytosolic HSP90 cochaperones HOP and FKBP interact with freshly synthesized chloroplast preproteins of Arabidopsis. *Mol Plant* **4** (6), 1133-1145. <https://doi.org/10.1093/mp/ssr037>.
- Fraering, P., Imhof, I., Meyer, U., Strub, J. M., van Dorsselaer, A., Vionnet, C. and Conzelmann, A.** (2001). The GPI transamidase complex of *Saccharomyces cerevisiae* contains Gaa1p, Gpi8p, and Gpi16p. *Mol Biol Cell* **12** (10), 3295-3306. <https://doi.org/10.1091/mbc.12.10.3295>.
- Fulga, T. A., Sinning, I., Dobberstein, B. and Pool, M. R.** (2001). SRbeta coordinates signal sequence release from SRP with ribosome binding to the translocon. *Embo j* **20** (9), 2338-2347. <https://doi.org/10.1093/emboj/20.9.2338>.
- Fumagalli, F., Noack, J., Bergmann, T. J., Cebollero, E., Pisoni, G. B., Fasana, E., Fregno, I., Galli, C., Loi, M., Soldà, T., D'Antuono, R., Raimondi, A., Jung, M., Melnyk, A., Schorr, S., Schreiber, A., Simonelli, L., Varani, L., Wilson-Zbinden, C., Zerbe, O., Hofmann, K., Peter, M., Quadroni, M., Zimmermann, R. and Molinari, M.** (2016). Translocon component Sec62 acts in endoplasmic reticulum turnover during stress recovery. *Nat Cell Biol* **18** (11), 1173-1184. <https://doi.org/10.1038/ncb3423>.
- Gilmore, R., Blobel, G. and Walter, P.** (1982a). Protein translocation across the endoplasmic reticulum. I. Detection in the microsomal membrane of a receptor for the signal recognition particle. *J Cell Biol* **95** (2 Pt 1), 463-469. <https://doi.org/10.1083/jcb.95.2.463>.
- Gilmore, R., Walter, P. and Blobel, G.** (1982b). Protein translocation across the endoplasmic reticulum. II. Isolation and characterization of the signal recognition particle receptor. *J Cell Biol* **95** (2 Pt 1), 470-477. <https://doi.org/10.1083/jcb.95.2.470>.
- Görlich, D. and Rapoport, T. A.** (1993). Protein translocation into proteoliposomes reconstituted from purified components of the endoplasmic reticulum membrane. *Cell* **75** (4), 615-630. [https://doi.org/10.1016/0092-8674\(93\)90483-7](https://doi.org/10.1016/0092-8674(93)90483-7).
- Graham, J. B., Canniff, N. P. and Hebert, D. N.** (2019). TPR-containing proteins control protein organization and homeostasis for the endoplasmic reticulum. *Crit Rev Biochem Mol Biol* **54** (2), 103-118. <https://doi.org/10.1080/10409238.2019.1590305>.
- Grefen, C. and Blatt, M. R.** (2012). A 2in1 cloning system enables ratiometric bimolecular fluorescence complementation (rBiFC). *Biotechniques* **53** (5), 311-314. <https://doi.org/10.2144/000113941>.
- Greiner, M., Kreutzer, B., Jung, V., Grobholz, R., Hasenfus, A., Stöhr, R. F., Tornillo, L., Dudek, J., Stöckle, M., Unteregger, G., Kamradt, J., Wullich, B. and Zimmermann, R.** (2011a). Silencing of the SEC62 gene inhibits migratory

- and invasive potential of various tumor cells. *Int J Cancer* **128** (10), 2284-2295. <https://doi.org/10.1002/ijc.25580>.
- Greiner, M., Kreutzer, B., Lang, S., Jung, V., Cavalié, A., Unteregger, G., Zimmermann, R. and Wullich, B.** (2011b). Sec62 protein level is crucial for the ER stress tolerance of prostate cancer. *Prostate* **71** (10), 1074-1083. <https://doi.org/10.1002/pros.21324>.
- Hanahan, D.** (1983). Studies on transformation of *Escherichia coli* with plasmids. *J Mol Biol* **166** (4), 557-580. [https://doi.org/10.1016/s0022-2836\(83\)80284-8](https://doi.org/10.1016/s0022-2836(83)80284-8).
- Harada, Y., Li, H., Wall, J. S., Li, H. and Lennarz, W. J.** (2011). Structural studies and the assembly of the heptameric post-translational translocon complex. *J Biol Chem* **286** (4), 2956-2965. <https://doi.org/10.1074/jbc.M110.159517>.
- Harrison, S. J., Mott, E. K., Parsley, K., Aspinall, S., Gray, J. C. and Cottage, A.** (2006). A rapid and robust method of identifying transformed *Arabidopsis thaliana* seedlings following floral dip transformation. *Plant Methods* **2**, 19. <https://doi.org/10.1186/1746-4811-2-19>.
- Haßdenteufel, S., Sicking, M., Schorr, S., Aviram, N., Fecher-Trost, C., Schuldiner, M., Jung, M., Zimmermann, R. and Lang, S.** (2017). hSnd2 protein represents an alternative targeting factor to the endoplasmic reticulum in human cells. *FEBS Letters* **591** (20), 3211-3224. <https://doi.org/10.1002/1873-3468.12831>.
- Hegde, R. S. and Keenan, R. J.** (2011). Tail-anchored membrane protein insertion into the endoplasmic reticulum. *Nat Rev Mol Cell Biol* **12** (12), 787-798. <https://doi.org/10.1038/nrm3226>.
- Hegde, R. S., Voigt, S., Rapoport, T. A. and Lingappa, V. R.** (1998). TRAM Regulates the Exposure of Nascent Secretory Proteins to the Cytosol during Translocation into the Endoplasmic Reticulum. *Cell* **92** (5), 621-631. [https://doi.org/10.1016/S0092-8674\(00\)81130-7](https://doi.org/10.1016/S0092-8674(00)81130-7).
- Hemm, M. R., Ruegger, M. O. and Chapple, C.** (2003). The *Arabidopsis* ref2 mutant is defective in the gene encoding CYP83A1 and shows both phenylpropanoid and glucosinolate phenotypes. *Plant Cell* **15** (1), 179-194. <https://doi.org/10.1105/tpc.006544>.
- Hu, H., Rappel, W. J., Occhipinti, R., Ries, A., Böhmer, M., You, L., Xiao, C., Engineer, C. B., Boron, W. F. and Schroeder, J. I.** (2015). Distinct Cellular Locations of Carbonic Anhydrases Mediate Carbon Dioxide Control of Stomatal Movements. *Plant Physiol* **169** (2), 1168-1178. <https://doi.org/10.1104/pp.15.00646>.
- Hu, S., Ye, H., Cui, Y. and Jiang, L.** (2020). AtSec62 is critical for plant development and is involved in ER-phagy in *Arabidopsis thaliana*. *J Integr Plant Biol* **62** (2), 181-200. <https://doi.org/10.1111/jipb.12872>.
- Huang, J., Li, Z., Biener, G., Xiong, E., Malik, S., Eaton, N., Zhao, C. Z., Raicu, V., Kong, H. and Zhao, D.** (2017). Carbonic Anhydrases Function in Anther Cell

- Differentiation Downstream of the Receptor-Like Kinase EMS1. *Plant Cell* **29** (6), 1335-1356. <https://doi.org/10.1105/tpc.16.00484>.
- Huang, M.-D., Chen, T.-L. and Huang, A. H.** (2013). Abundant type III lipid transfer proteins in Arabidopsis tapetum are secreted to the locule and become a constituent of the pollen exine. *Plant Physiol* **163** (3), 1218-1229. <https://doi.org/10.1104/pp.113.225706>.
- Ichikawa, M., Hirano, T., Enami, K., Fuselier, T., Kato, N., Kwon, C., Voigt, B., Schulze-Lefert, P., Baluška, F. and Sato, M. H.** (2014). Syntaxin of plant proteins SYP123 and SYP132 mediate root hair tip growth in Arabidopsis thaliana. *Plant Cell Physiol* **55** (4), 790-800. <https://doi.org/10.1093/pcp/pcu048>.
- Ishiguro, S., Watanabe, Y., Ito, N., Nonaka, H., Takeda, N., Sakai, T., Kanaya, H. and Okada, K.** (2002). SHEPHERD is the Arabidopsis GRP94 responsible for the formation of functional CLAVATA proteins. *Embo j* **21** (5), 898-908. <https://doi.org/10.1093/emboj/21.5.898>.
- Itskanov, S. and Park, E.** (2019). Structure of the posttranslational Sec protein-translocation channel complex from yeast. *Science* **363** (6422), 84-87. <https://doi.org/10.1126/science.aav6740>.
- Jakobsen, M. K., Poulsen, L. R., Schulz, A., Fleurat-Lessard, P., Møller, A., Husted, S., Schiøtt, M., Amtmann, A. and Palmgren, M. G.** (2005). Pollen development and fertilization in Arabidopsis is dependent on the MALE GAMETOGENESIS IMPAIRED ANTHEIRS gene encoding a type V P-type ATPase. *Genes Dev* **19** (22), 2757-2769. <https://doi.org/10.1101/gad.357305>.
- Jancowski, S., Catching, A., Pighin, J., Kudo, T., Foissner, I. and Wasteneys, G. O.** (2014). Trafficking of the myosinase-associated protein GLL23 requires NUC/MVP1/GOLD36/ERMO3 and the p24 protein CYB. *Plant J* **77** (4), 497-510. <https://doi.org/10.1111/tpj.12408>.
- Jaquinod, M., Villiers, F., Kieffer-Jaquinod, S., Hugouvieux, V., Bruley, C., Garin, J. and Bourguignon, J.** (2007). A proteomics dissection of Arabidopsis thaliana vacuoles isolated from cell culture. *Mol Cell Proteomics* **6** (3), 394-412. <https://doi.org/10.1074/mcp.M600250-MCP200>.
- Johnson, N., Vildardi, F., Lang, S., Leznicki, P., Zimmermann, R. and High, S.** (2012). TRC40 can deliver short secretory proteins to the Sec61 translocon. *J Cell Sci* **125** (Pt 15), 3612-3620. <https://doi.org/10.1242/jcs.102608>.
- Jones, D. T., Taylor, W. R. and Thornton, J. M.** (1992). The rapid generation of mutation data matrices from protein sequences. *Comput Appl Biosci* **8** (3), 275-282. <https://doi.org/10.1093/bioinformatics/8.3.275>.
- Jung, S. J., Jung, Y. and Kim, H.** (2019). Proper insertion and topogenesis of membrane proteins in the ER depend on Sec63. *Biochim Biophys Acta Gen Subj* **1863** (9), 1371-1380. <https://doi.org/10.1016/j.bbagen.2019.06.005>.
- Jung, S. J., Kim, J. E., Reithinger, J. H. and Kim, H.** (2014). The Sec62-Sec63 translocon facilitates translocation of the C-terminus of membrane proteins. *J Cell Sci* **127** (Pt 19), 4270-4278. <https://doi.org/10.1242/jcs.153650>.

- Karimi, M., Depicker, A. and Hilson, P.** (2007). Recombinational cloning with plant gateway vectors. *Plant Physiol* **145** (4), 1144-1154. <https://doi.org/10.1104/pp.107.106989>.
- Karimi, M., Inzé, D. and Depicker, A.** (2002). GATEWAY vectors for Agrobacterium-mediated plant transformation. *Trends Plant Sci* **7** (5), 193-195. [https://doi.org/10.1016/S1360-1385\(02\)02251-3](https://doi.org/10.1016/S1360-1385(02)02251-3).
- Kim, S. J. and Bassham, D. C.** (2013). Functional redundancy between trans-Golgi network SNARE family members in *Arabidopsis thaliana*. *BMC Biochem* **14**, 22. <https://doi.org/10.1186/1471-2091-14-22>.
- Knittler, M. R., Dirks, S. and Haas, I. G.** (1995). Molecular chaperones involved in protein degradation in the endoplasmic reticulum: quantitative interaction of the heat shock cognate protein BiP with partially folded immunoglobulin light chains that are degraded in the endoplasmic reticulum. *Proc Natl Acad Sci U S A* **92** (5), 1764-1768. <https://doi.org/10.1073/pnas.92.5.1764>.
- Koop, H.-U., Steinmüller, K., Wagner, H., Rößler, C., Eibl, C. and Sacher, L.** (1996). Integration of foreign sequences into the tobacco plastome via polyethylene glycol-mediated protoplast transformation. *Planta* **199** (2), 193-201. <https://doi.org/10.1007/BF00196559>.
- Kriechbaumer, V., von Löffelholz, O. and Abell, B. M.** (2012). Chaperone receptors: guiding proteins to intracellular compartments. *Protoplasma* **249** (1), 21-30. <https://doi.org/10.1007/s00709-011-0270-9>.
- Krieg, U. C., Walter, P. and Johnson, A. E.** (1986). Photocrosslinking of the signal sequence of nascent preprolactin to the 54-kilodalton polypeptide of the signal recognition particle. *Proc Natl Acad Sci U S A* **83** (22), 8604-8608. <https://doi.org/10.1073/pnas.83.22.8604>.
- Krishna, P. and Gloor, G.** (2001). The Hsp90 family of proteins in *Arabidopsis thaliana*. *Cell Stress Chaperones* **6** (3), 238-246. [https://doi.org/10.1379/1466-1268\(2001\)006<0238:thfopi>2.0.co;2](https://doi.org/10.1379/1466-1268(2001)006<0238:thfopi>2.0.co;2).
- Kuehn, M. J., Herrmann, J. M. and Schekman, R.** (1998). COPII-cargo interactions direct protein sorting into ER-derived transport vesicles. *Nature* **391** (6663), 187-190. <https://doi.org/10.1038/344438>.
- Kumar, S., Stecher, G., Li, M., Knyaz, C. and Tamura, K.** (2018). MEGA X: Molecular Evolutionary Genetics Analysis across Computing Platforms. *Mol Biol Evol* **35** (6), 1547-1549. <https://doi.org/10.1093/molbev/msy096>.
- Kurzchalia, T. V., Wiedmann, M., Girshovich, A. S., Bochkareva, E. S., Bielka, H. and Rapoport, T. A.** (1986). The signal sequence of nascent preprolactin interacts with the 54K polypeptide of the signal recognition particle. *Nature* **320** (6063), 634-636. <https://doi.org/10.1038/320634a0>.
- Laemmli, U. K.** (1970). Cleavage of structural proteins during the assembly of the head of bacteriophage T4. *Nature* **227** (5259), 680-685.
- Lakkaraju, A. K., Thankappan, R., Mary, C., Garrison, J. L., Taunton, J. and Strub, K.** (2012). Efficient secretion of small proteins in mammalian cells relies on Sec62-

- dependent posttranslational translocation. *Mol Biol Cell* **23** (14), 2712-2722. <https://doi.org/10.1091/mbc.E12-03-0228>.
- Lang, S., Benedix, J., Fedeles, S. V., Schorr, S., Schirra, C., Schäuble, N., Jalal, C., Greiner, M., Haßdenteufel, S., Tatzelt, J., Kreutzer, B., Edelmann, L., Krause, E., Rettig, J., Somlo, S., Zimmermann, R. and Dudek, J.** (2012). Different effects of Sec61alpha, Sec62 and Sec63 depletion on transport of polypeptides into the endoplasmic reticulum of mammalian cells. *J Cell Sci* **125** (Pt 8), 1958-1969. <https://doi.org/10.1242/jcs.096727>.
- Lerouxel, O., Mouille, G., Andème-Onzighi, C., Bruyant, M. P., Séveno, M., Loutelier-Bourhis, C., Driouich, A., Höfte, H. and Lerouge, P.** (2005). Mutants in DEFECTIVE GLYCOSYLATION, an Arabidopsis homolog of an oligosaccharyltransferase complex subunit, show protein underglycosylation and defects in cell differentiation and growth. *Plant J* **42** (4), 455-468. <https://doi.org/10.1111/j.1365-313X.2005.02392.x>.
- Li, Q., Wei, H., Liu, L., Yang, X., Zhang, X. and Xie, Q.** (2017). Unfolded protein response activation compensates endoplasmic reticulum-associated degradation deficiency in Arabidopsis. *J Integr Plant Biol* **59** (7), 506-521. <https://doi.org/10.1111/jipb.12544>.
- Linxweiler, M., Schick, B. and Zimmermann, R.** (2017). Let's talk about Secs: Sec61, Sec62 and Sec63 in signal transduction, oncology and personalized medicine. *Signal Transduct Target Ther* **2**, 17002. <https://doi.org/10.1038/sigtrans.2017.2>.
- Linxweiler, M., Schorr, S., Schäuble, N., Jung, M., Linxweiler, J., Langer, F., Schäfers, H. J., Cavalié, A., Zimmermann, R. and Greiner, M.** (2013). Targeting cell migration and the endoplasmic reticulum stress response with calmodulin antagonists: a clinically tested small molecule phenocopy of SEC62 gene silencing in human tumor cells. *BMC Cancer* **13**, 574. <https://doi.org/10.1186/1471-2407-13-574>.
- Lister, R., Carrie, C., Duncan, O., Ho, L. H. M., Howell, K. A., Murcha, M. W. and Whelan, J.** (2007). Functional Definition of Outer Membrane Proteins Involved in Preprotein Import into Mitochondria. *The Plant Cell* **19** (11), 3739-3759. <https://doi.org/10.1105/tpc.107.050534>.
- Liu, D. Y., Smith, P. M., Barton, D. A., Day, D. A. and Overall, R. L.** (2017). Characterisation of Arabidopsis calnexin 1 and calnexin 2 in the endoplasmic reticulum and at plasmodesmata. *Protoplasma* **254** (1), 125-136. <https://doi.org/10.1007/s00709-015-0921-3>.
- Liu, J. and Qu, L.-J.** (2008). Meiotic and mitotic cell cycle mutants involved in gametophyte development in Arabidopsis. *Mol Plant* **1** (4), 564-574. <https://doi.org/10.1093/mp/ssn033>.
- Löoke, M., Kristjuhan, K. and Kristjuhan, A.** (2011). Extraction of genomic DNA from yeasts for PCR-based applications. *Biotechniques* **50** (5), 325-328. <https://doi.org/10.2144/000113672>.

- Lu, P., Chai, M., Yang, J., Ning, G., Wang, G. and Ma, H.** (2014). The Arabidopsis CALLOSE DEFECTIVE MICROSPORE1 gene is required for male fertility through regulating callose metabolism during microsporogenesis. *Plant Physiol* **164** (4), 1893-1904. <https://doi.org/10.1104/pp.113.233387>.
- Lütcke, H., High, S., Römisch, K., Ashford, A. J. and Dobberstein, B.** (1992). The methionine-rich domain of the 54 kDa subunit of signal recognition particle is sufficient for the interaction with signal sequences. *Embo j* **11** (4), 1543-1551.
- Lyman, S. K. and Schekman, R.** (1997). Binding of Secretory Precursor Polypeptides to a Translocon Subcomplex Is Regulated by BiP. *Cell* **88** (1), 85-96. [https://doi.org/10.1016/s0092-8674\(00\)81861-9](https://doi.org/10.1016/s0092-8674(00)81861-9).
- Malhotra, H., Vandana, Sharma, S. and Pandey, R.** (2018). Phosphorus Nutrition: Plant Growth in Response to Deficiency and Excess. In *Plant Nutrients and Abiotic Stress Tolerance* (M. Hasanuzzaman, M. Fujita, H. Oku, K. Nahar and B. Hawrylak-Nowak, eds). Singapore: Springer Nature, pp. 171-190. [https://doi.org/10.1007/978-981-10-9044-8\\_7](https://doi.org/10.1007/978-981-10-9044-8_7).
- Mariappan, M., Li, X., Stefanovic, S., Sharma, A., Mateja, A., Keenan, R. J. and Hegde, R. S.** (2010). A ribosome-associating factor chaperones tail-anchored membrane proteins. *Nature* **466** (7310), 1120-1124. <https://doi.org/10.1038/nature09296>.
- Marshall, R. D.** (1972). Glycoproteins. *Annu Rev Biochem* **41**, 673-702. <https://doi.org/10.1146/annurev.bi.41.070172.003325>.
- Maruyama, D., Endo, T. and Nishikawa, S.** (2010). BiP-mediated polar nuclei fusion is essential for the regulation of endosperm nuclei proliferation in Arabidopsis thaliana. *Proc Natl Acad Sci U S A* **107** (4), 1684-1689. <https://doi.org/10.1073/pnas.0905795107>.
- Maruyama, D., Sugiyama, T., Endo, T. and Nishikawa, S.** (2014). Multiple BiP genes of Arabidopsis thaliana are required for male gametogenesis and pollen competitiveness. *Plant Cell Physiol* **55** (4), 801-810. <https://doi.org/10.1093/pcp/pcu018>.
- Mateja, A., Paduch, M., Chang, H.-Y., Szydlowska, A., Kossiakoff, A. A., Hegde, R. S. and Keenan, R. J.** (2015). Structure of the Get3 targeting factor in complex with its membrane protein cargo. *Science* **347** (6226), 1152-1155. <https://doi.org/10.1126/science.1261671>.
- Matlack, K. E., Misselwitz, B., Plath, K. and Rapoport, T. A.** (1999). BiP acts as a molecular ratchet during posttranslational transport of prepro-alpha factor across the ER membrane. *Cell* **97** (5), 553-564. [https://doi.org/10.1016/s0092-8674\(00\)80767-9](https://doi.org/10.1016/s0092-8674(00)80767-9).
- Matsushima, R., Kondo, M., Nishimura, M. and Hara-Nishimura, I.** (2003). A novel ER-derived compartment, the ER body, selectively accumulates a beta-glucosidase with an ER-retention signal in Arabidopsis. *Plant J* **33** (3), 493-502.

- May, T. and Soll, J.** (2000). 14-3-3 proteins form a guidance complex with chloroplast precursor proteins in plants. *Plant Cell* **12** (1), 53-64. <https://doi.org/10.1105/tpc.12.1.53>.
- Meyer, D. I., Krause, E. and Dobberstein, B.** (1982). Secretory protein translocation across membranes—the role of the ‘docking protein’. *Nature* **297** (5868), 647-650. <https://doi.org/10.1038/297647a0>.
- Meyer, H.-A., Grau, H., Kraft, R., Kostka, S., Prehn, S., Kalies, K.-U. and Hartmann, E.** (2000). Mammalian Sec61 is associated with Sec62 and Sec63. *J Biol Chem* **275** (19), 14550-14557. <https://doi.org/10.1074/jbc.275.19.14550>.
- Mitterreiter, M.J., Bosch, F.A., Brylok, T. and Schwenkert, S.** (2020). The ER luminal C-terminus of AtSec62 is critical for male fertility and plant growth in *Arabidopsis thaliana*. *Plant J* **101** (1), 5-17. <https://doi.org/10.1111/tpj.14483>.
- Müller, L., de Escauriaza, M. D., Lajoie, P., Theis, M., Jung, M., Müller, A., Burgard, C., Greiner, M., Snapp, E. L., Dudek, J. and Zimmermann, R.** (2010). Evolutionary gain of function for the ER membrane protein Sec62 from yeast to humans. *Mol Biol Cell* **21** (5), 691-703. <https://doi.org/10.1091/mbc.E09-08-0730>.
- Nagano, A. J., Fukao, Y., Fujiwara, M., Nishimura, M. and Hara-Nishimura, I.** (2008). Antagonistic jacalin-related lectins regulate the size of ER body-type beta-glucosidase complexes in *Arabidopsis thaliana*. *Plant Cell Physiol* **49** (6), 969-980. <https://doi.org/10.1093/pcp/pcn075>.
- Nagano, A. J., Matsushima, R. and Hara-Nishimura, I.** (2005). Activation of an ER-body-localized beta-glucosidase via a cytosolic binding partner in damaged tissues of *Arabidopsis thaliana*. *Plant Cell Physiol* **46** (7), 1140-1148. <https://doi.org/10.1093/pcp/pci126>.
- Naur, P., Petersen, B. L., Mikkelsen, M. D., Bak, S., Rasmussen, H., Olsen, C. E. and Halkier, B. A.** (2003). CYP83A1 and CYP83B1, two nonredundant cytochrome P450 enzymes metabolizing oximes in the biosynthesis of glucosinolates in *Arabidopsis*. *Plant Physiol* **133** (1), 63-72. <https://doi.org/10.1104/pp.102.019240>.
- Nelson, B. K., Cai, X. and Nebenführ, A.** (2007). A multicolored set of in vivo organelle markers for co-localization studies in *Arabidopsis* and other plants. *Plant J* **51** (6), 1126-1136. <https://doi.org/10.1111/j.1365-313X.2007.03212.x>.
- Ng, D. T., Brown, J. D. and Walter, P.** (1996). Signal sequences specify the targeting route to the endoplasmic reticulum membrane. *J Cell Biol* **134** (2), 269-278. <https://doi.org/10.1083/jcb.134.2.269>.
- Ngosuwon, J., Wang, N. M., Fung, K. L. and Chirico, W. J.** (2003). Roles of cytosolic Hsp70 and Hsp40 molecular chaperones in post-translational translocation of presecretory proteins into the endoplasmic reticulum. *J Biol Chem* **278** (9), 7034-7042. <https://doi.org/10.1074/jbc.M210544200>.
- Noël, P. and Cartwright, I. L.** (1994). A Sec62p-related component of the secretory protein translocon from *Drosophila* displays developmentally complex behavior. *Embo j* **13** (22), 5253-5261. <https://doi.org/10.1002/j.1460-2075.1994.tb06859.x>.

- Osborne, A. R., Rapoport, T. A. and van den Berg, B.** (2005). Protein translocation by the Sec61/SecY channel. *Annu Rev Cell Dev Biol* **21**, 529-550. <https://doi.org/10.1146/annurev.cellbio.21.012704.133214>.
- Panzner, S., Dreier, L., Hartmann, E., Kostka, S. and Rapoport, T. A.** (1995). Posttranslational protein transport in yeast reconstituted with a purified complex of Sec proteins and Kar2p. *Cell* **81** (4), 561-570. [https://doi.org/10.1016/0092-8674\(95\)90077-2](https://doi.org/10.1016/0092-8674(95)90077-2).
- Park, E. and Rapoport, T. A.** (2012). Mechanisms of Sec61/SecY-mediated protein translocation across membranes. *Annu Rev Biophys* **41**, 21-40. <https://doi.org/10.1146/annurev-biophys-050511-102312>.
- Pastor-Cantizano, N., Ko, D. K., Angelos, E., Pu, Y. and Brandizzi, F.** (2020). Functional Diversification of ER Stress Responses in Arabidopsis. *Trends in Biochemical Sciences* **45** (2), 123-136. <https://doi.org/10.1016/j.tibs.2019.10.008>.
- Pérez-Torres, C.-A., López-Bucio, J., Cruz-Ramírez, A., Ibarra-Laclette, E., Dharmasiri, S., Estelle, M. and Herrera-Estrella, L.** (2008). Phosphate Availability Alters Lateral Root Development in Arabidopsis by Modulating Auxin Sensitivity via a Mechanism Involving the TIR1 Auxin Receptor. *The Plant Cell* **20** (12), 3258-3272. <https://doi.org/10.1105/tpc.108.058719>.
- Pfeffer, S., Dudek, J., Schaffer, M., Ng, B. G., Albert, S., Plitzko, J. M., Baumeister, W., Zimmermann, R., Freeze, H. H., Engel, B. D. and Förster, F.** (2017). Dissecting the molecular organization of the translocon-associated protein complex. *Nature Communications* **8** (1), 14516. <https://doi.org/10.1038/ncomms14516>.
- Pilon, M., Schekman, R. and Römisch, K.** (1997). Sec61p mediates export of a misfolded secretory protein from the endoplasmic reticulum to the cytosol for degradation. *Embo j* **16** (15), 4540-4548. <https://doi.org/10.1093/emboj/16.15.4540>.
- Plath, K., Mothes, W., Wilkinson, B. M., Stirling, C. J. and Rapoport, T. A.** (1998). Signal sequence recognition in posttranslational protein transport across the yeast ER membrane. *Cell* **94** (6), 795-807. [https://doi.org/10.1016/S0092-8674\(00\)81738-9](https://doi.org/10.1016/S0092-8674(00)81738-9).
- Plemper, R. K., Böhmler, S., Bordallo, J., Sommer, T. and Wolf, D. H.** (1997). Mutant analysis links the translocon and BiP to retrograde protein transport for ER degradation. *Nature* **388** (6645), 891-895. <https://doi.org/10.1038/42276>.
- Prasad, B. D., Goel, S. and Krishna, P.** (2010). In silico identification of carboxylate clamp type tetratricopeptide repeat proteins in Arabidopsis and rice as putative co-chaperones of Hsp90/Hsp70. *PLoS One* **5** (9), e12761. <https://doi.org/10.1371/journal.pone.0012761>.
- R Core Team** (2019). R: A language and environment for statistical computing. *R Foundation for Statistical Computing*, Vienna. <https://www.R-project.org/>.

- Rapoport, T. A.** (2007). Protein translocation across the eukaryotic endoplasmic reticulum and bacterial plasma membranes. *Nature* **450** (7170), 663-669. <https://doi.org/10.1038/nature06384>.
- Reithinger, J. H., Kim, J. E. and Kim, H.** (2013). Sec62 protein mediates membrane insertion and orientation of moderately hydrophobic signal anchor proteins in the endoplasmic reticulum (ER). *J Biol Chem* **288** (25), 18058-18067. <https://doi.org/10.1074/jbc.M113.473009>.
- Rhee, S. Y., Osborne, E., Poindexter, P. D. and Somerville, C. R.** (2003). Microspore separation in the quartet 3 mutants of *Arabidopsis* is impaired by a defect in a developmentally regulated polygalacturonase required for pollen mother cell wall degradation. *Plant Physiol* **133** (3), 1170-1180. <https://doi.org/10.1104/pp.103.028266>.
- Rome, M. E., Rao, M., Clemons, W. M. and Shan, S.-o.** (2013). Precise timing of ATPase activation drives targeting of tail-anchored proteins. *Proceedings of the National Academy of Sciences* **110** (19), 7666-7671. <https://doi.org/10.1073/pnas.1222054110>.
- Römisch, K., Webb, J., Lingelbach, K., Gausepohl, H. and Dobberstein, B.** (1990). The 54-kD protein of signal recognition particle contains a methionine-rich RNA binding domain. *J Cell Biol* **111** (5 Pt 1), 1793-1802. <https://doi.org/10.1083/jcb.111.5.1793>.
- Saraogi, I. and Shan, S. O.** (2011). Molecular mechanism of co-translational protein targeting by the signal recognition particle. *Traffic* **12** (5), 535-542. <https://doi.org/10.1111/j.1600-0854.2011.01171.x>.
- Scheufler, C., Brinker, A., Bourenkov, G., Pegoraro, S., Moroder, L., Bartunik, H., Hartl, F. U. and Moarefi, I.** (2000). Structure of TPR Domain Peptide Complexes: Critical Elements in the Assembly of the Hsp70/Hsp90 Multichaperone Machine. *Cell* **101** (2), 199-210. [https://doi.org/10.1016/S0092-8674\(00\)80830-2](https://doi.org/10.1016/S0092-8674(00)80830-2).
- Schibich, D., Gloge, F., Pöhner, I., Björkholm, P., Wade, R. C., von Heijne, G., Bukau, B. and Kramer, G.** (2016). Global profiling of SRP interaction with nascent polypeptides. *Nature* **536** (7615), 219-223. <https://doi.org/10.1038/nature19070>.
- Schlegel, T., Mirus, O., von Haeseler, A. and Schleiff, E.** (2007). The tetratricopeptide repeats of receptors involved in protein translocation across membranes. *Mol Biol Evol* **24** (12), 2763-2774. <https://doi.org/10.1093/molbev/msm211>.
- Schuldiner, M., Metz, J., Schmid, V., Denic, V., Rakwalska, M., Schmitt, H. D., Schwappach, B. and Weissman, J. S.** (2008). The GET Complex Mediates Insertion of Tail-Anchored Proteins into the ER Membrane. *Cell* **134** (4), 634-645. <https://doi.org/10.1016/j.cell.2008.06.025>.
- Schwartz, T. and Blobel, G.** (2003). Structural basis for the function of the beta subunit of the eukaryotic signal recognition particle receptor. *Cell* **112** (6), 793-803. [https://doi.org/10.1016/S0092-8674\(03\)00161-2](https://doi.org/10.1016/S0092-8674(03)00161-2).

- Schweiger, R., Müller, N. C., Schmitt, M. J., Soll, J. and Schwenkert, S.** (2012). AtTPR7 is a chaperone-docking protein of the Sec translocon in Arabidopsis. *J Cell Sci* **125** (Pt 21), 5196-5207. <https://doi.org/10.1242/jcs.111054>.
- Schweiger, R. and Schwenkert, S.** (2013). AtTPR7 as part of the Arabidopsis Sec post-translocon. *Plant Signal Behav* **8** (8). <https://doi.org/10.4161/psb.25286>.
- Schweiger, R. and Schwenkert, S.** (2014). Protein-protein interactions visualized by bimolecular fluorescence complementation in tobacco protoplasts and leaves. *J Vis Exp* (85). <https://doi.org/10.3791/51327>.
- Schweiger, R., Soll, J., Jung, K., Heermann, R. and Schwenkert, S.** (2013). Quantification of interaction strengths between chaperones and tetratricopeptide repeat domain-containing membrane proteins. *J Biol Chem* **288** (42), 30614-30625. <https://doi.org/10.1074/jbc.M113.493015>.
- Schwenkert, S., Dittmer, S. and Soll, J.** (2018). Structural components involved in plastid protein import. *Essays Biochem* **62** (1), 65-75. <https://doi.org/10.1042/EBC20170093>.
- Shao, S., Rodrigo-Brenni, M. C., Kivlen, M. H. and Hegde, R. S.** (2017). Mechanistic basis for a molecular triage reaction. *Science* **355** (6322), 298-302. <https://doi.org/10.1126/science.aah6130>.
- Sikorski, R. S., Boguski, M. S., Goebel, M. and Hieter, P.** (1990). A repeating amino acid motif in CDC23 defines a family of proteins and a new relationship among genes required for mitosis and RNA synthesis. *Cell* **60** (2), 307-317. [https://doi.org/10.1016/0092-8674\(90\)90745-z](https://doi.org/10.1016/0092-8674(90)90745-z).
- Sommer, N., Junne, T., Kalies, K. U., Spiess, M. and Hartmann, E.** (2013). TRAP assists membrane protein topogenesis at the mammalian ER membrane. *Biochim Biophys Acta* **1833** (12), 3104-3111. <https://doi.org/10.1016/j.bbamcr.2013.08.018>.
- Song, W., Raden, D., Mandon, E. C. and Gilmore, R.** (2000). Role of Sec61alpha in the regulated transfer of the ribosome-nascent chain complex from the signal recognition particle to the translocation channel. *Cell* **100** (3), 333-343. [https://doi.org/10.1016/s0092-8674\(00\)80669-8](https://doi.org/10.1016/s0092-8674(00)80669-8).
- Spitzer, M., Wildenhain, J., Rappsilber, J. and Tyers, M.** (2014). BoxPlotR: a web tool for generation of box plots. *Nat Methods* **11** (2), 121-122. <https://doi.org/10.1038/nmeth.2811>.
- Srivastava, R., Zalisko, B. E., Keenan, R. J. and Howell, S. H.** (2017). The GET System Inserts the Tail-Anchored Protein, SYP72, into Endoplasmic Reticulum Membranes. *Plant Physiol* **173** (2), 1137-1145. <https://doi.org/10.1104/pp.16.00928>.
- Staudinger, J., Zhou, J., Burgess, R., Elledge, S. J. and Olson, E. N.** (1995). PICK1: a perinuclear binding protein and substrate for protein kinase C isolated by the yeast two-hybrid system. *J Cell Biol* **128** (3), 263-271. <https://doi.org/10.1083/jcb.128.3.263>.

- Stefanovic, S. and Hegde, R. S.** (2007). Identification of a Targeting Factor for Posttranslational Membrane Protein Insertion into the ER. *Cell* **128** (6), 1147-1159. <https://doi.org/10.1016/j.cell.2007.01.036>.
- Stieglitz, H.** (1977). Role of beta-1,3-glucanase in postmeiotic microspore release. *Dev Biol* **57** (1), 87-97. [https://doi.org/10.1016/0012-1606\(77\)90356-6](https://doi.org/10.1016/0012-1606(77)90356-6).
- Strasser, R.** (2018). Protein Quality Control in the Endoplasmic Reticulum of Plants. *Annu Rev Plant Biol* **69**, 147-172. <https://doi.org/10.1146/annurev-arplant-042817-040331>.
- Sze, H., Schumacher, K., Müller, M. L., Padmanaban, S. and Taiz, L.** (2002). A simple nomenclature for a complex proton pump: VHA genes encode the vacuolar H(+)-ATPase. *Trends Plant Sci* **7** (4), 157-161. [https://doi.org/10.1016/s1360-1385\(02\)02240-9](https://doi.org/10.1016/s1360-1385(02)02240-9).
- Tajima, S., Lauffer, L., Rath, V. L. and Walter, P.** (1986). The signal recognition particle receptor is a complex that contains two distinct polypeptide chains. *J Cell Biol* **103** (4), 1167-1178. <https://doi.org/10.1083/jcb.103.4.1167>.
- Tamborero, S., Vilar, M., Martínez-Gil, L., Johnson, A. E. and Mingarro, I.** (2011). Membrane insertion and topology of the translocating chain-associating membrane protein (TRAM). *J Mol Biol* **406** (4), 571-582. <https://doi.org/10.1016/j.jmb.2011.01.009>.
- Tripathi, A., Mandon, E. C., Gilmore, R. and Rapoport, T. A.** (2017). Two alternative binding mechanisms connect the protein translocation Sec71-Sec72 complex with heat shock proteins. *Journal of Biological Chemistry* **292** (19), 8007-8018. <https://doi.org/10.1074/jbc.M116.761122>.
- Tyedmers, J., Lerner, M., Bies, C., Dudek, J., Skowronek, M. H., Haas, I. G., Heim, N., Nastainczyk, W., Volkmer, J. and Zimmermann, R.** (2000). Homologs of the yeast Sec complex subunits Sec62p and Sec63p are abundant proteins in dog pancreas microsomes. *Proc Natl Acad Sci U S A* **97** (13), 7214-7219. <https://doi.org/10.1073/pnas.97.13.7214>.
- Van Aken, O., Pečenková, T., van de Cotte, B., De Rycke, R., Eeckhout, D., Fromm, H., De Jaeger, G., Witters, E., Beemster, G. T., Inzé, D. and Van Breusegem, F.** (2007). Mitochondrial type-I prohibitins of *Arabidopsis thaliana* are required for supporting proficient meristem development. *Plant J* **52** (5), 850-864. <https://doi.org/10.1111/j.1365-313X.2007.03276.x>.
- Van Puyenbroeck, V. and Vermeire, K.** (2018). Inhibitors of protein translocation across membranes of the secretory pathway: novel antimicrobial and anticancer agents. *Cell Mol Life Sci* **75** (9), 1541-1558. <https://doi.org/10.1007/s00018-017-2743-2>.
- Villarejo, A., Burén, S., Larsson, S., Déjardin, A., Monné, M., Rudhe, C., Karlsson, J., Jansson, S., Lerouge, P., Rolland, N., von Heijne, G., Grebe, M., Bako, L. and Samuelsson, G.** (2005). Evidence for a protein transported through the secretory pathway en route to the higher plant chloroplast. *Nat Cell Biol* **7** (12), 1224-1231. <https://doi.org/10.1038/ncb1330>.

- von Loeffelholz, O., Kriechbaumer, V., Ewan, R. A., Jonczyk, R., Lehmann, S., Young, J. C. and Abell, B. M. (2011). OEP61 is a chaperone receptor at the plastid outer envelope. *Biochem J* **438** (1), 143-153. <https://doi.org/10.1042/BJ20110448>.
- Vu, K. V., Nguyen, N. T., Jeong, C. Y., Lee, Y.-H., Lee, H. and Hong, S.-W. (2017). Systematic deletion of the ER lectin chaperone genes reveals their roles in vegetative growth and male gametophyte development in Arabidopsis. *Plant J* **89** (5), 972-983. <https://doi.org/10.1111/tpj.13435>.
- Wang, F., Brown, E. C., Mak, G., Zhuang, J. and Denic, V. (2010a). A Chaperone Cascade Sorts Proteins for Posttranslational Membrane Insertion into the Endoplasmic Reticulum. *Molecular Cell* **40** (1), 159-171. <https://doi.org/10.1016/j.molcel.2010.08.038>.
- Wang, X., Xu, M., Gao, C., Zeng, Y., Cui, Y., Shen, W. and Jiang, L. (2020). The roles of endomembrane trafficking in plant abiotic stress responses. *J Integr Plant Biol* **62** (1), 55-69. <https://doi.org/10.1111/jipb.12895>.
- Wang, Y., Ries, A., Wu, K., Yang, A. and Crawford, N. M. (2010b). The Arabidopsis Prohibitin Gene PHB3 Functions in Nitric Oxide-Mediated Responses and in Hydrogen Peroxide-Induced Nitric Oxide Accumulation. *Plant Cell* **22** (1), 249-259. <https://doi.org/10.1105/tpc.109.072066>.
- Wiertz, E. J., Tortorella, D., Bogyo, M., Yu, J., Mothes, W., Jones, T. R., Rapoport, T. A. and Ploegh, H. L. (1996). Sec61-mediated transfer of a membrane protein from the endoplasmic reticulum to the proteasome for destruction. *Nature* **384** (6608), 432-438. <https://doi.org/10.1038/384432a0>.
- Wild, R., Kowal, J., Eyring, J., Ngwa, E. M., Aebi, M. and Locher, K. P. (2018). Structure of the yeast oligosaccharyltransferase complex gives insight into eukaryotic N-glycosylation. *Science* **359** (6375), 545-550. <https://doi.org/10.1126/science.aar5140>.
- Willer, M., Jermy, A. J., Young, B. P. and Stirling, C. J. (2003). Identification of novel protein-protein interactions at the cytosolic surface of the Sec63 complex in the yeast ER membrane. *Yeast* **20** (2), 133-148. <https://doi.org/10.1002/yea.954>.
- Winter, D., Vinegar, B., Nahal, H., Ammar, R., Wilson, G. V. and Provart, N. J. (2007). An "Electronic Fluorescent Pictograph" browser for exploring and analyzing large-scale biological data sets. *PLoS One* **2** (8), e718. <https://doi.org/10.1371/journal.pone.0000718>.
- Wittke, S., Dünwald, M. and Johnsson, N. (2000). Sec62p, a component of the endoplasmic reticulum protein translocation machinery, contains multiple binding sites for the Sec-complex. *Mol Biol Cell* **11** (11), 3859-3871. <https://doi.org/10.1091/mbc.11.11.3859>.
- Wu, X., Cabanos, C. and Rapoport, T. A. (2019). Structure of the post-translational protein translocation machinery of the ER membrane. *Nature* **566** (7742), 136-139. <https://doi.org/10.1038/s41586-018-0856-x>.

- Xie, W., Nielsen, M. E., Pedersen, C. and Thordal-Christensen, H.** (2017). A Split-GFP Gateway Cloning System for Topology Analyses of Membrane Proteins in Plants. *PLoS One* **12** (1), e0170118. <https://doi.org/10.1371/journal.pone.0170118>.
- Xing, S., Mehlhorn, D. G., Wallmeroth, N., Asseck, L. Y., Kar, R., Voss, A., Denninger, P., Schmidt, V. A., Schwarzländer, M., Stierhof, Y.-D., Grossmann, G. and Grefen, C.** (2017). Loss of GET pathway orthologs in *Arabidopsis thaliana* causes root hair growth defects and affects SNARE abundance. *Proc Natl Acad Sci U S A* **114** (8), E1544-E1553. <https://doi.org/10.1073/pnas.1619525114>.
- Yamamoto, M., Maruyama, D., Endo, T. and Nishikawa, S.** (2008). *Arabidopsis thaliana* has a set of J proteins in the endoplasmic reticulum that are conserved from yeast to animals and plants. *Plant Cell Physiol* **49** (10), 1547-1562. <https://doi.org/10.1093/pcp/pcn119>.
- Yamamoto, Y. and Sakisaka, T.** (2012). Molecular Machinery for Insertion of Tail-Anchored Membrane Proteins into the Endoplasmic Reticulum Membrane in Mammalian Cells. *Molecular Cell* **48** (3), 387-397. <https://doi.org/10.1016/j.molcel.2012.08.028>.
- Yang, K.-Z., Xia, C., Liu, X.-L., Dou, X.-Y., Wang, W., Chen, L.-Q., Zhang, X.-Q., Xie, L.-F., He, L., Ma, X. and Ye, D.** (2009). A mutation in Thermosensitive Male Sterile 1, encoding a heat shock protein with DnaJ and PDI domains, leads to thermosensitive gametophytic male sterility in *Arabidopsis*. *Plant J* **57** (5), 870-882. <https://doi.org/10.1111/j.1365-313X.2008.03732.x>.
- Yim, C., Jung, S. J., Kim, J. E. H., Jung, Y., Jeong, S. D. and Kim, H.** (2018). Profiling of signal sequence characteristics and requirement of different translocation components. *Biochim Biophys Acta Mol Cell Res* **1865** (11 Pt A), 1640-1648. <https://doi.org/10.1016/j.bbamcr.2018.08.018>.
- Young, J. C., Ursini, J., Legate, K. R., Miller, J. D., Walter, P. and Andrews, D. W.** (1995). An Amino-terminal Domain Containing Hydrophobic and Hydrophilic Sequences Binds the Signal Recognition Particle Receptor  $\alpha$  Subunit to the  $\beta$  Subunit on the Endoplasmic Reticulum Membrane. *Journal of Biological Chemistry* **270** (26), 15650-15657. <https://doi.org/10.1074/jbc.270.26.15650>.
- Zhang, X., Schaffitzel, C., Ban, N. and Shan, S. O.** (2009). Multiple conformational switches in a GTPase complex control co-translational protein targeting. *Proc Natl Acad Sci U S A* **106** (6), 1754-1759. <https://doi.org/10.1073/pnas.0808573106>.
- Zhao, Z., Zhang, W., Stanley, B. A. and Assmann, S. M.** (2008). Functional proteomics of *Arabidopsis thaliana* guard cells uncovers new stomatal signaling pathways. *Plant Cell* **20** (12), 3210-3226. <https://doi.org/10.1105/tpc.108.063263>.
- Zhou, Z., Pang, Z., Li, G., Lin, C., Wang, J., Lv, Q., He, C. and Zhu, L.** (2016). Endoplasmic reticulum membrane-bound MoSec62 is involved in the suppression of rice immunity and is essential for the pathogenicity of *Magnaporthe oryzae*. *Mol Plant Pathol* **17** (8), 1211-1222. <https://doi.org/10.1111/mpp.12357>.
- Zhu, Y., Fraering, P., Vionnet, C. and Conzelmann, A.** (2005). Gpi17p does not stably interact with other subunits of glycosylphosphatidylinositol transamidase in

- Saccharomyces cerevisiae*. *Biochim Biophys Acta* **1735** (1), 79-88. <https://doi.org/10.1016/j.bbaliip.2005.05.001>.
- Zimmermann, R., Eyrisch, S., Ahmad, M. and Helms, V.** (2011). Protein translocation across the ER membrane. *Biochim Biophys Acta* **1808** (3), 912-924. <https://doi.org/10.1016/j.bbamem.2010.06.015>.
- Zimmermann, R., Müller, L. and Wullich, B.** (2006). Protein transport into the endoplasmic reticulum: mechanisms and pathologies. *Trends Mol Med* **12** (12), 567-573. <https://doi.org/10.1016/j.molmed.2006.10.004>.
- Zimmermann, R., Sagstetter, M., Lewis, M. J. and Pelham, H. R.** (1988). Seventy-kilodalton heat shock proteins and an additional component from reticulocyte lysate stimulate import of M13 procoat protein into microsomes. *Embo j* **7** (9), 2875-2880. <https://doi.org/10.1002/j.1460-2075.1988.tb03144.x>.
- Zopf, D., Bernstein, H. D., Johnson, A. E. and Walter, P.** (1990). The methionine-rich domain of the 54 kd protein subunit of the signal recognition particle contains an RNA binding site and can be crosslinked to a signal sequence. *Embo j* **9** (13), 4511-4517.
- Zopf, D., Bernstein, H. D. and Walter, P.** (1993). GTPase domain of the 54-kD subunit of the mammalian signal recognition particle is required for protein translocation but not for signal sequence binding. *J Cell Biol* **120** (5), 1113-1121. <https://doi.org/10.1083/jcb.120.5.1113>.

## Appendix

**Table A1: Complete list of potential AtSec62 interacting/ associating proteins.** Proteins were identified by GFP-trap® pull-down with AtSec62-GFP or GFP-AtSec62 and subsequent mass spectrometric analysis resulting in the given score. Two biological replicates (R1 and R2) were analysed for AtSec62-GFP.

Accession number	Protein name <sup>1</sup>	Score AtSec62-GFP <sup>2</sup>		Score GFP-AtSec62 <sup>2</sup>
		R1	R2	
AT1G08450.2	AtCRT3/ AtPSL1	n.d.	n.d.	160.46
AT1G11860.3	AtGDT1/ AtGDC-T1	n.d.	108.57	107.69
AT1G12900.2	AtGAPa-2	113.70	n.d.	n.d.
AT1G13100.1	AtCYP71B29	n.d.	NaN	160.18
AT1G14320.1	AtRPL10A	n.d.	119.21	NaN
AT1G15690.1	AtVHP1.1/ AtAVP1/ AtFUGU5	85.807	n.d.	n.d.
AT1G16410.2	AtCYP79F1/ AtSPS	n.d.	102.07	331.368
AT1G20620.4	AtCAT3/ AtSEN2	82.831	n.d.	n.d.
AT1G22530.1	AtPATL2	270.191	n.d.	n.d.
AT1G42970.1	AtGAPb	489.94	n.d.	n.d.
AT1G43170.4	AtRPL3A	n.d.	157.75	63.864
AT1G52370.3	-	57.047	n.d.	n.d.
AT1G56070.1	AtLOS1	n.d.	104.75	96.253
AT1G59870.1	AtABCG36/ AtPDR8/ AtPEN3	n.d.	238.88	549.61
AT1G78900.2	AtVHA-A	607.63	951.937	739.36
AT2G01250.1	AtRPL7B	n.d.	109.79	200.93
AT2G01720.1	AtOST1a	n.d.	125.22	n.d.
AT2G21160.2	-	n.d.	128.91	77.192
AT2G28900.1	AtOep16-1	329.95	n.d.	n.d.
AT2G34420.1	AtLHCb1.5	231.54	n.d.	n.d.
AT2G37270.2	AtRPS5A	n.d.	120.45	NaN
AT2G39730.3	AtRCA	903.708	n.d.	n.d.
AT2G44060.2	-	n.d.	NaN	184.96
AT2G45470.1	AtFLA8	n.d.	n.d.	155
AT2G45960.2	AtPIP1.2/ AtPIP1b/ AtTMPa	136.27	n.d.	n.d.
AT2G47470.4	AtPDI-S/ AtPDIL4-1/ AtPDI11	n.d.	289.9	263.42

Accession number	Protein name <sup>1</sup>	Score AtSec62-GFP <sup>2</sup>		Score GFP-AtSec62 <sup>2</sup>
		R1	R2	
AT3G01500.1	AtBCA1/ AtCA1	861.56	n.d.	n.d.
AT3G02650.1	-	47.067	n.d.	n.d.
AT3G04920.1	AtRPS24A	n.d.	n.d.	392.73
AT3G13870.2	AtRHD3	n.d.	97.779	177.048
AT3G14210.1	AtESM	160.52	n.d.	n.d.
AT3G14420.3	AtGOX1	582.448	n.d.	n.d.
AT3G14600.1	AtRPL18aC	n.d.	149.4	146.94
AT3G16240.1	AtTIP2.1	n.d.	112.17	n.d.
AT3G17390.1	AtMAT4/ AtSAMS3/ AtMTO3	n.d.	NaN	113.89
AT3G18740.1	AtRPL30C	n.d.	n.d.	258.07
AT3G18780.1	AtACT2	300.844	n.d.	n.d.
AT3G19820.3	AtDIM/ DWF1	77.279	91.123	164.68
AT3G20920.2	AtSec62	342.704	404.671	1703.046
AT3G25520.2	AtRPL5A	n.d.	NaN	240.46
AT3G26520.1	AtTIP1.2	247.73	n.d.	n.d.
AT3G43950.1	-	58.699	n.d.	n.d.
AT3G46740.1	AtToc75-III	99.732	n.d.	n.d.
AT3G47370.3	AtRPS20B	n.d.	155.47	285.32
AT3G52590.1	AtRPL40B/ AtUBQ1	105.17	n.d.	n.d.
AT3G53020.1	AtRPL24b/ AtSTV	n.d.	125.97	159.5
AT3G53420.2	AtPIP2.1/ AtPIP2a	769.83	n.d.	n.d.
AT3G55410.1	-	n.d.	NaN	1120.25
AT3G58510.3	AtRH11	n.d.	n.d.	123.35
AT3G61430.2	AtPIP1.1/ AtPIP1a	313.69	n.d.	n.d.
AT3G63160.1	AtOEP7.2	146.79	n.d.	n.d.
AT3G63410.1	AtAPG1/ AtVTE3	160.48	n.d.	n.d.
AT3G63520.1	AtCCD1/ AtNCED1	n.d.	NaN	150.1
AT4G02080.1	AtSARA1c	n.d.	NaN	255.86
AT4G09800.1	AtRPS18C	n.d.	120.99	n.d.
AT4G10450.1	AtRPL90D	n.d.	NaN	99.136
AT4G12320.1	AtCYP706A6	n.d.	NaN	261.17

Accession number	Protein name <sup>1</sup>	Score AtSec62-GFP <sup>2</sup>		Score GFP-AtSec62 <sup>2</sup>
		R1	R2	
AT4G12420.2	AtSKU5	n.d.	n.d.	248.96
AT4G12800.1	AtPsaL	n.d.	204.42	71.501
AT4G13770.1	AtCYP83A1	n.d.	602.83	674.437
AT4G14960.1	AtTUA6	n.d.	156.927	625.75
AT4G15000.2	AtRPL27C	n.d.	n.d.	127.83
AT4G16920.1	-	17.943	n.d.	n.d.
AT4G20360.1	AtTufA/ AtRABE1b/ AtSVR11	157.34	116.37	134.48
AT4G21150.2	AtHAP6	n.d.	217.659	735.238
AT4G21770.1	-	n.d.	n.d.	116.84
AT4G21960.1	AtPer42/ AtPRXR1	n.d.	n.d.	294.082
AT4G24190.2	AtHSP90.7/ AtSHD	n.d.	348.6	1136.636
AT4G28390.1	AtAAC3	n.d.	n.d.	332.83
AT4G28750.1	AtPsaE1	n.d.	153.1	218.02
AT4G30190.1	AtAHA2	122.28	314.83	340.259
AT4G31490.1	AtCopB1	n.d.	n.d.	269.14
AT4G31500.1	AtCYP83B1/ AtSUR2/ AtRED1	n.d.	152.54	278.83
AT4G33010.1	AtGDP1/ AtGDC-P1/ AtGLDP1	n.d.	112.85	304.036
AT4G33240.3	AtFab1a	n.d.	n.d.	84.916
AT4G34450.1	-	n.d.	279.12	277.37
AT4G34670.1	AtRPS3aB	n.d.	n.d.	109.16
AT4G35000.1	AtAPX3	n.d.	NaN	56.632
AT4G35100.2	AtPIP2.7/ AtPIP3a	315.429	n.d.	n.d.
AT4G35860.2	AtRAB-B1c	n.d.	n.d.	143.96
AT4G36130.1	AtRPL8C	n.d.	161.51	n.d.
AT5G02500.2	AtHsp70-1	n.d.	487.71	276.34
AT5G02870.2	AtRPL4D	n.d.	238.2	278.38
AT5G03850.1	AtRPS28B	n.d.	189.24	n.d.
AT5G06660.1	-	n.d.	n.d.	301.35
AT5G08690.1	AtmtATP-beta2	317.245	n.d.	n.d.
AT5G09660.2	AtpMDH2	n.d.	n.d.	591.37
AT5G12470.1	AtRER4	66.621	n.d.	n.d.

Accession number	Protein name <sup>1</sup>	Score AtSec62-GFP <sup>2</sup>		Score GFP-AtSec62 <sup>2</sup>
		R1	R2	
AT5G14740.2	AtBCA2/ AtCA2	257.92	n.d.	n.d.
AT5G17920.2	AtMS1/ AtCIMS/ AtMETS1	91.961	NaN	418.88
AT5G25980.2	AtBGLU37/ AtTGG2	n.d.	561.03	789.01
AT5G26000.2	AtBGLU38/ AtTGG1	n.d.	234.623	591.76
AT5G26742.3	AtRH3	n.d.	424.463	888.13
AT5G27850.1	AtRPL18C	n.d.	169.37	205.585
AT5G28540.1	AtBiP1/ AtBP1/ AtHsp70-11	n.d.	835.156	1416.834
AT5G35630.3	AtGLN2/ AtGSL1	113.61	n.d.	n.d.
AT5G42020.2	AtBiP2/ AtBP2/ AtHsp70-12	468.91	n.d.	n.d.
AT5G42650.1	AtCYP74A/ AtAOS	n.d.	407.683	708.4
AT5G44340.1	AtTUB4	170.178	n.d.	n.d.
AT5G45620.2	-	n.d.	82.75	n.d.
AT5G45770.1	AtSNC3/ AtRLP55	17.647	n.d.	n.d.
AT5G46110.2	AtTPT	248.66	n.d.	n.d.
AT5G50920.1	AtClpC1/ AtHSP93-V	375.144	400.13	286.56
AT5G59840.1	AtRAB-E1b	n.d.	270.02	n.d.
AT5G60390.2	-	1237.849	599.237	1073.969
AT5G61790.1	AtCNX1	760.788	865.66	1250.723
AT5G64990.1	AtRAB-H1a	n.d.	123.21	126.31
AT5G66680.1	AtDGL1	n.d.	186.78	611.146
AT5G67560.1	AtARLA1d/ AtARL8b	n.d.	85.533	184.36

<sup>1</sup> Protein name according to aramemnon (<http://aramemnon.uni-koeln.de/>).

<sup>2</sup> n.d.: not detected in mass spectrometric analysis. NaN: not a number.

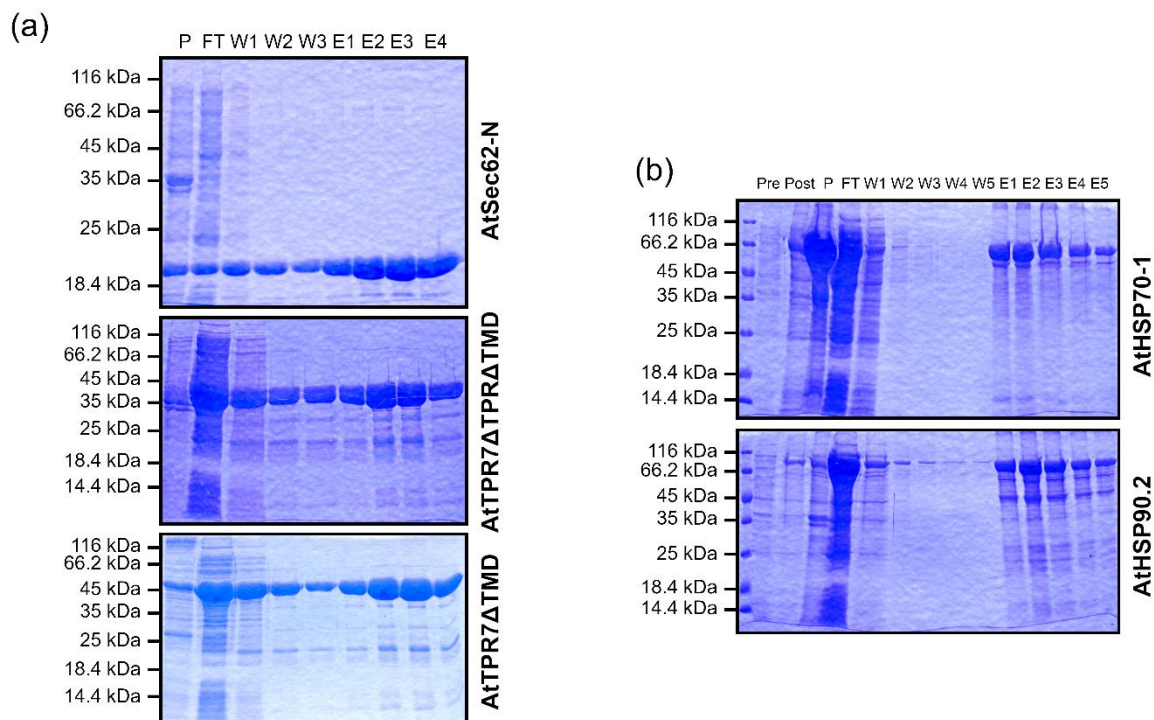


**Figure A1: Protein purification for subsequent antibody generation or *in vitro* pull-down analysis.** AtSec62-N, AtTPR7 $\Delta$ TPR $\Delta$ TMD and AtTPR7 $\Delta$ TMD were expressed with a C-terminal His-tag (a), whereas AtHSP70-1 and AtHSP90.2 were expressed with a C-terminal Strep-tag (b). Fractions indicated on Coomassie stained SDS-PAGE gels correspond to 5  $\mu$ l pre-induction (Pre) and post-induction sample (Post), 3  $\mu$ l of the resuspended pellet (P), 15  $\mu$ l flow-through (FT) and washes (W1 – W5) and 5  $\mu$ l of the elutions (E1 – E5) (compare to 2.2.18. and 2.2.19.).

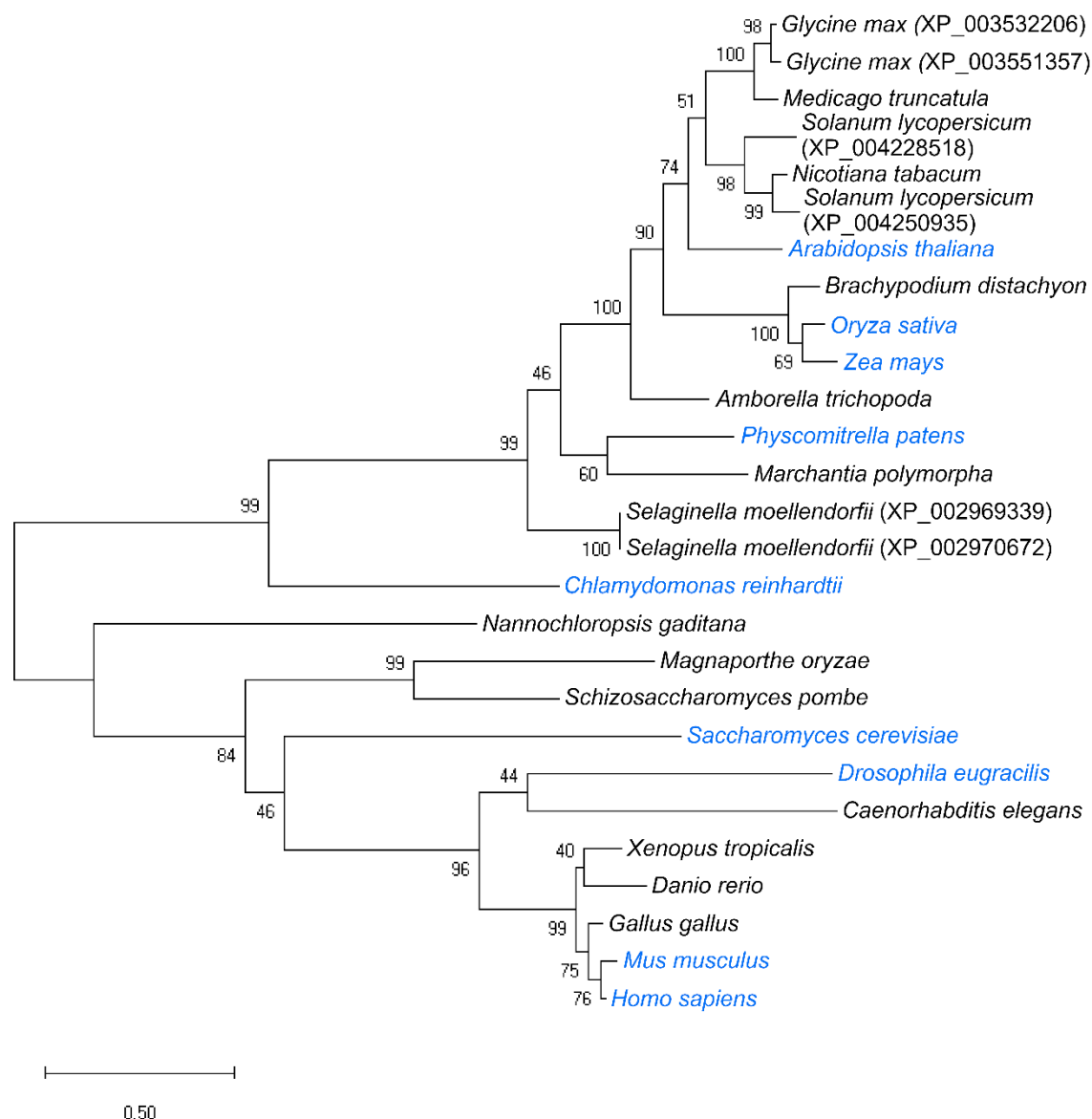


**Figure A2: Phylogenetic analysis of Sec62 homologues.** The phylogenetic tree was generated with MEGA-X (Kumar *et al.* 2018), using the Maximum Likelihood method, having 500 bootstrap replications and applying the Jones-Taylor-Thornton substitution model (Jones *et al.* 1992) and Nearest-Neighbour-Interchange. It is drawn to scale with branch length measured in the number of substitutions per site. The percentage of trees in which the associated taxa clustered together is shown next to the branches. Detailed information regarding accession numbers is given in section 2.1.7. Species marked in blue were used for amino acid sequence alignment (compare to Figure 9a).

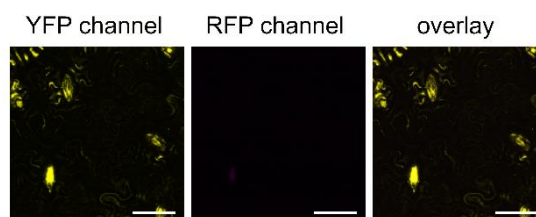


**Figure A3: Untransformed leaf sample for rBiFC analysis.** Fluorescent signals were detected by confocal laser scanning microscopy. Scale bars represent 50  $\mu\text{m}$ .

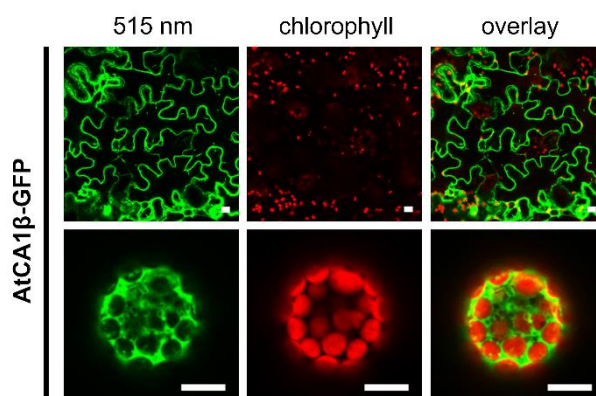


**Figure A4: AtCA1 $\beta$ -GFP localisation.** Fluorescent signals were detected by confocal laser scanning microscopy in transiently transformed tobacco leaves (upper panel) or isolated *Arabidopsis* protoplasts (lower panel). Scale bars represent 10  $\mu\text{m}$ .



### Conference contributions

EMBO Workshop – Current advances in protein translocation across membranes.

23<sup>rd</sup> – 27<sup>th</sup> March 2019 (Sant Feliu de Guixols, Spain).

Poster: Mitterreiter, M.J., Soll, J., Schwenkert, S.: The plant homologue of Sec62 has a unique topology and is indispensable for male fertility in *Arabidopsis*.

SFB1035-Conference on conformational transitions in proteins.

3<sup>rd</sup> – 6<sup>th</sup> May 2018 (Island of San Servolo, Venice, Italy).

Poster: Mitterreiter, M.J., Schwenkert, S.: Protein translocation into the endoplasmic reticulum in *Arabidopsis thaliana*.

## Acknowledgements

First of all, I am grateful to PD Dr. Serena Schwenkert for giving me the opportunity to work in her research group and for her supervision and support.

I would like to thank Prof. Dr. Jürgen Soll for providing work space, equipment and for helpful discussions. Moreover, I am thankful to Prof. Dr. Wolfgang Frank and Prof. Dr. Thorben Cordes for useful advices and support.

Prof. Dr. Christopher Grefen is acknowledged for helpful discussions and suggestions and for providing 2in1-rBiFC vectors, while Prof. Dr. Hans Thordal-Christensen is acknowledged for supplying Split-GFP vectors. I would like to give thanks to Dr. Chris Carrie for providing yeast vectors and for advice on yeast experiments.

I am grateful to my former colleague Dr. Thomas Brylok for initial screening of *atsec62* mutant plants,  $\alpha$ AtSec62 antibody generation and for adjusting instructions on microsomal membrane preparation. Furthermore, I would like to thank my research student Franziska Bosch for performing and analysing root length as well as ER stress experiments. Tamara Bergius is acknowledged for technical assistance and help with gDNA isolation.

I would like to give thanks to my current and former colleagues Inga, Manali, Roberto, Li, Ahmed, Renuka, Petra, Kerstin, Carina, the other Melanie, Şebnem, Tamara and Annabel for their constant support and encouragement not only in the laboratory but also over coffee and cake, during cheerful evenings and extensive forest walks.

Finally, I want to express my deepest gratitude to my family and friends ...